



From Half Metal To Spintronics

(從半金屬到自旋電子學)

Jauyn Grace Lin

Cener for Condensed Matter sciences
National Taiwan Univsersity

2008/11/20

Context



Chapter One *Half Metal*

Chapter Two *Colossal Magnetoresistance*

Chapter Three *Experiments for Spintronics*



Chapter One

Half Metal



Outline

1. *Definition of half metal*
2. *Material classification*
3. *Polarization measurement*
4. *Applications*

New Class of Materials: Half-Metallic Ferromagnets

R. A. de Groot and F. M. Mueller

Research Institute for Materials, Faculty of Science, Toernooiveld, 6525 ED Nijmegen, The Netherlands

and

P. G. van Engen and K. H. J. Buschow

Philips Research Laboratories, 5600 JA Eindhoven, The Netherlands

(Received 21 March 1983)

The band structure of Mn-based Heusler alloys of the $C1_b$ crystal structure (MgAgAs type) has been calculated with the augmented-spherical-wave method. Some of these magnetic compounds show unusual electronic properties. The majority-spin electrons are metallic, whereas the minority-spin electrons are semiconducting.

Compound	$N(E)\uparrow$	$N(E)\downarrow$	$n_{3d}^{Mn\uparrow}$	$n_{3d}^{Mn\downarrow}$	μ_{tot}^{cacl}	μ_{tot}^{exp}
NiMnSb	9.90	0	4.51	0.87	4.00	3.85
PtMnSb	10.05	0	4.57	0.79	4.00	3.97
PdMnSb	9.04	2.97	4.58	0.71	4.05	3.95
PtMnSn	9.78	19.31	4.40	0.78	3.60	3.42

Half metals are the extreme case of strong ferromagnet, where not only 3d electrons are fully polarized, but also other (sp) down-spin bands do not cross the Fermi level.
 (examples: NiMnSb, PtMnSb--- Hesuler phases.)

Augmented-spherical-wave method

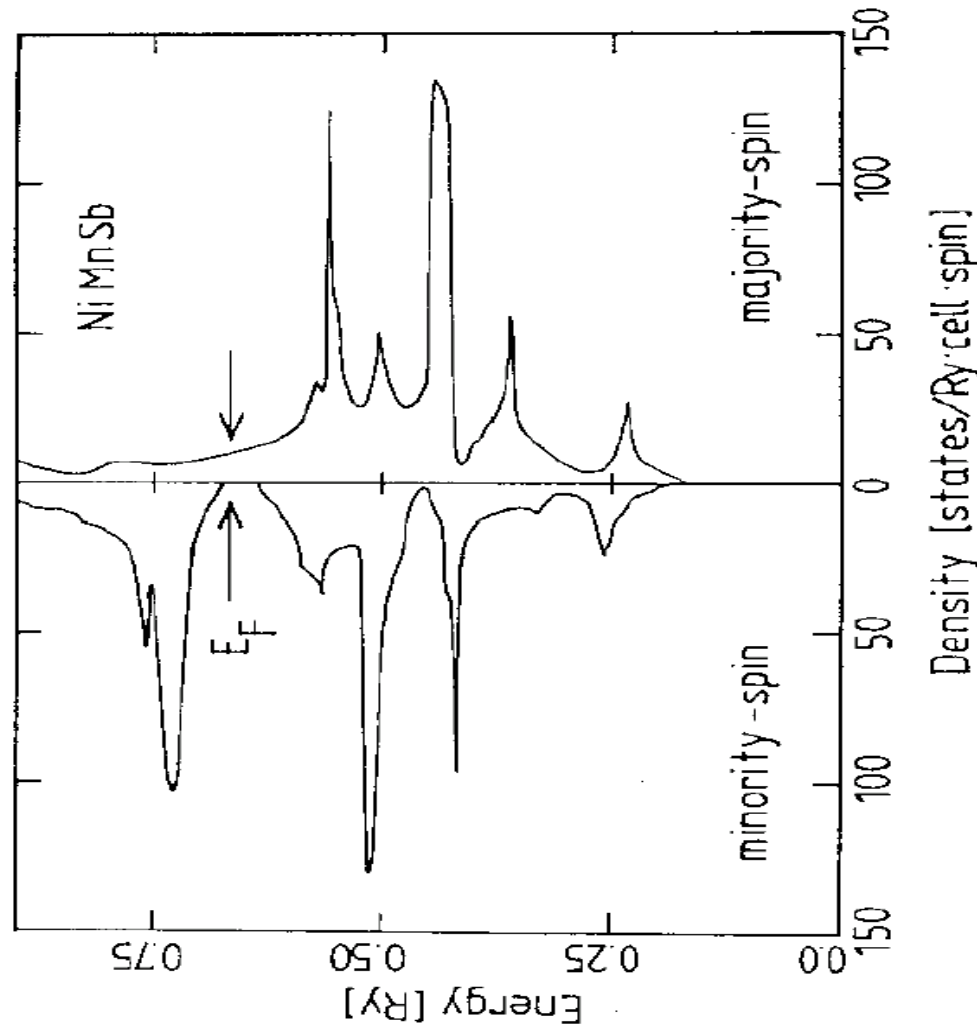


Fig.1. Band structure for NiMnSb [1].

JOURNAL OF APPLIED PHYSICS VOLUME 91 (2002)

Half-metallic ferromagnetism: Example of CrO₂ (invited)

J. M. D. Coey and M. Venkatesan

Physics Department, Trinity College, Dublin 2, Ireland

A **half metal** is a solid with an unusual electronic structure. For electrons of one spin it is a metal with a Fermi surface, but for the opposite spin there is a gap in the spin-polarized density of states, like a semiconductor or insulator. This definition presupposes a magnetically ordered state to define the spin quantization axis. The responses of a half metal to electric and magnetic field at zero temperature are quite different. There is electric conductivity, but no high-field magnetic susceptibility.

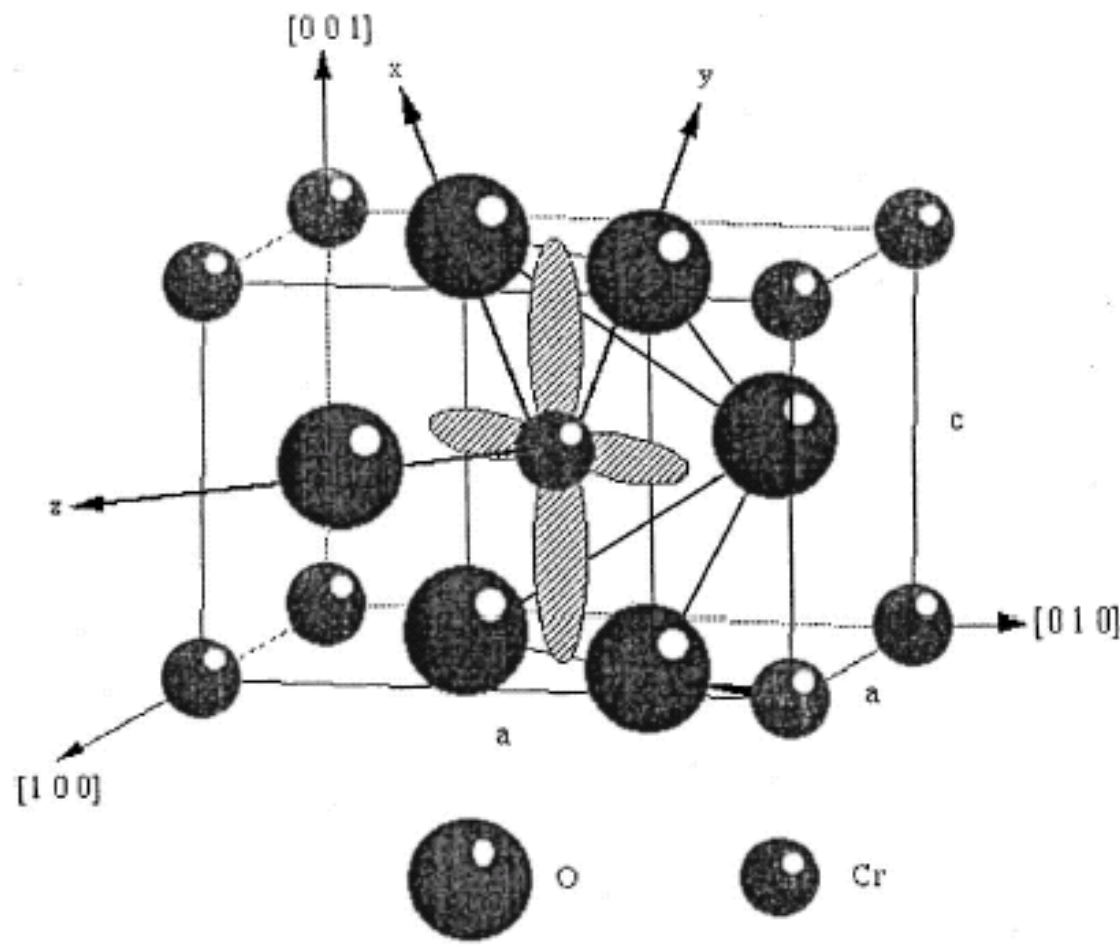


FIG. 4. The rutile structure of CrO_2 . The local axis frame for the t_{2g} orbitals is shown.

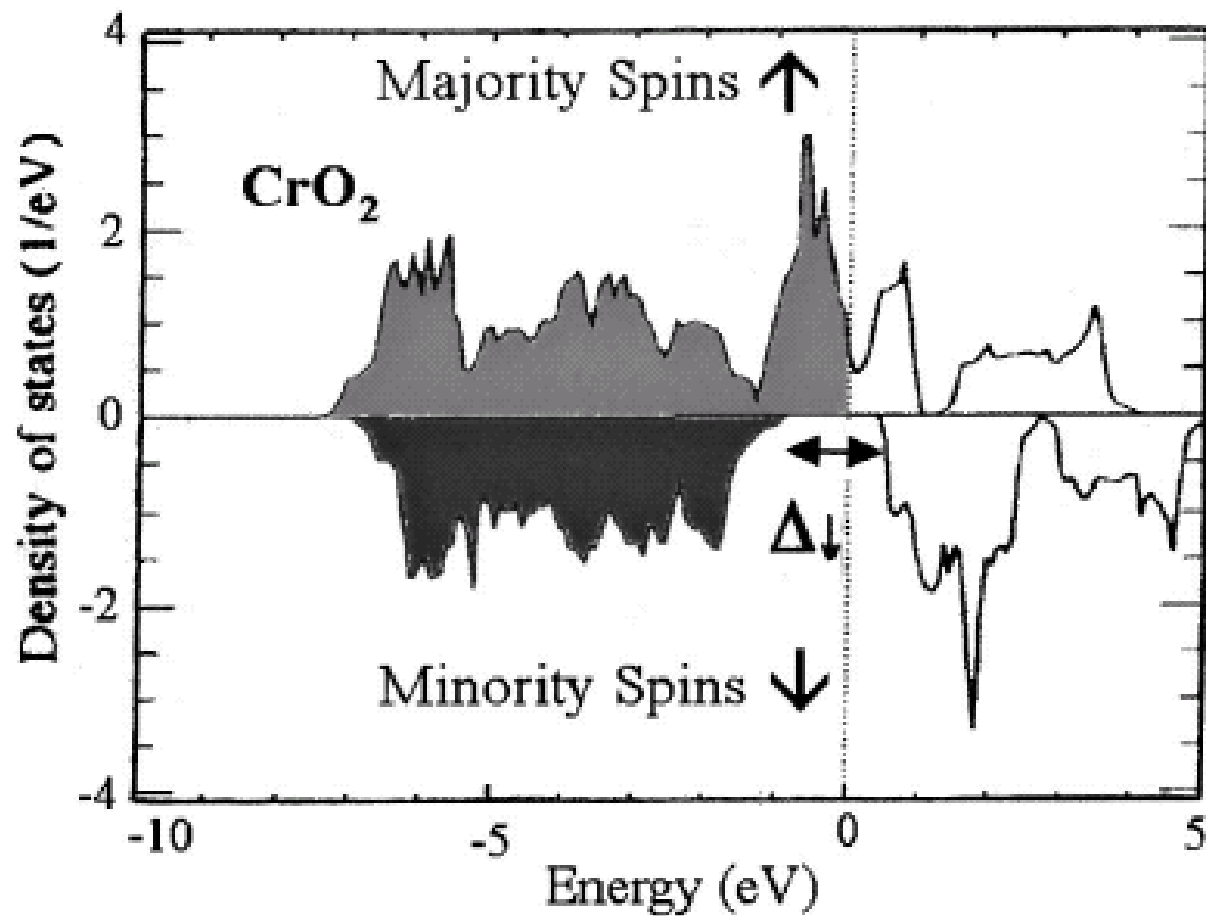
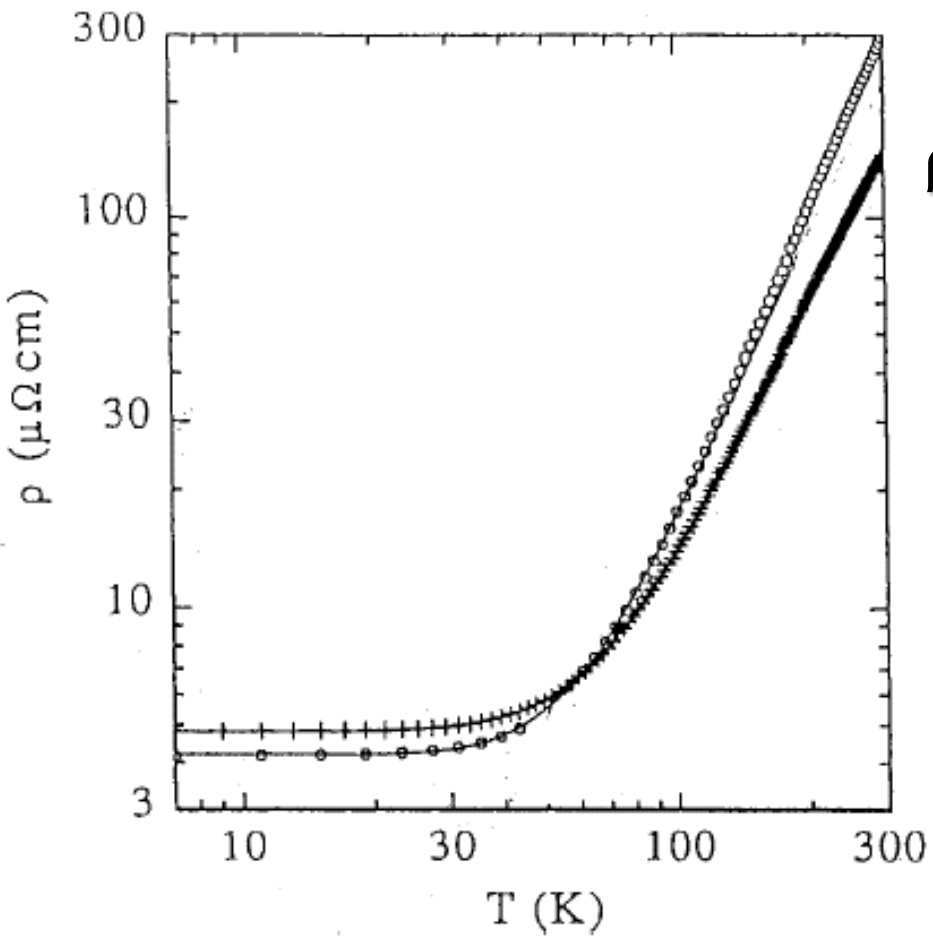


FIG. 5. Spin polarization of the density of states of CrO_2 .

TABLE III. Some electronic structure calculation on CrO₂.

Author		Δ_{\downarrow} (eV)	Δ_{sf} (eV)	N_{\uparrow} eV ⁻¹ f.u ⁻¹
Schwarz	Ref. 26 LSDA-ASW	1.3	0.3	0.8
Lewis <i>et al.</i>	Ref. 2 LSDA-PWPP	1.4	0.3	0.69
Korotin <i>et al.</i>	Ref. 27 LSDA+U(3 eV)	2.4	1.7	0.4
Mazin <i>et al.</i>	Ref. 31 LSDA/GGA	1.3	0.2–0.7	0.95
Brener <i>et al.</i>	Ref. 32 LSDA-LCGO	1.3	0.2	1.16
Kunes <i>et al.</i>	Ref. 28 GGA	1.8	0.7	0.3

 Δ_{Sf} : spin-flip gap



$\rho_0 = 4 \times 10^{-8} \text{ ohm-m}$
 $\sim 90 \text{ nm mean-free path}$

$$\rho = \rho_0 T^2 e^{-\Delta/T}$$

with $\Delta \sim 80 \text{ K}$

FIG. 6. Resistivity of CrO_2 thin films.

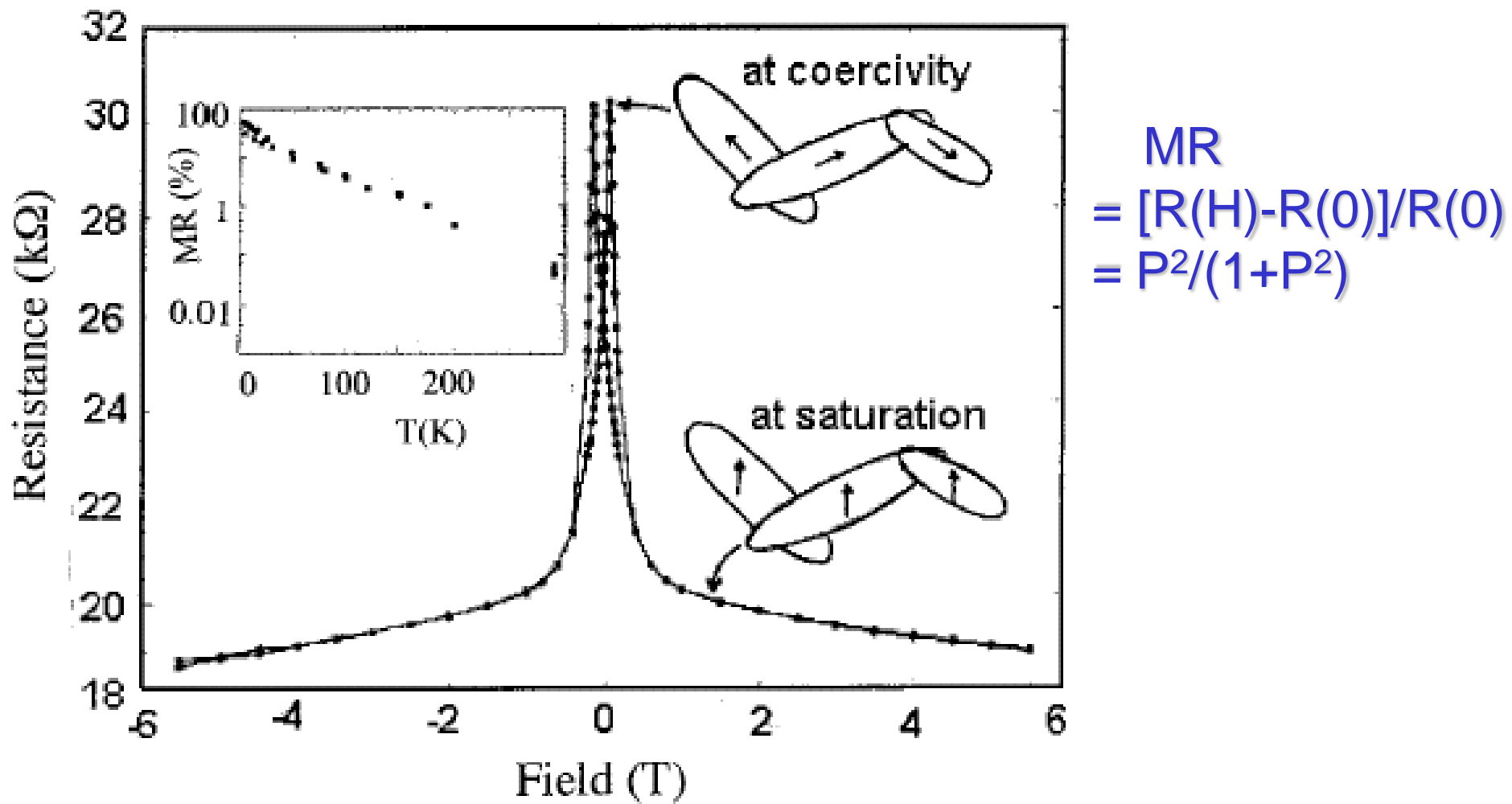


FIG. 7. Magnetoresistance of a CrO_2 – Cr_2O_3 pressed powder compact, with temperature dependence shown in the inset.

TABLE I. Summary of the classification of half-metals.

Type	Density of states	Conductivity	\uparrow electrons at E_F	\downarrow electrons at E_F
IA	Half-metal	Metallic	Itinerant	None (<chem>CrO2</chem> , <chem>NiMnSb</chem>)
IB	Half-metal	Metallic	None	Itinerant (<chem>Sr2FeMoO6</chem>)
IIA	Half-metal	Nonmetallic	Localized	None
IIB	Half-metal	Nonmetallic	None	Localized
IIIA	Metal	Metallic	Itinerant	Localized (<chem>Magnetite</chem>)
IIIB	Metal	Metallic	Localized	Itinerant (<chem>La0.7Sr0.3MnO6</chem>)
IVA	Semimetal	Metallic	Itinerant	Localized
IVB	Semimetal	Metallic	Localized	Itinerant (<chem>Tl2Mn2O7</chem>)
V A	Semiconductor	Semiconducting	Few, itinerant	None (<chem>Doped EuO</chem> & <chem>EuS</chem>)
VB	Semiconductor	Semiconducting	None	Few, itinerant (<chem>GaAsMn</chem>)

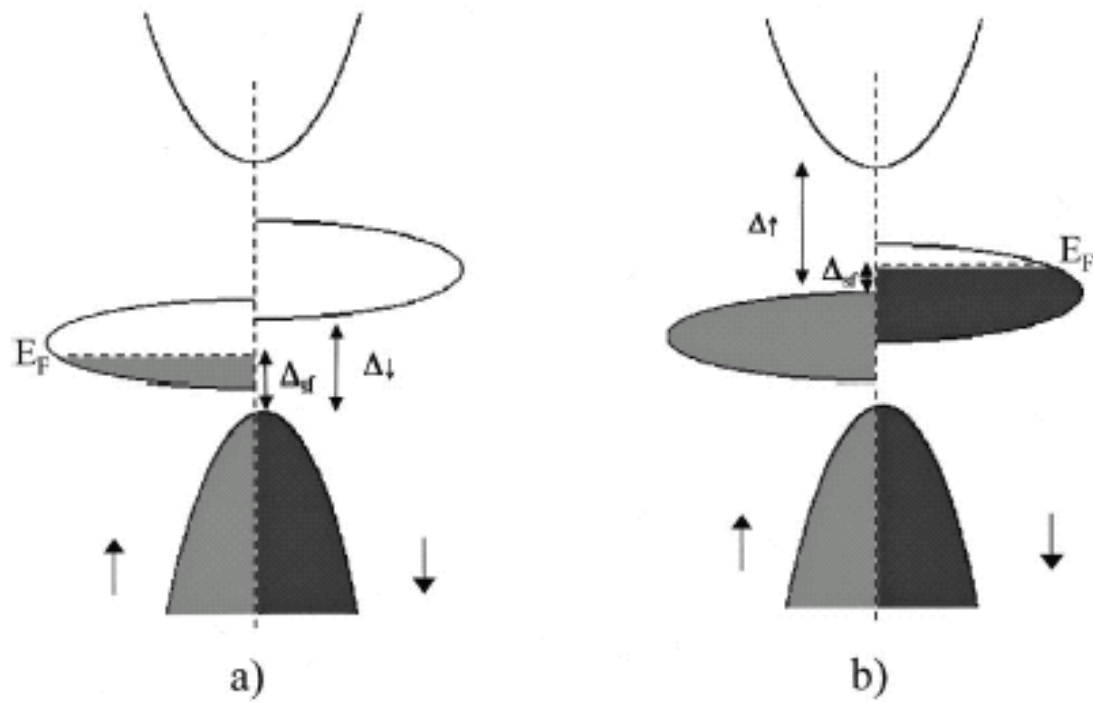


FIG. 1. Schematic density of states for a half metal, (a) Type I_A with only \uparrow electrons at E_F and (b) Type I_B with only \downarrow electrons at E_F . In narrow d bands, the states at E_F may be localized (type II).

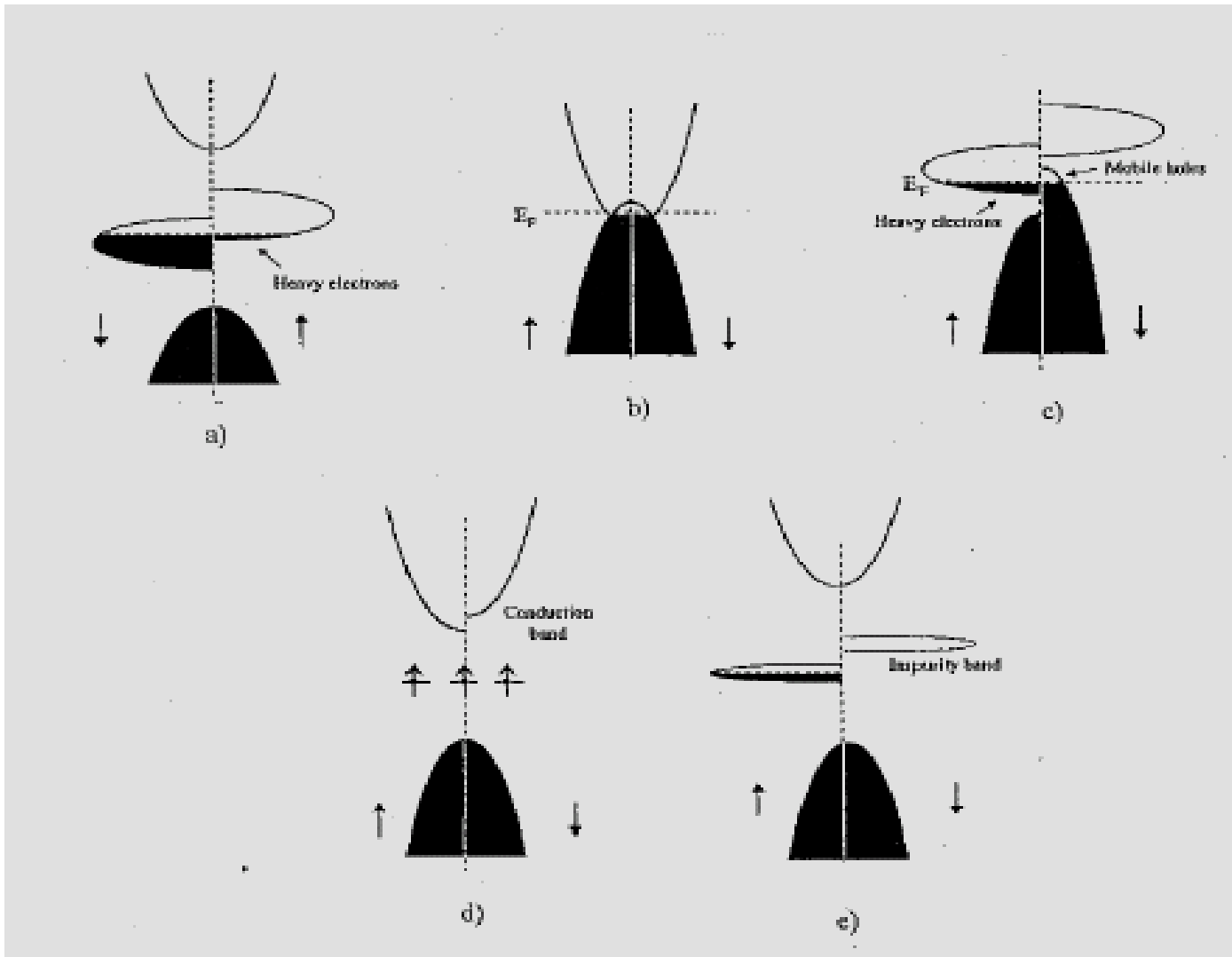


FIG. 2. Schematic density of states for (a) a type III_A half metal, where electrons of one spin direction are itinerant and the others are localized, (b) a semimetal, (c) a type IV_A half metal, and (d), (e) two types of ferromagnetic semiconductor.

Definition of polarization

$$P_0 = (N^\dagger - N^\downarrow) / (N^\dagger + N^\downarrow),$$

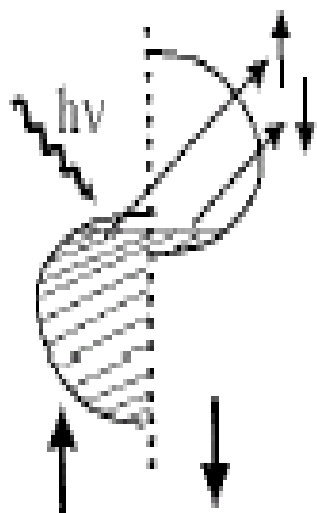
--- straightforward

$$P_n = (\langle N^\dagger v^{\dagger n} \rangle - \langle N^\downarrow v^{\downarrow n} \rangle) / (\langle N^\dagger v^{\dagger n} \rangle + \langle N^\downarrow v^{\downarrow n} \rangle).$$

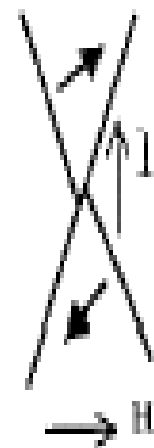
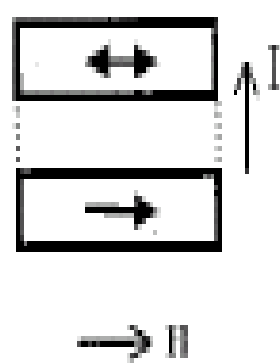
--- real measurement

v: fermi velocity of electrons

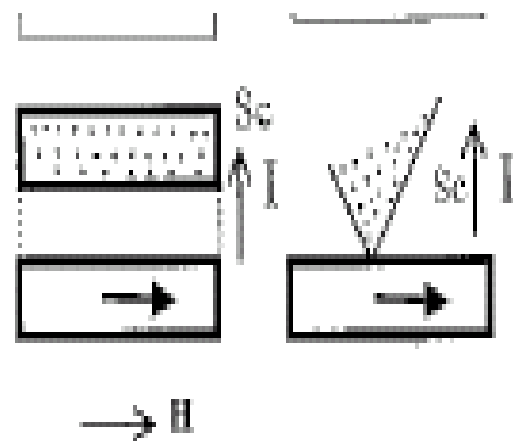
1. Photoemission



3. Point Contact



5. Andreev



2. Magn. Tunnel Junc.

4. Tedrow-Meservey

FIG. 3. Comparison of five methods of measuring P : Photoemission, tunnel junction, point contact, Tedrow–Meservey experiment, Andreev reflection.

TABLE II. Calculated spin polarization in ferromagnetic oxides.

	CrO_2 (Ref. 2)	$(\text{La}_{0.67}\text{Ca}_{0.33})\text{MnO}_3$ (Ref. 7)	$\text{Tl}_2\text{Mn}_2\text{O}_7$ (Ref. 8)
N^\uparrow ($\text{eV}^{-1} \text{f.u}^{-1}$)	0.69	0.58	1.25
N^\downarrow ($\text{eV}^{-1} \text{f.u}^{-1}$)		0.27	0.24
V_F^\uparrow (10^6 ms^{-1})	0.25	0.76	0.06
V_F^\downarrow (10^6 ms^{-1})		0.22	0.33
P_0 %	100	36	66
P_1 %	100	76	-5
P_2 %	100	92	-71

Applications of Half metals

a. **Magneto-optical effects**

Large Kerr rotation in PtMnSb.

b. **Magneto-resistance applications**

Spin-valve system --- pick-up head, MRAM

c. **Spin electronics**--- Injection of polarized carriers

- i) The spin injection in a normal metal can give information on the spin diffusion length in this metal.
- ii) Spin injection may act as a pair-breaking agent in a superconductor.
- iii) Half metals can also be used to build a spin transistor
- iv) Another possible application is as polarized tips in STM, in order to visualize the orientation of magnetic domains.



Chapter Two

Colossal Magnetoresistance

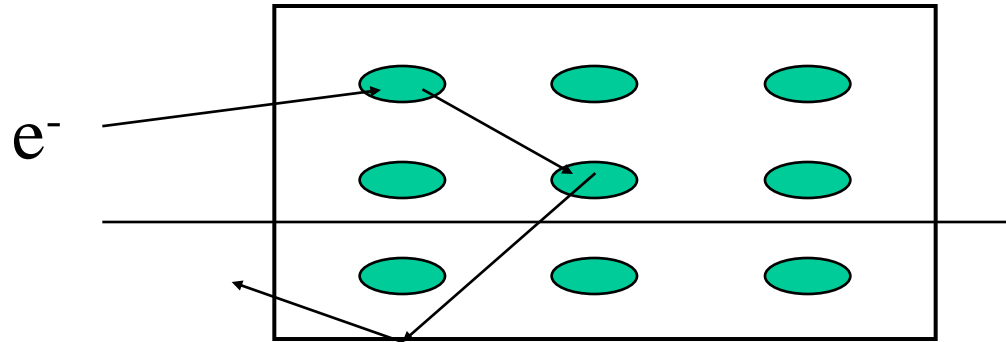


Outline

1. *Introduction*
2. *Material structure*
3. *Physical Properties & Mechanism*

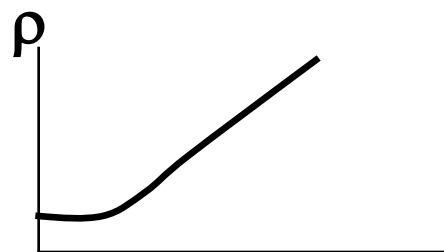


1. Introduction --- 何謂電阻(率)

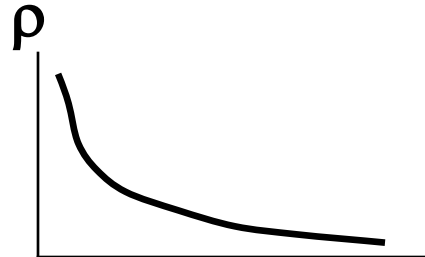


$$\xrightarrow{\hspace{1cm}} \text{電阻 } \mathbf{R}$$

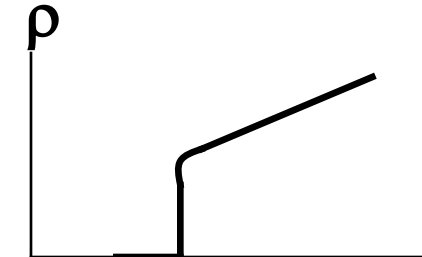
$$\rho = R * A / w$$



金屬



半導體



超導體

T



Introduction --- 物質的基本磁性

順磁



鐵磁



反鐵磁



亞鐵磁

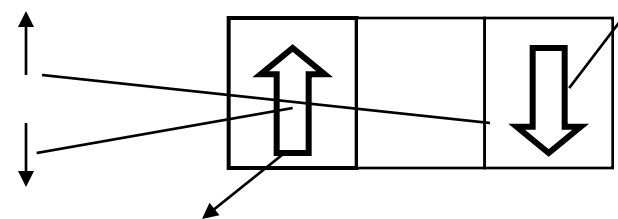


斜磁

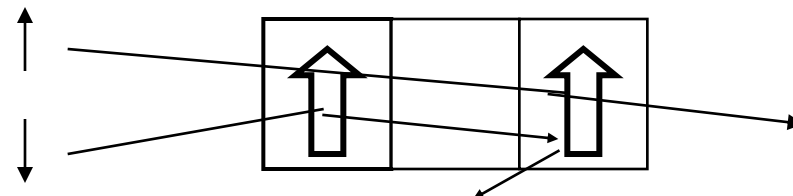
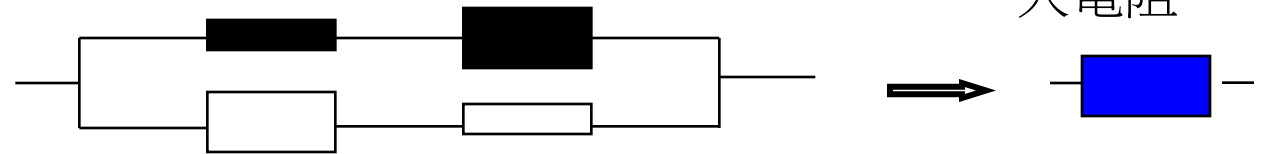




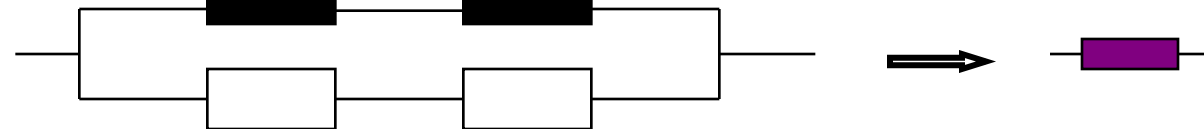
Introduction ---何謂磁阻



$$H = 0$$

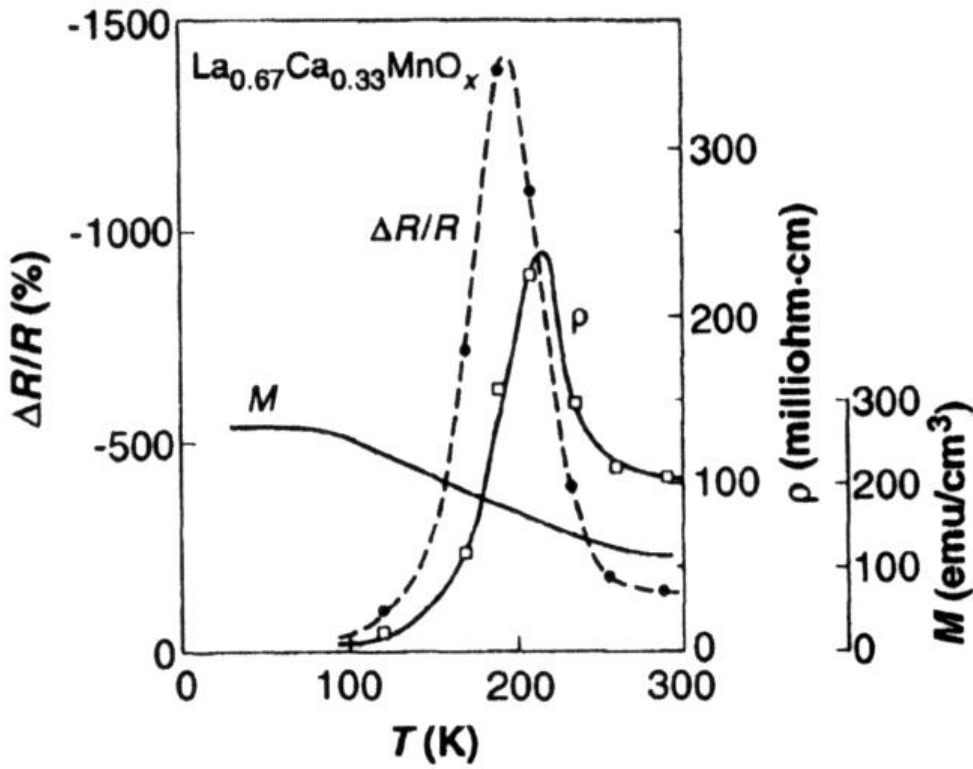


$$H = H_a$$





Introduction --- 何謂龐磁阻(CMR)



- 1) Very high magnetoresistance (99% at T_p)
- 2) Polarization 100% (half metal)
- 3) M- I (F/AF) transition
- 4) Phase separation
- 5) Charge ordering
- 6) Orbital ordering

$$MR = [\rho(H) - \rho(0)] / \rho(H=6 \text{ tesla})$$



MR ratio of spintronic materials

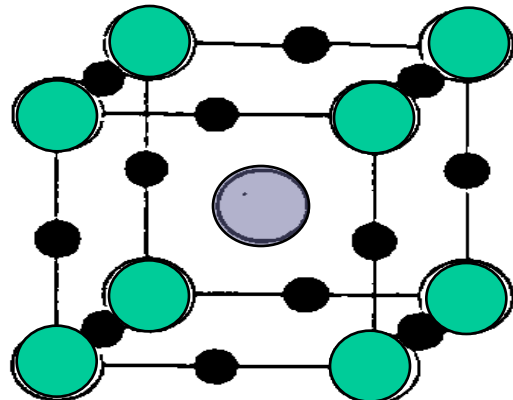
Type	MR	Field	Temp.	Sample
OMR	0.01%	~Tesla	RT	Cu,Al
AMR	2 %	10 Oe	RT	Fe,Co,Ni
GMR	10 %	2 Oe	RT	Fe/Cr/Fe
TMR	40 %	10 Oe	RT	Co/AlO/Co
CMR	10 (99)%	~Tesla	RT(LT)	La-Sr-Mn-O

2. Material Perovskite layered structure

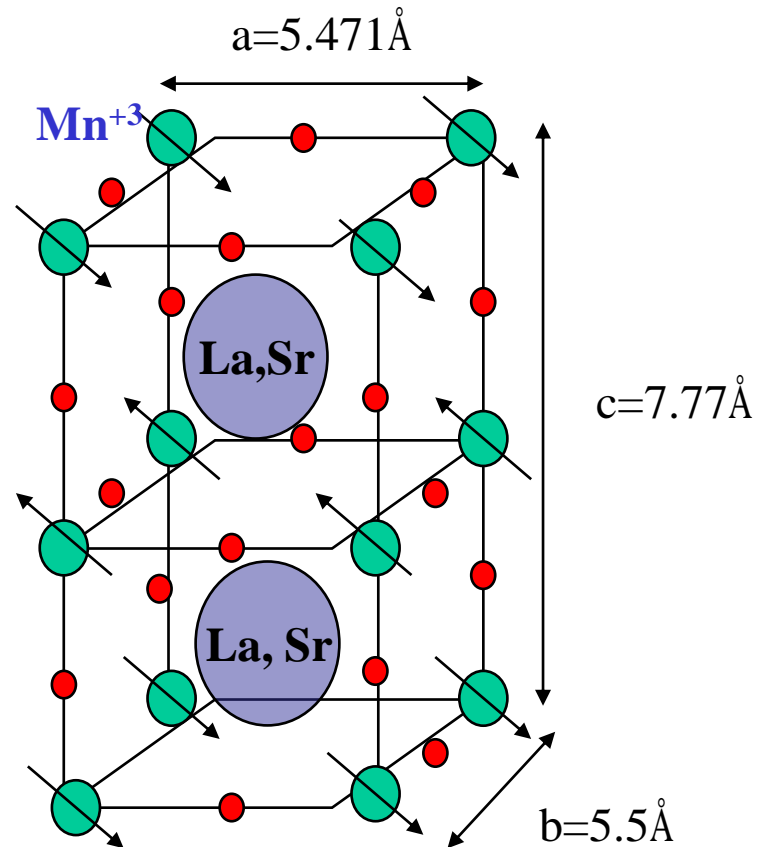
LaMnO_3 : Cubic (insulator, Antiferromagnetic)



Mn (0.70 Å)
O (1.32 Å)
La (1.216 Å)

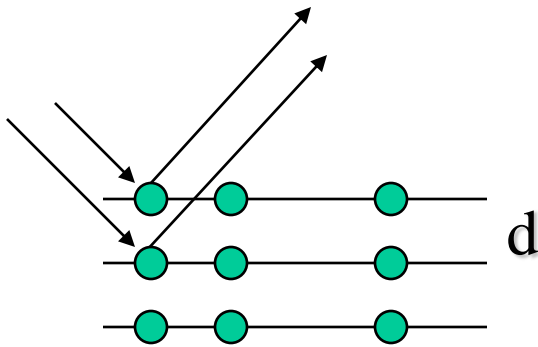


$(\text{La},\text{Sr})\text{MnO}_3$: orthorhombic (Metal, Ferromagnetic)



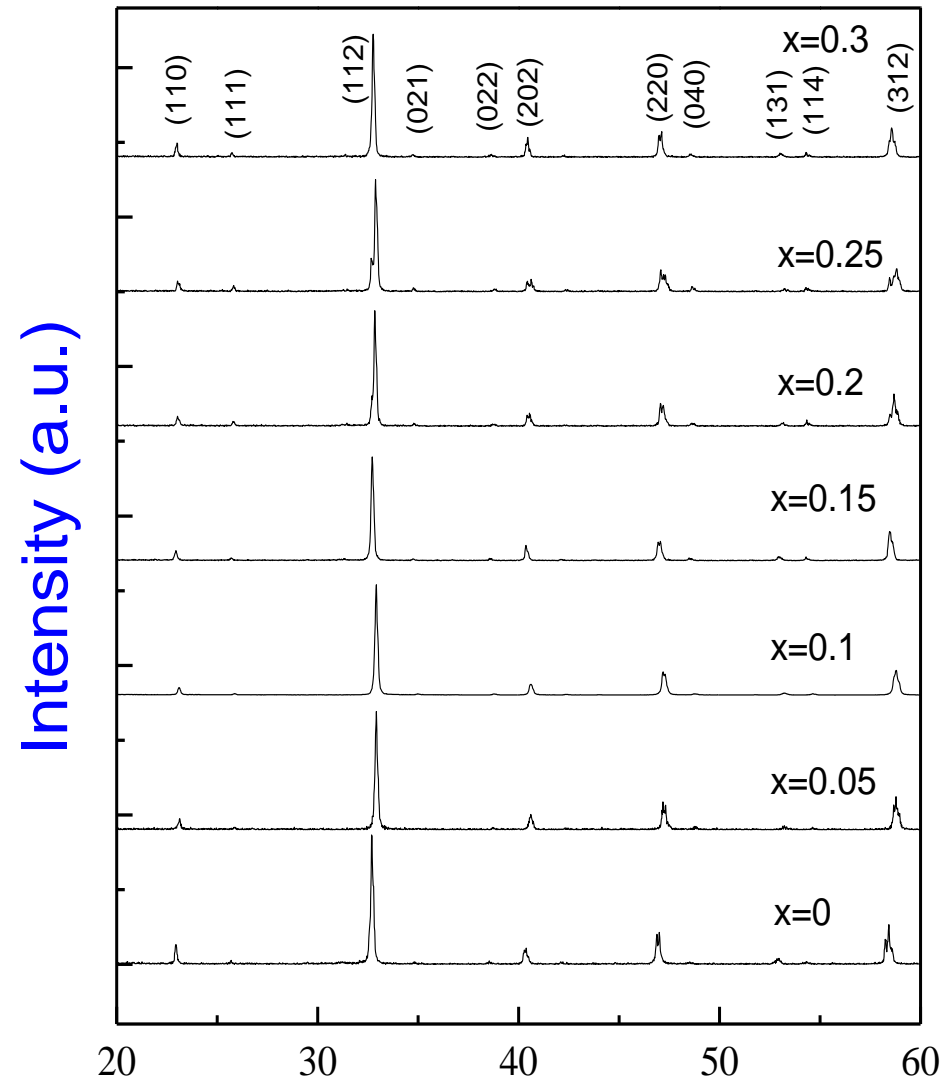


X – ray diffraction pattern



Bragg condition:

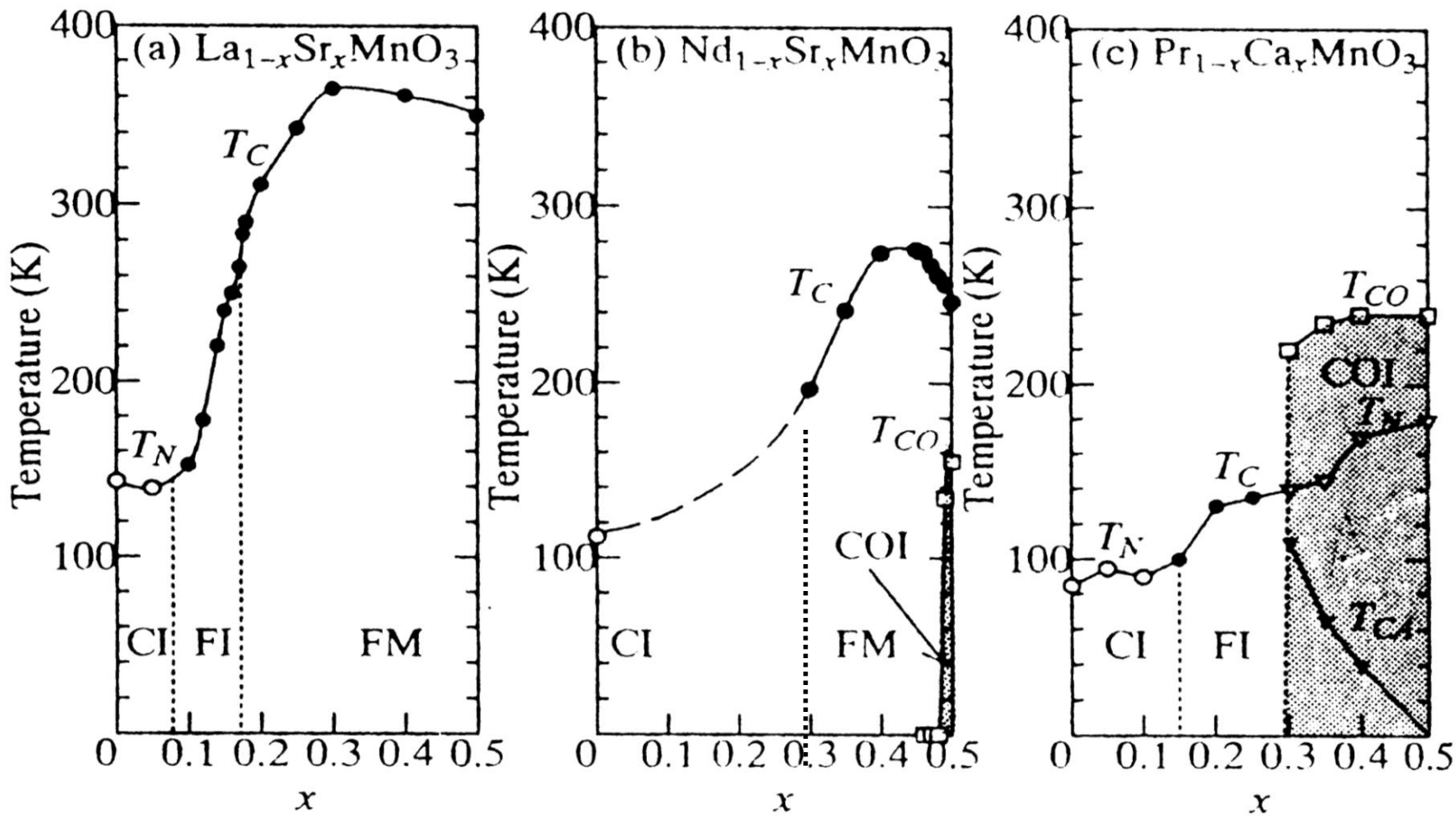
$$n\lambda = 2d\sin\theta$$





Phase diagrams of $R_{1-x}A_xMnO_3$

degrees of freedom: charge, spin, orbital



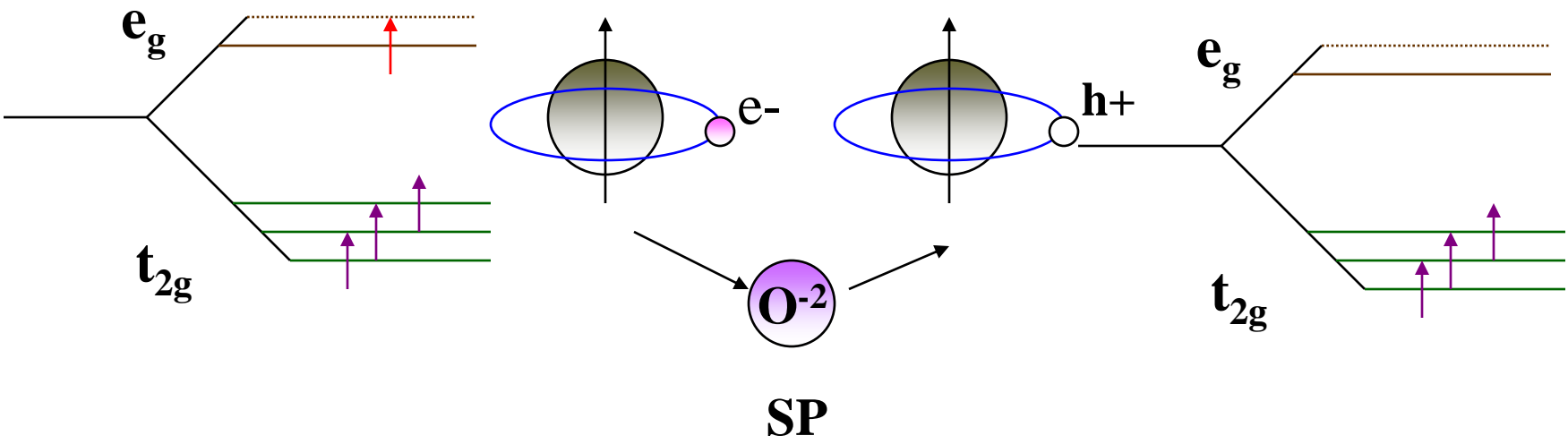
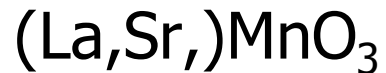


3. Physical properties & mechanism

What's the new physics



Double exchange (1951, Zener)





Mechanism vs. degree of freedom

- ♣ FM/AFM superexchange --- spin
- ♣ Charge/orbital ordering --- charge/orbital
- ♣ double exchange --- charge/spin
- ♣ Lattice distortion
(John-Teller effect) --- lattice

Phase diagram of manganese oxide

Ryo Maezono, Surnio Ishihara, and Naoto Nagaosa

Department of Applied Physics, University of Tokyo, Bunkyo-ku, Tokyo 113, Japan

$$H = H_K + H_{Hund} + H_{\text{onsite}} + H_S$$

$$H_K = \sum_{\sigma\gamma\gamma'(ij)} t_{ij}^{\gamma\gamma'} d_{i\sigma\gamma}^+ d_{j\sigma\gamma'}^- \quad (\text{Kinetic energy of } e_g \text{ electrons})$$

$$H_{Hund} = -J_H \sum_i \vec{S}_{t_{2g}i} \cdot \vec{S}_{e_{gi}} \quad (\text{Hund coupling between } e_g \text{ & } t_{2g} \text{ spins})$$

$$H_{\text{onsite}} = -\sum_i (\tilde{\beta} T_i^2 + \tilde{\alpha} S_{e_{gi}}^2) \quad (\text{Coulomb interaction between } e_g\text{-electrons})$$

$$H_S = J_S \sum_{(ij)} \vec{S}_{t_{2g}i} \cdot \vec{S}_{t_{2g}j} \quad (\text{Super exchange } t_{2g} \text{ spins})$$

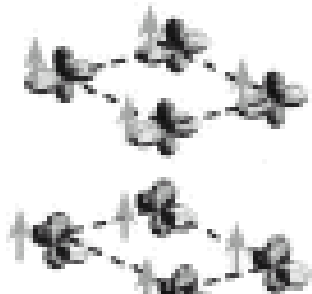
2D-F



($x=0.0$) ; spin F

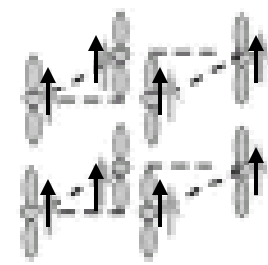


($x=0.3$) ; spin F



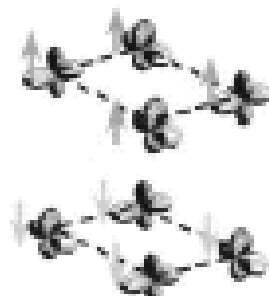
($0.3 < x < 0.8$) ; spin F

1D-F

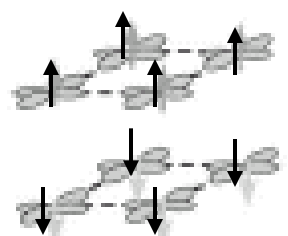


($x=0.8$) ; spin F

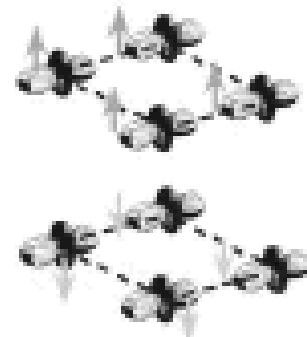
A



($x=0.0$) ; spin A



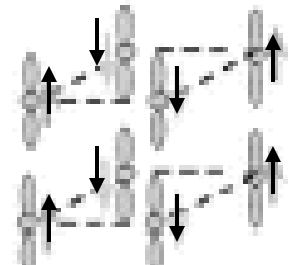
($0.1 < x < 0.45$) ; spin A



($0.45 < x < 0.75$) ; spin A

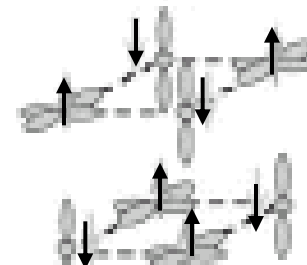


($x=0.0$) ; spin C



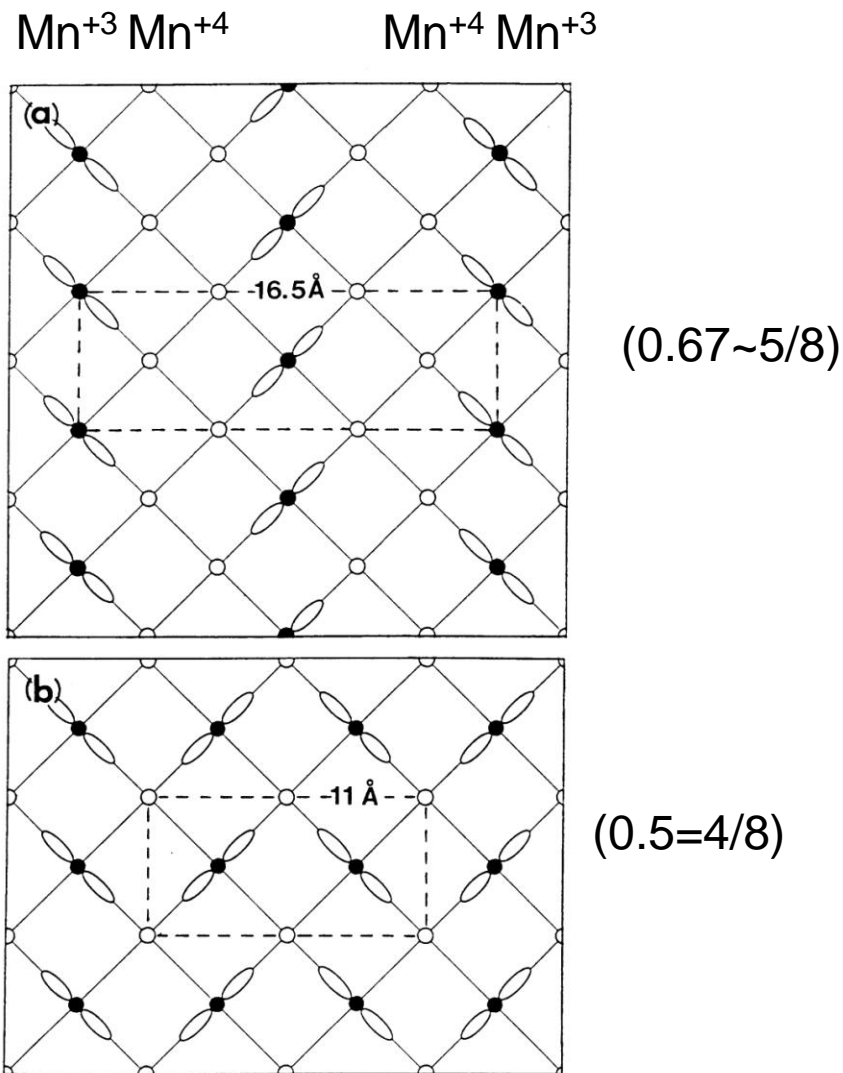
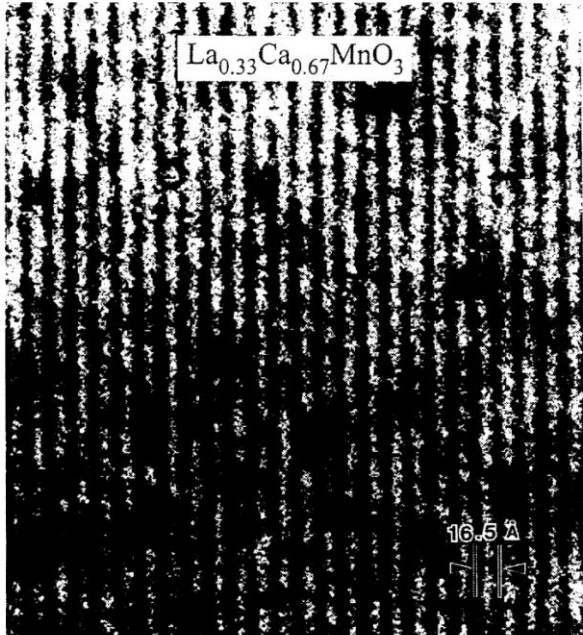
($x \neq 0.0$) ; spin C

G



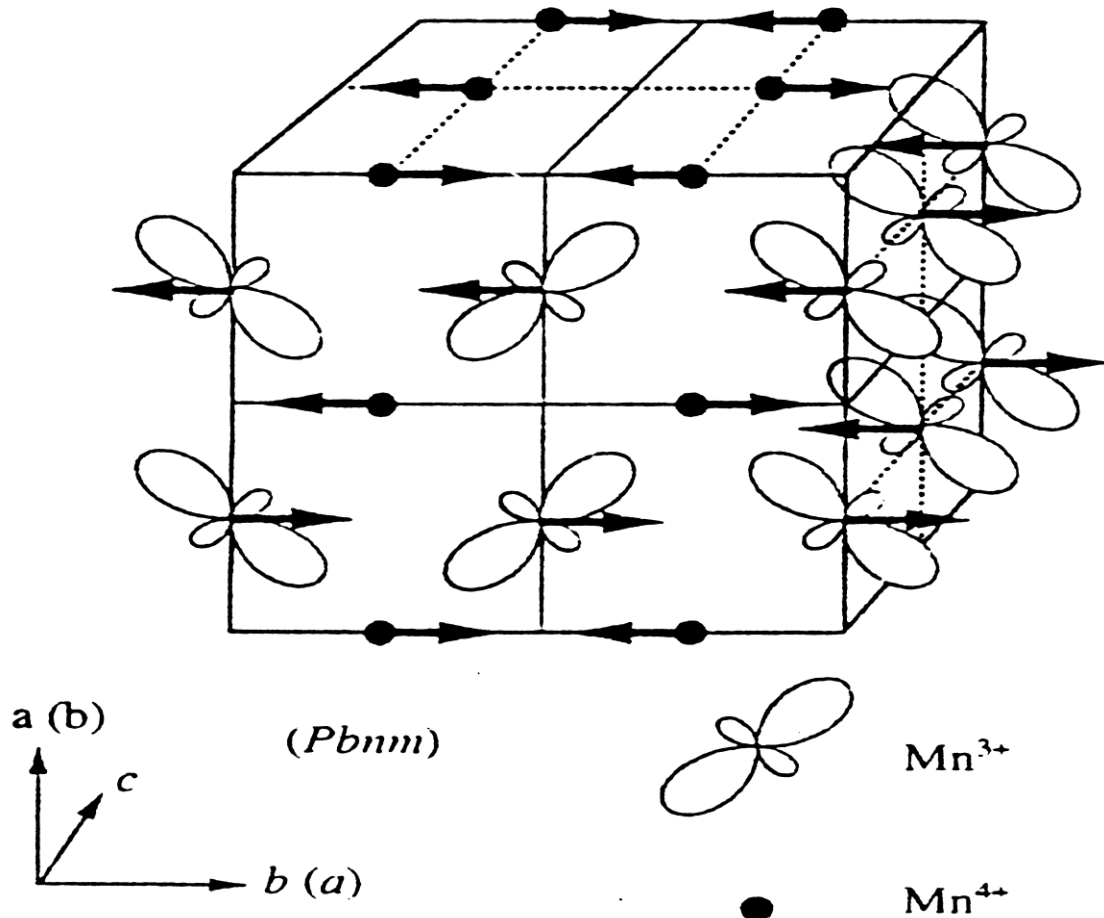
($x=0.0$) ; spin G

Charge Ordering ($Mn^{+4}/Mn^{+3} = n/8$)



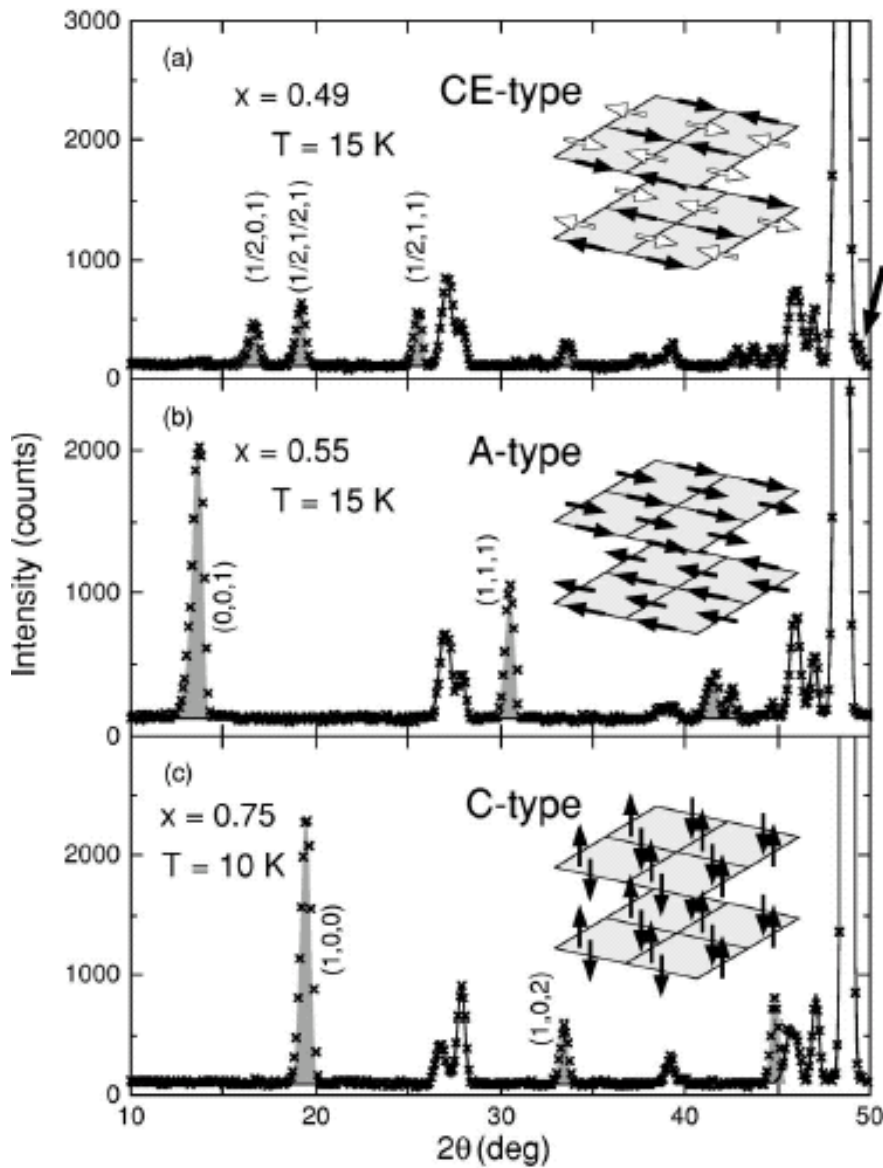
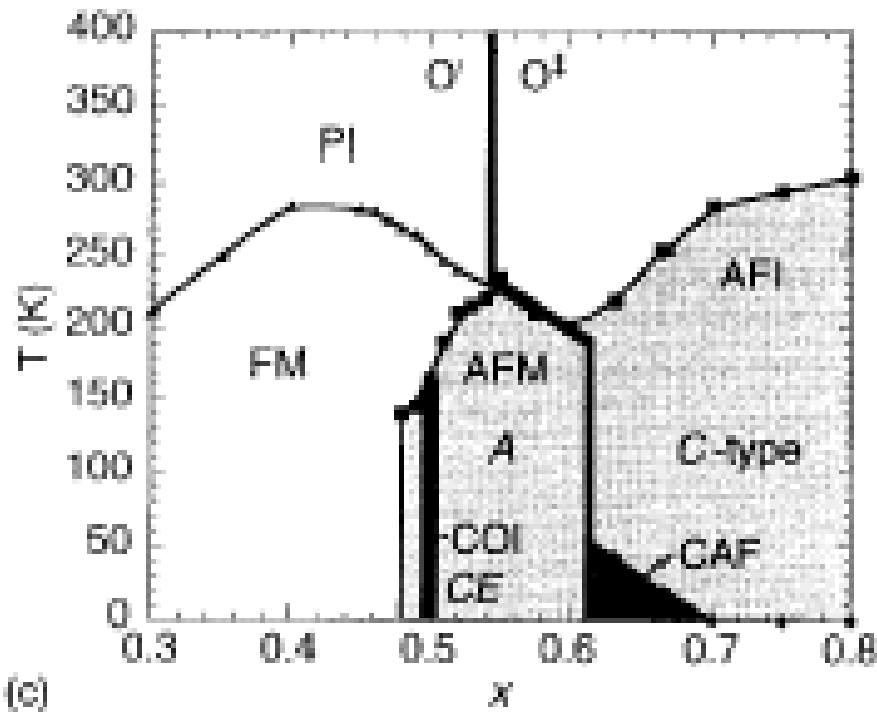
Chen et al., J. Appl. Phys. 81 (1997)

Spin/orbital structure

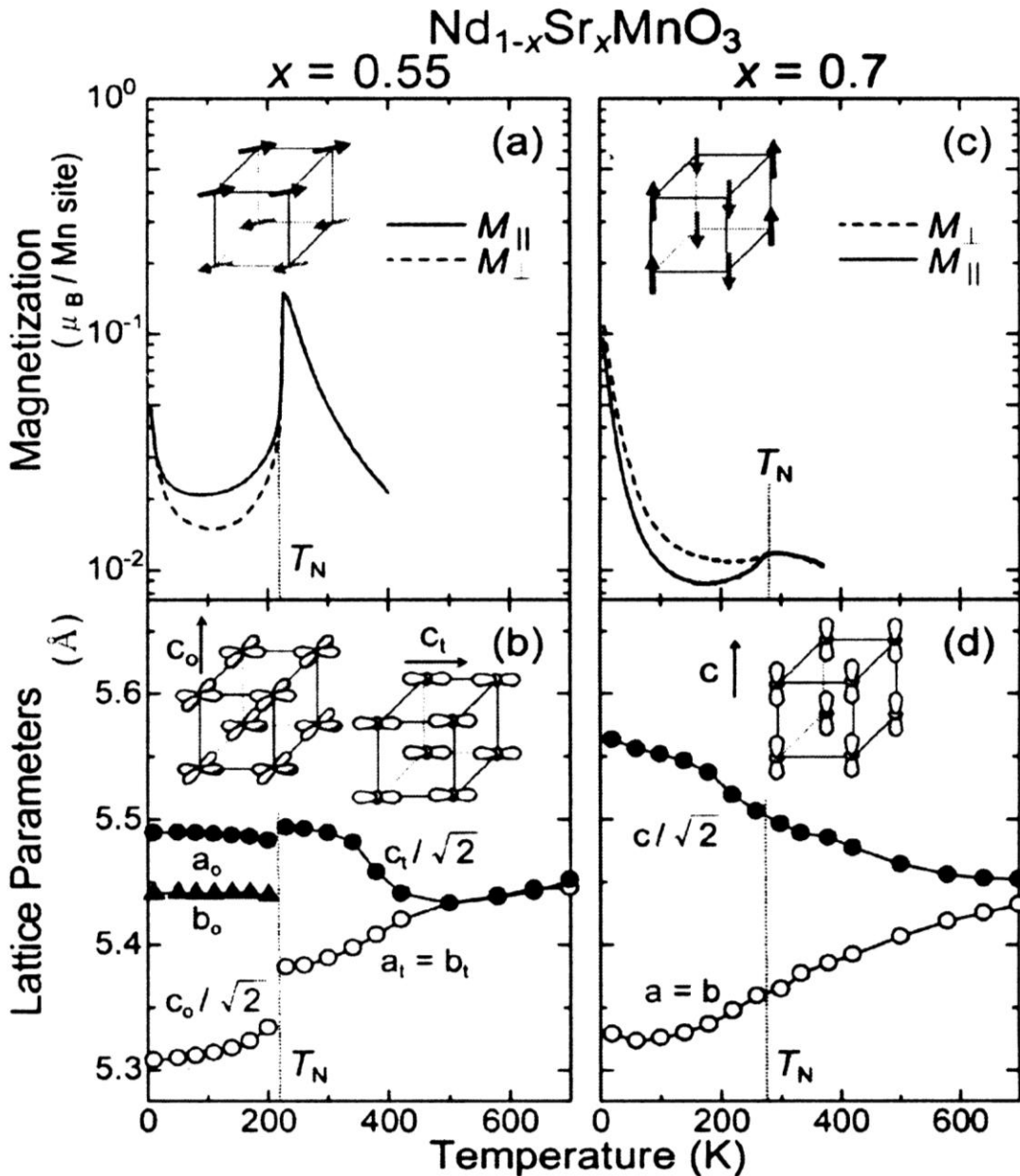


Neutron diffraction
Magnetic Dichroism

$\text{Nd}_{1-x}\text{Sr}_x\text{MnO}_3$



Orbital switching in A-type spin state



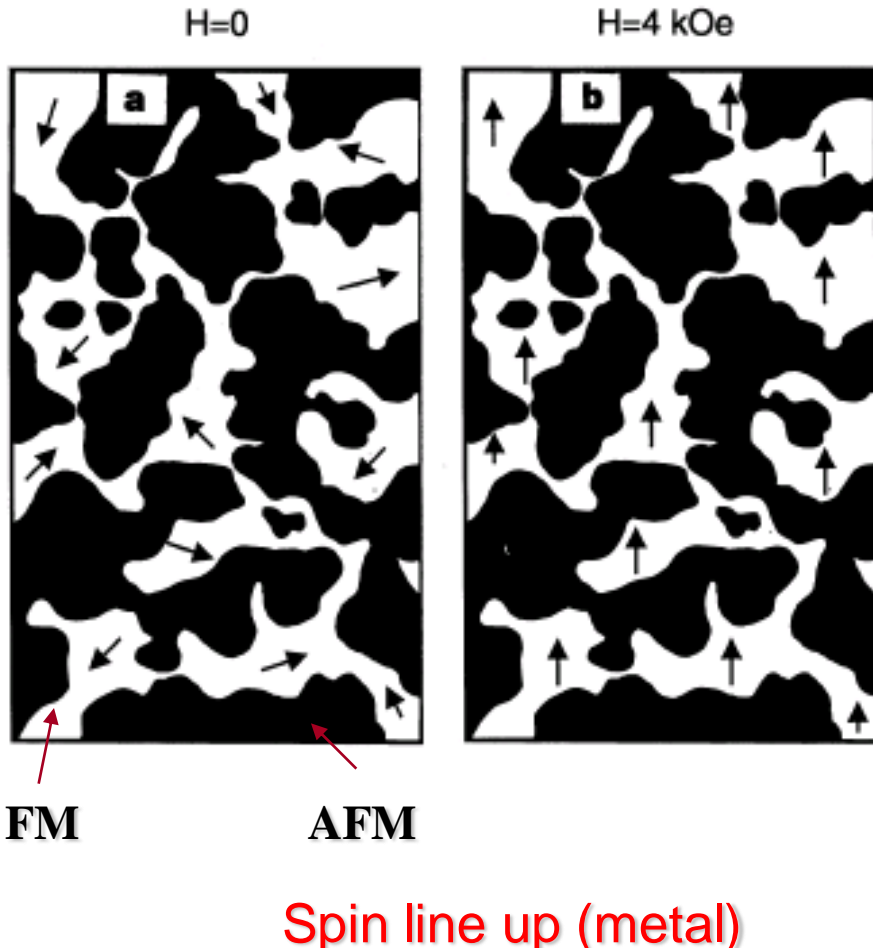
Spin A-Type :

from $d_{3z^2-r^2}$ to $d_{x^2-y^2}$
at $T_N \sim 220$ K

Spin C-type :

remains $d_{3z^2-r^2}$
with $T_N \sim 270$ K

Origin of CMR: Phase separation



AFM Melting as $H \geq 1$ Tesla (insulator)



M. Uehara, et al, Nature 399 (1999)



Chapter Three

Experiments for Spintronics



III-1. Bulk

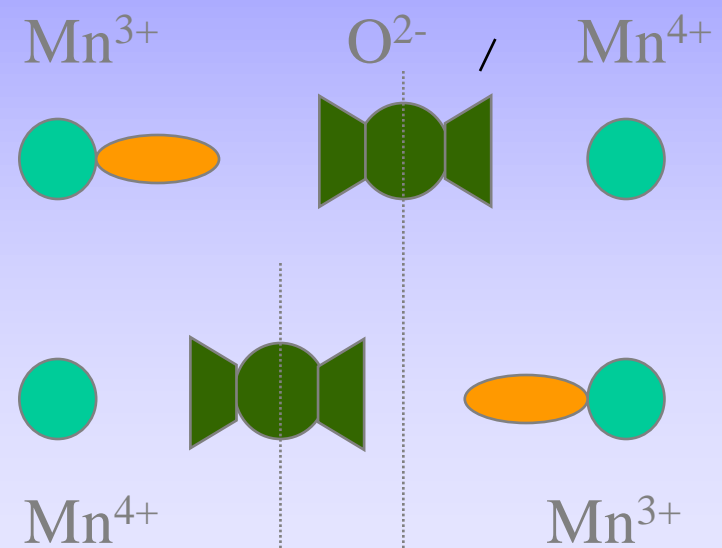
Phase separation

--- fine tuning the MR value by
Ionic radius size



Key parameters

- hole concentration
(charge/orbital/spin)
- radius of A-site
(lattice/ spin)





Bulk Making



Step 1 Pre-heating R_2O_3 : 900°C / 3 h .

Step 2 Mix R_2O_3 , CaCO_3 , SrCO_3 , MnCO_3

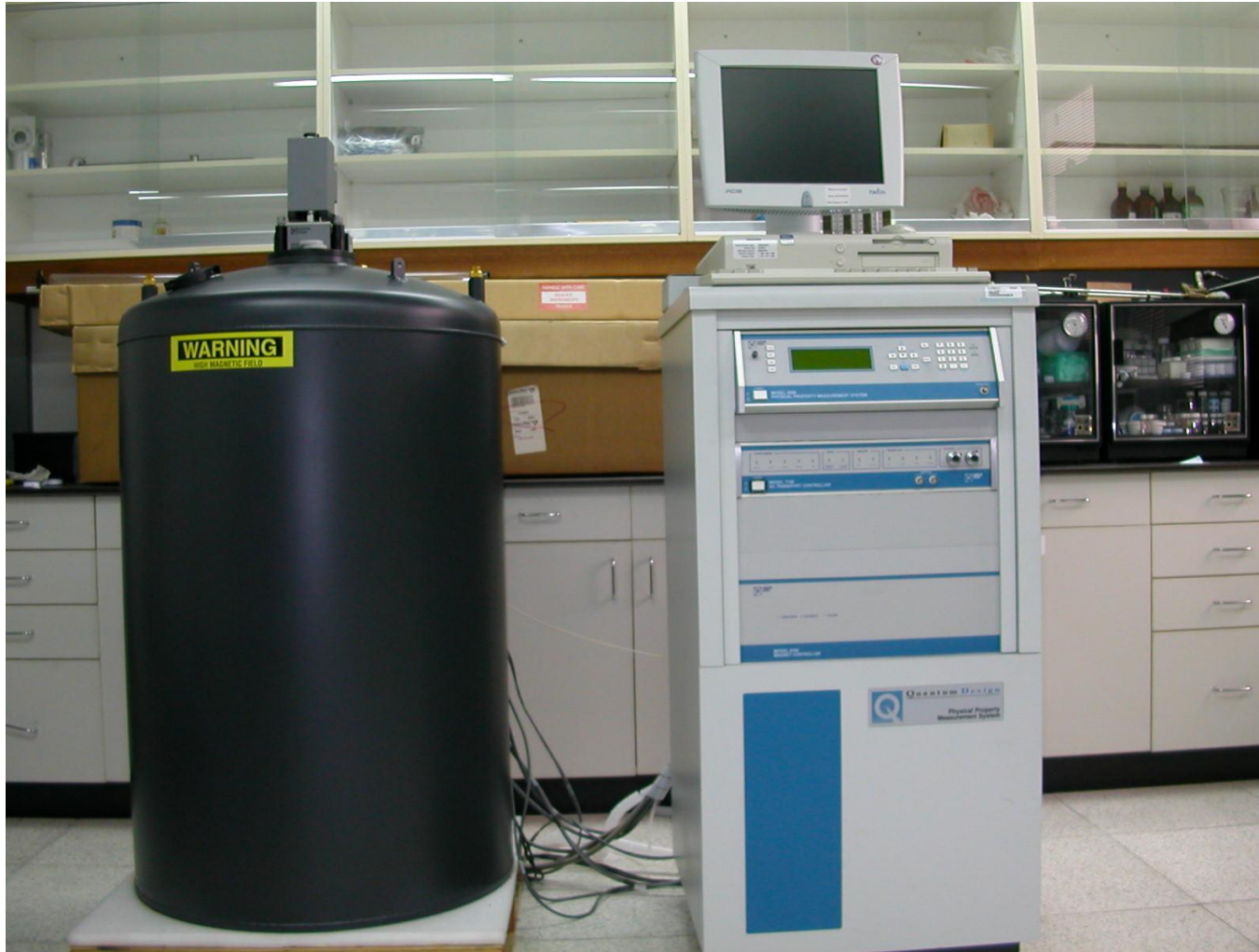
Step 3 Reaction: 1200°C / 24 h

Step 4 Pellet : $d = 1 \text{ cm}$, Thickness = 3 mm , 3 tons/cm^{-2}

Step 5 Anneal: 1400°C /16 h



Physical Property measurement System (PPMS)

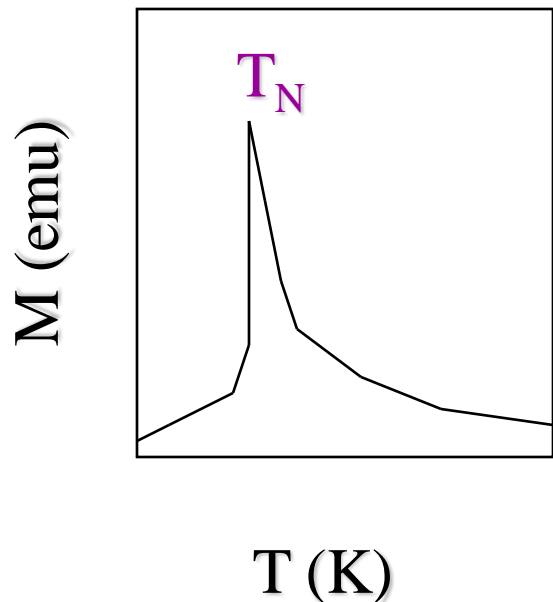


0 – 7 Tesla
1.4 – 400 K
Hall effect
resisitiviy
AC susceptibility

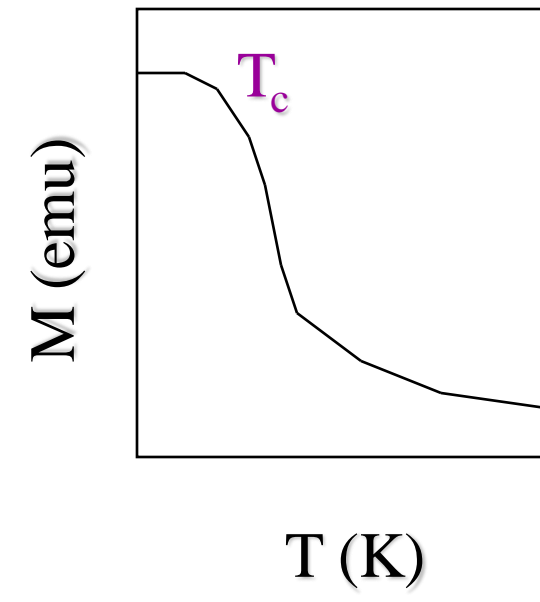


Basic M – T curve

Para- to antiferromagnetic



Para- to ferromagnetic



$$M \sim C/T, C/(T+T_N), C/(T-T_c)$$

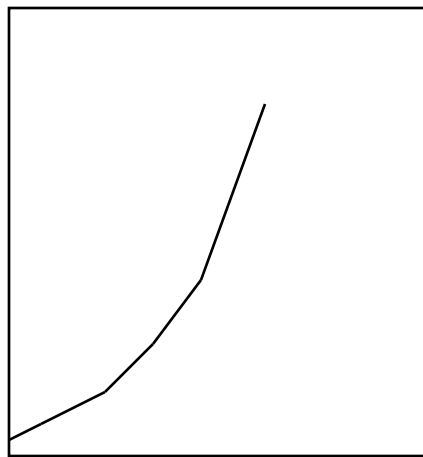


Basic R – T curve

$$\rho = \rho_0 + \rho_1 T^\alpha$$

metal

$$\rho \text{ (ohm-cm)}$$

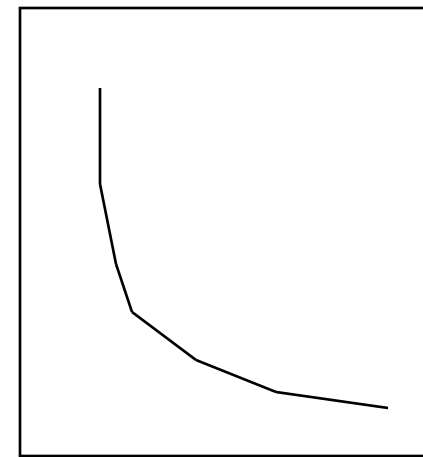


$$T \text{ (K)}$$

$$\rho = \rho_0 \exp(C/T^\beta)$$

insulator

$$\rho \text{ (ohm-cm)}$$

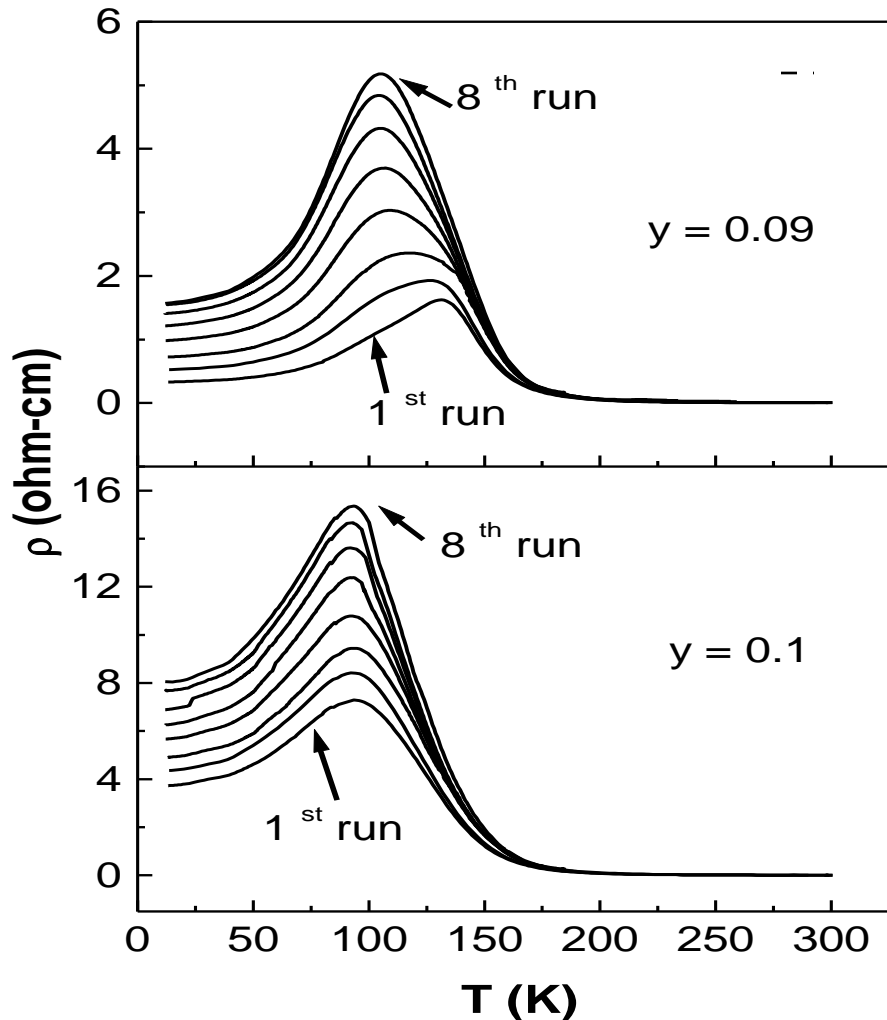


$$T \text{ (K)}$$

Thermal and magnetic instability near the percolation threshold of $\text{Nd}_{0.5}\text{Ca}_{0.5-y}\text{Sr}_y\text{MnO}_3$

C. W. Chang,* A. K. Debnath,† and J. G. Lin‡

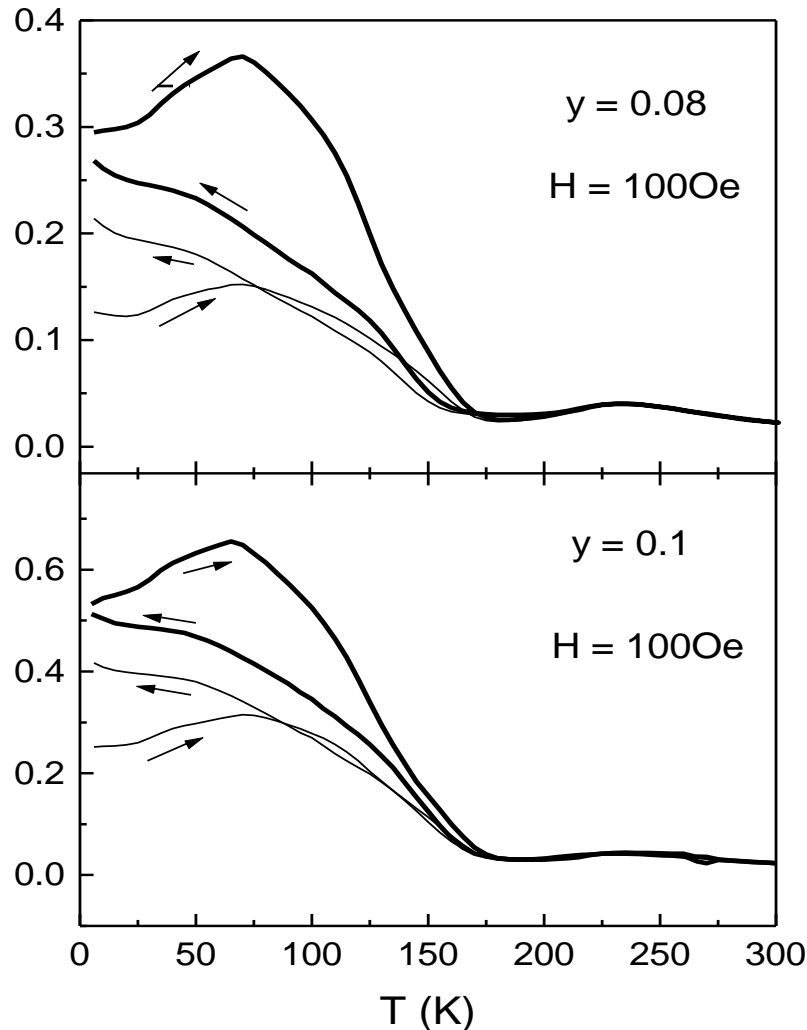
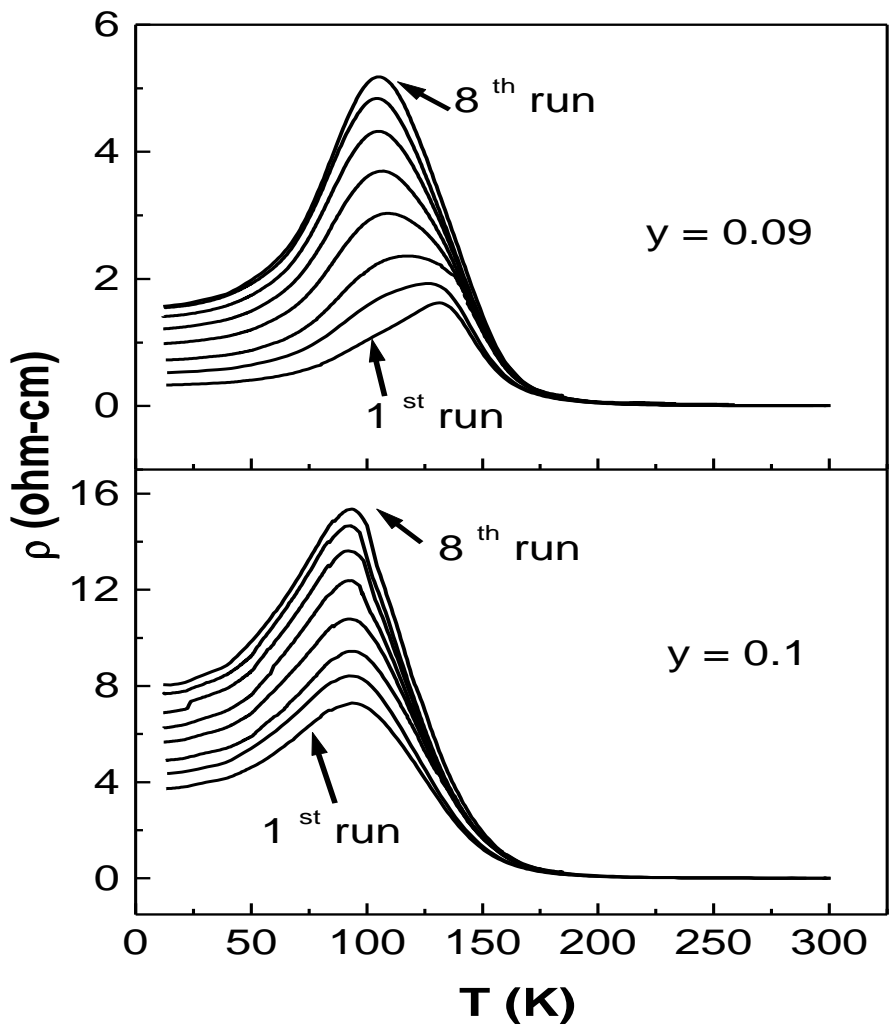
Center for Condensed Matter Science, National Taiwan University, Taipei, Taiwan



**Thermal and magnetic instability near the percolation threshold of
 $\text{Nd}_{0.5}\text{Ca}_{0.5-y}\text{Sr}_y\text{MnO}_3$**

C. W. Chang,* A. K. Debnath,[†] and J. G. Lin[‡]

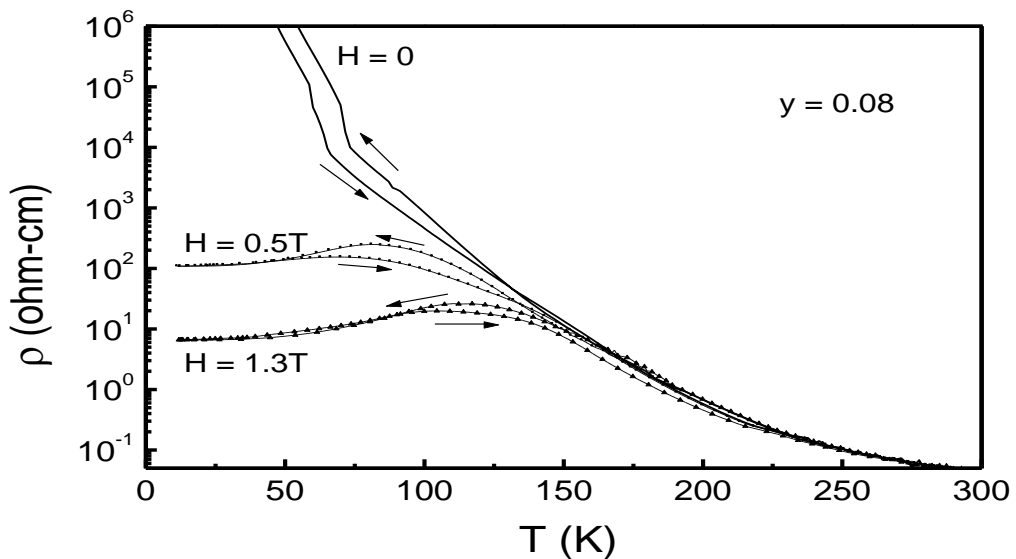
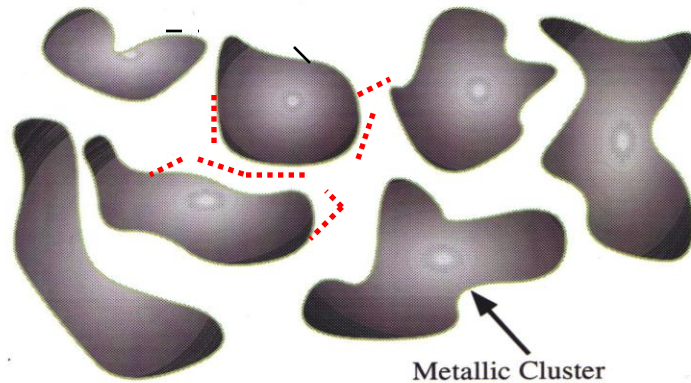
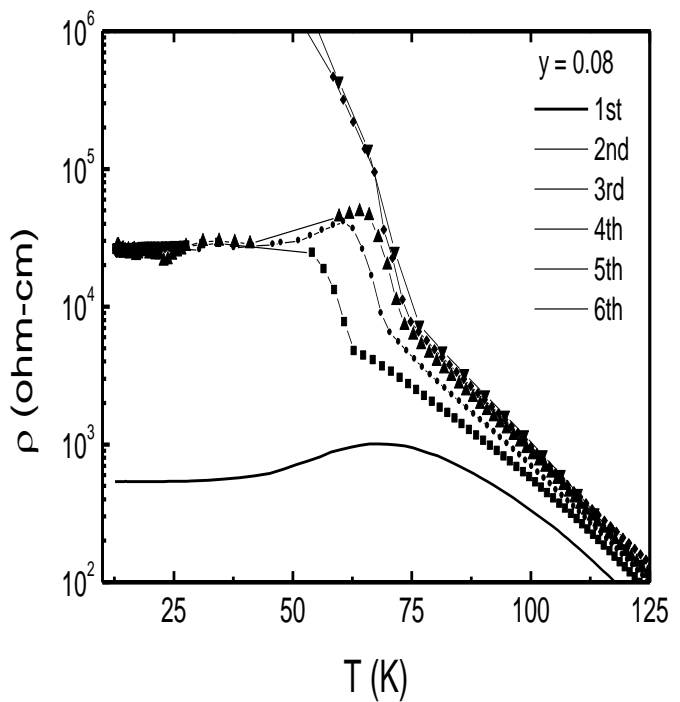
Center for Condensed Matter Science, National Taiwan University, Taipei, Taiwan



Termal and magnetic instability near the percolation threshold of $\text{Nd}_{0.5}\text{Ca}_{0.5-y}\text{Sr}_y\text{MnO}_3$

C. W. Chang,* A. K. Debnath,[†] and J. G. Lin[‡]

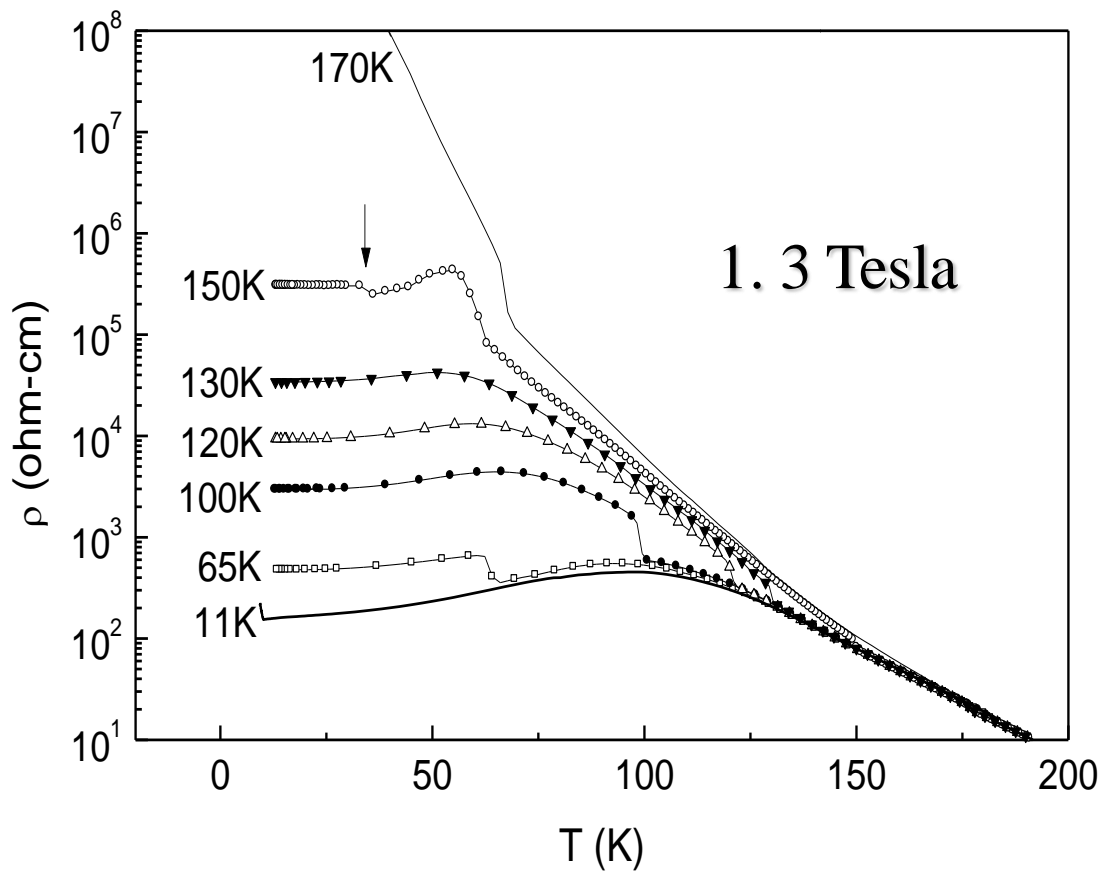
Center for Condensed Matter Science, National Taiwan University, Taipei, Taiwan



Thermal and magnetic instability near the percolation threshold of $\text{Nd}_{0.5}\text{Ca}_{0.5-y}\text{Sr}_y\text{MnO}_3$

C. W. Chang,* A. K. Debnath,† and J. G. Lin‡

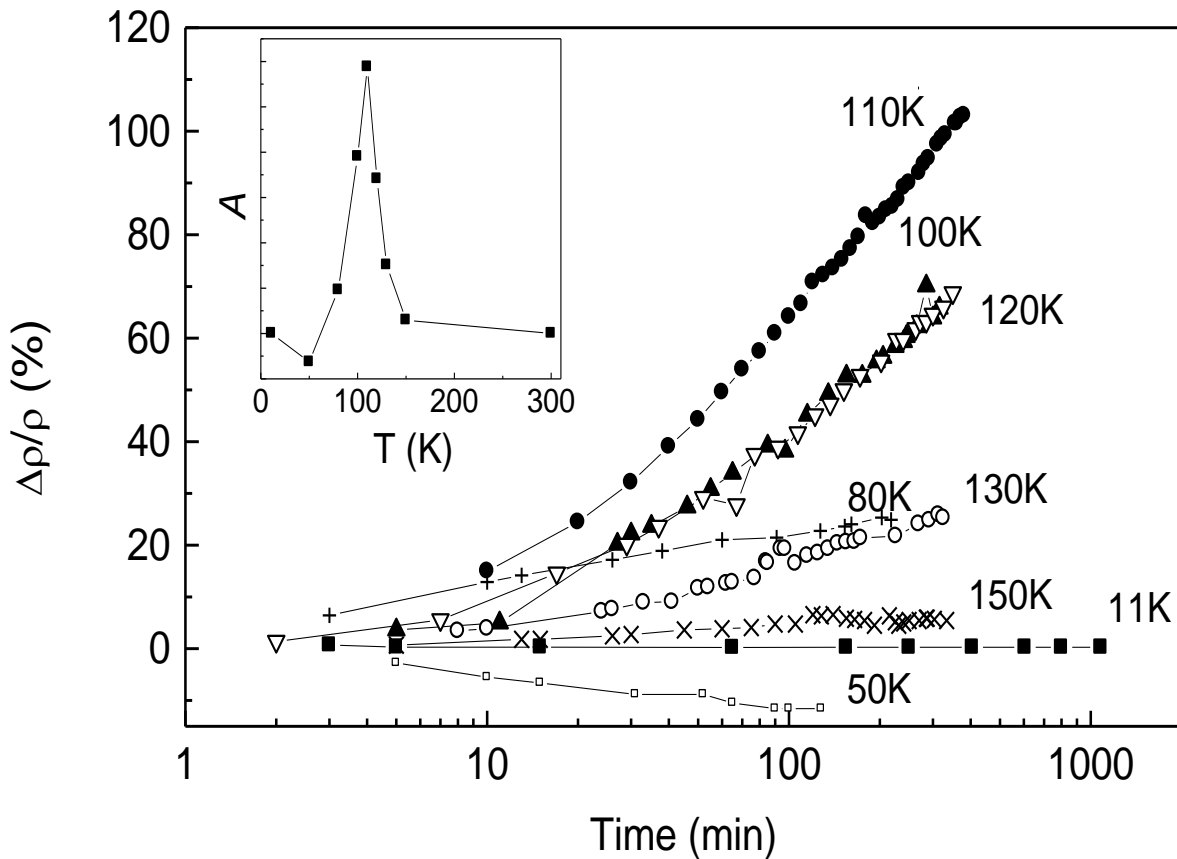
Center for Condensed Matter Science, National Taiwan University, Taipei, Taiwan



Thermal and magnetic instability near the percolation threshold of $\text{Nd}_{0.5}\text{Ca}_{0.5-y}\text{Sr}_y\text{MnO}_3$

C. W. Chang,* A. K. Debnath,[†] and J. G. Lin[‡]

Center for Condensed Matter Science, National Taiwan University, Taipei, Taiwan



$$\Delta\rho/\rho = A \ln t + \text{const.}$$

Enhancement of magnetoresistance in the intermediate state of $\text{Pr}_{0.5}\text{Sr}_{0.3}\text{Ca}_{0.2}\text{MnO}_3$

C. W. Chang and J. G. Lin

Center for Condensed Matter Science, National Taiwan University, Taipei, Taiwan 10764

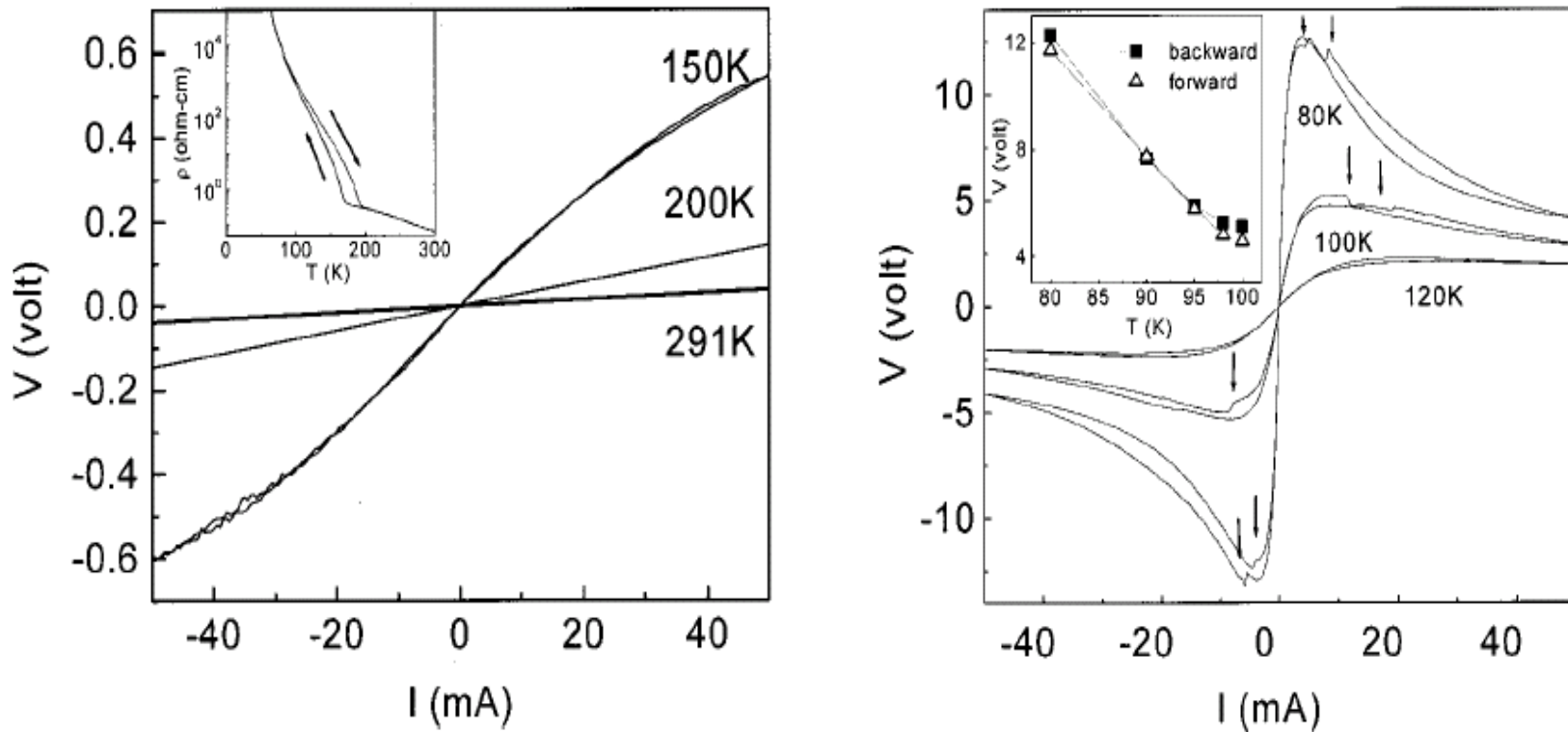
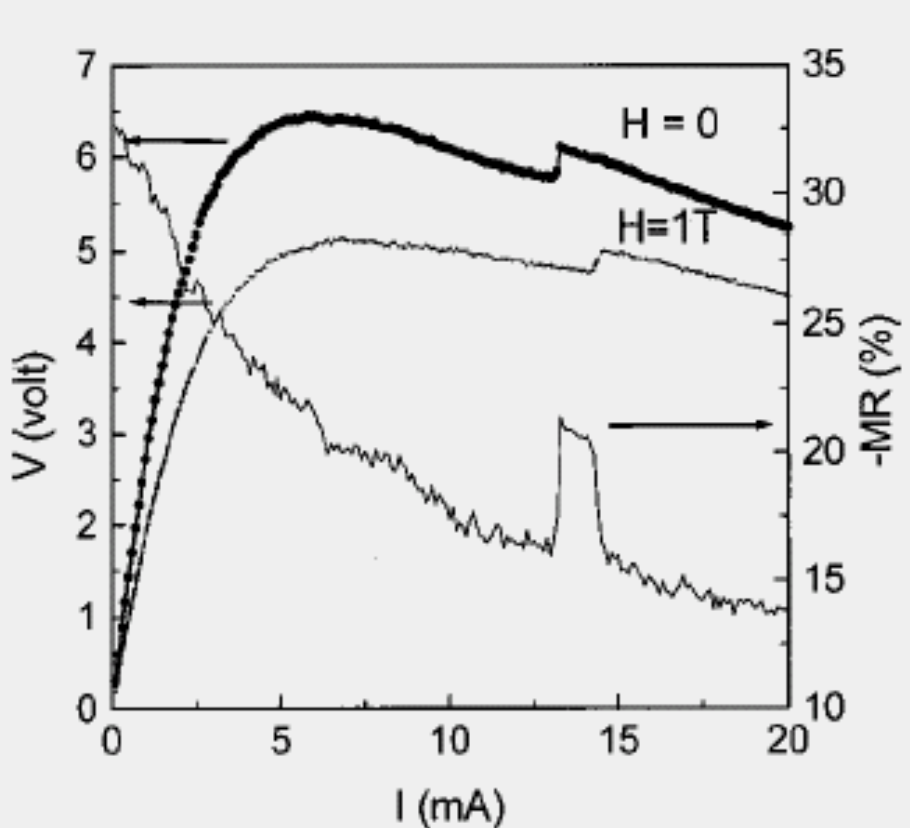


FIG. 2. $I - V$ curves for $\text{Pr}_{0.5}\text{Sr}_{0.3}\text{Ca}_{0.2}\text{MnO}_3$ at 120, 100, and 80 K, respectively. The arrows denote the jumps of voltage. The inset shows the temperature dependence of the onset voltage of the jump with the forward scan (increasing) and the backward scan (decreasing).

Enhancement of magnetoresistance in the intermediate state of $\text{Pr}_{0.5}\text{Sr}_{0.3}\text{Ca}_{0.2}\text{MnO}_3$

C. W. Chang and J. G. Lin

Center for Condensed Matter Science, National Taiwan University, Taipei, Taiwan 10764



$$\text{MR} = \frac{R(H) - R(0)}{R(0)} = \frac{V(H) - V(0)}{V(0)},$$

FIG. 3. Current dependence of V and MR ratio at 95 K with different magnetic fields.

Enhancement of magnetoresistance in the intermediate state of $\text{Pr}_{0.5}\text{Sr}_{0.3}\text{Ca}_{0.2}\text{MnO}_3$

C. W. Chang and J. G. Lin

Center for Condensed Matter Science, National Taiwan University, Taipei, Taiwan 10764

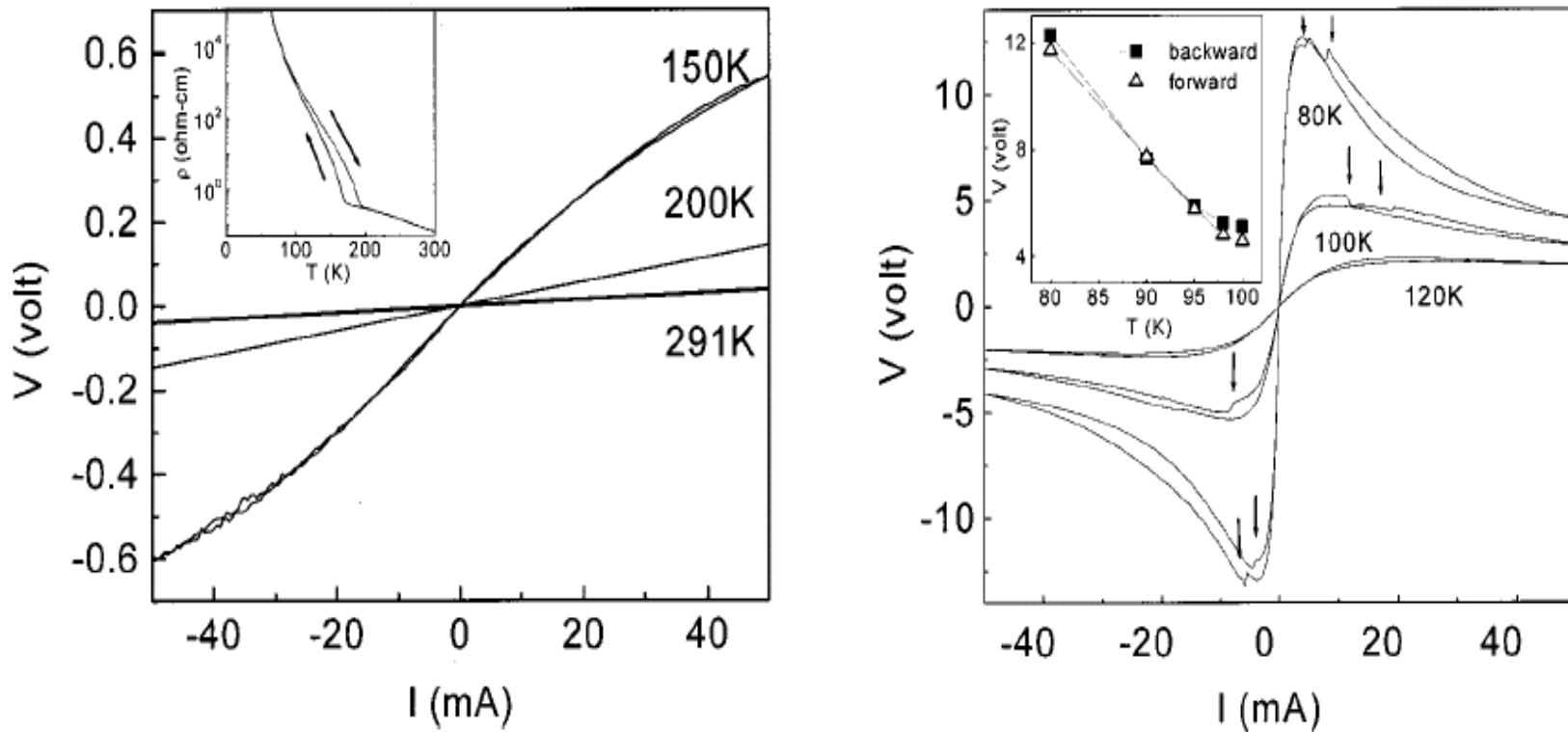


FIG. 2. $I - V$ curves for $\text{Pr}_{0.5}\text{Sr}_{0.3}\text{Ca}_{0.2}\text{MnO}_3$ at 120, 100, and 80 K, respectively. The arrows denote the jumps of voltage. The inset shows the temperature dependence of the onset voltage of the jump with the forward scan (increasing) and the backward scan (decreasing).



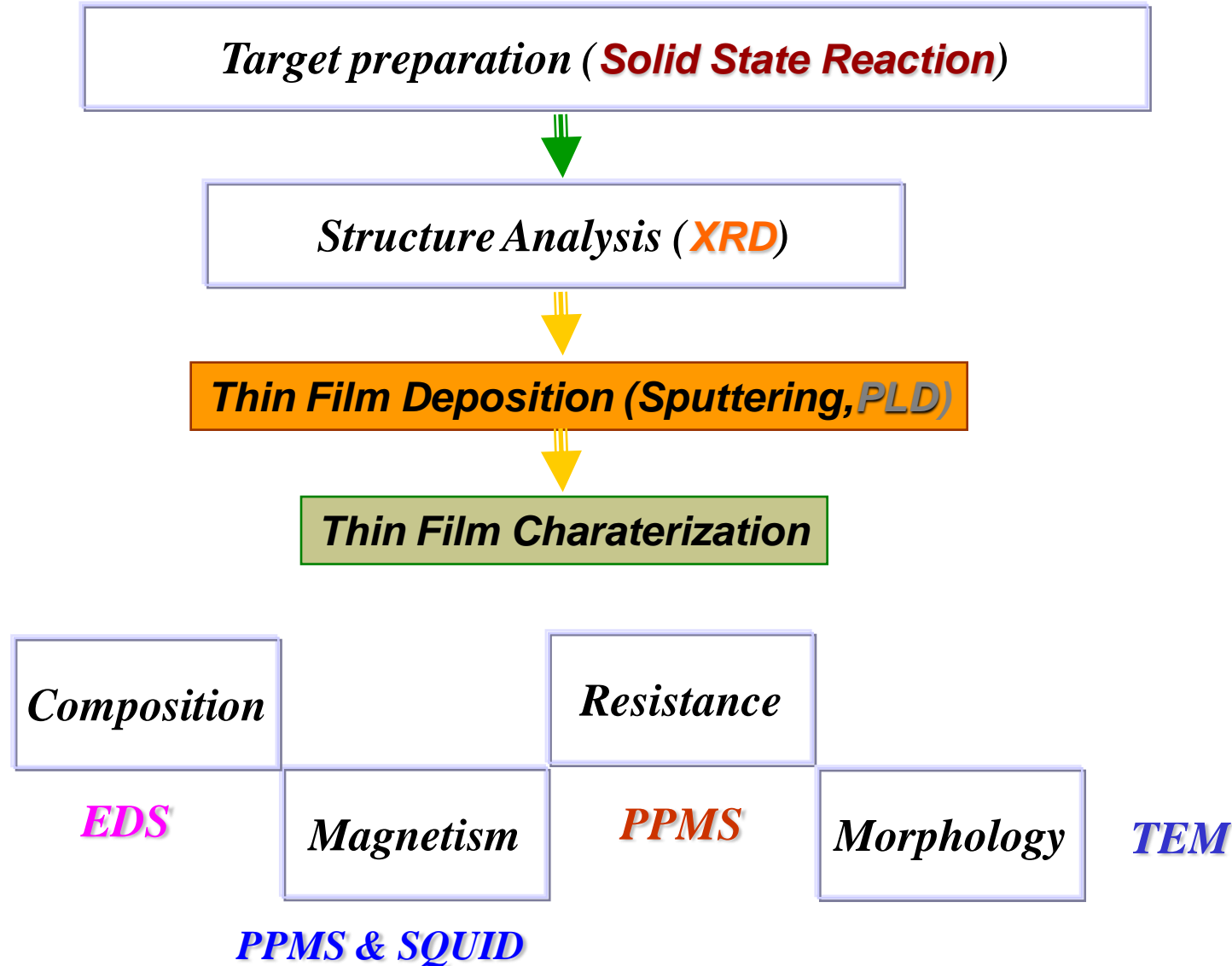
III-2 films & bilayers



Subject (1): Nanocrystalline LSMO films

--- High electroresistance
& low field MR effects

Experiment Flow Chart





Target preparation

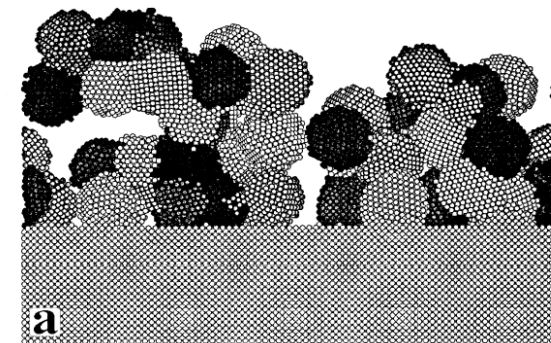
- ❖ $\text{Nd}_{0.7}\text{Ca}_{0.3}\text{MnO}_3$ (NCMO):

Nd_2O_3 , CaCO_3 , MnCO_3 Powder
100°C (3 hrs.) in air
1100°C (24 hrs.) in air

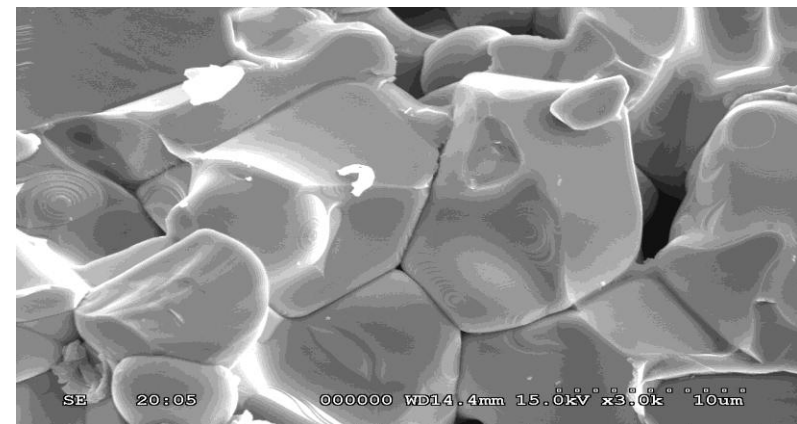
- ❖ $\text{YBa}_2\text{Cu}_3\text{O}_7$ (YBCO)

Y_2O_3 , BaCO_3 , CuO_2 Powder
100°C (3 hrs.) in air
1050°C (36 hrs.) in oxygen
400°C (12 hrs.) in oxygen

Powders



Solid state reaction



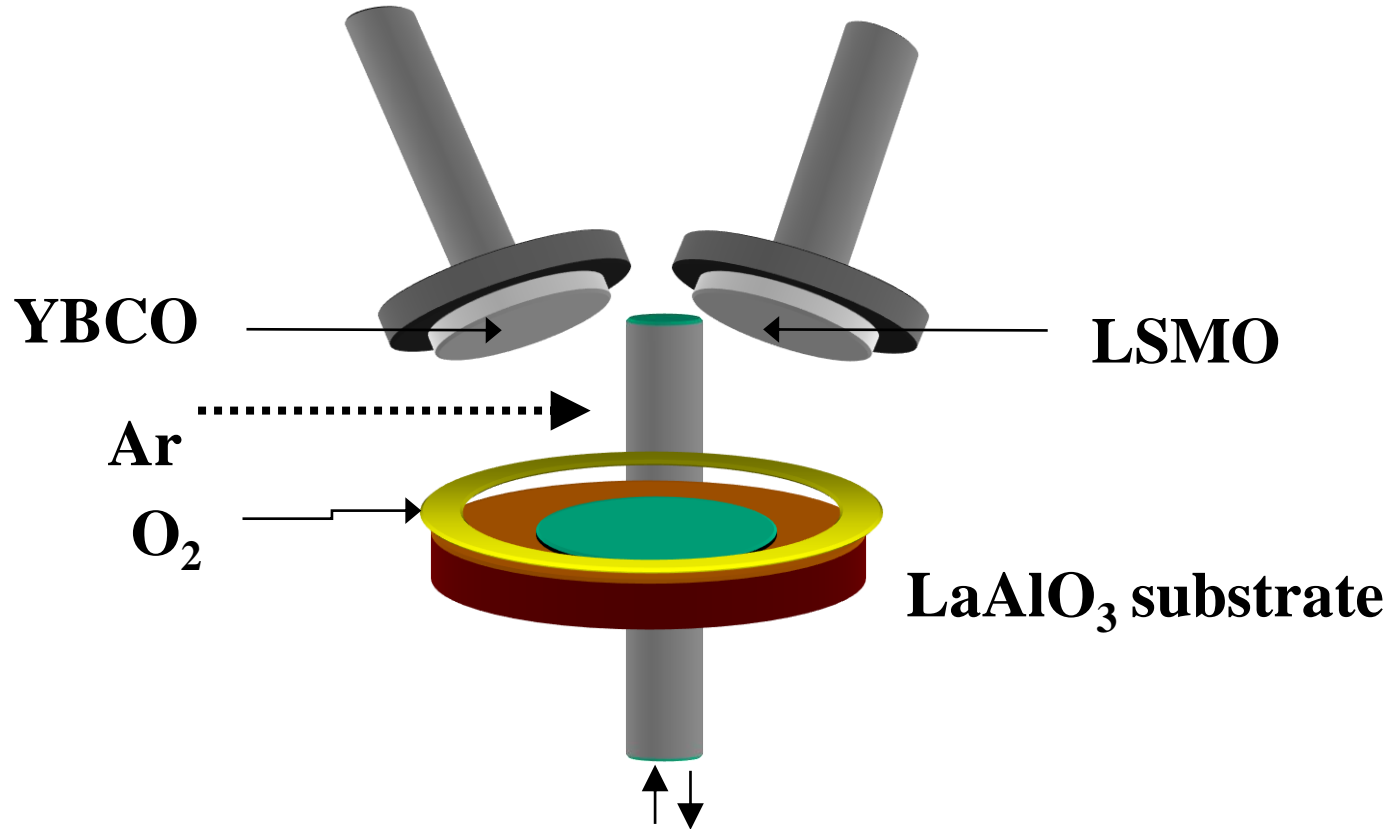


RF sputter system (Millton CVT, 13.6 MHz)



10^{-8} torr
four guns
 1000°C

Film making

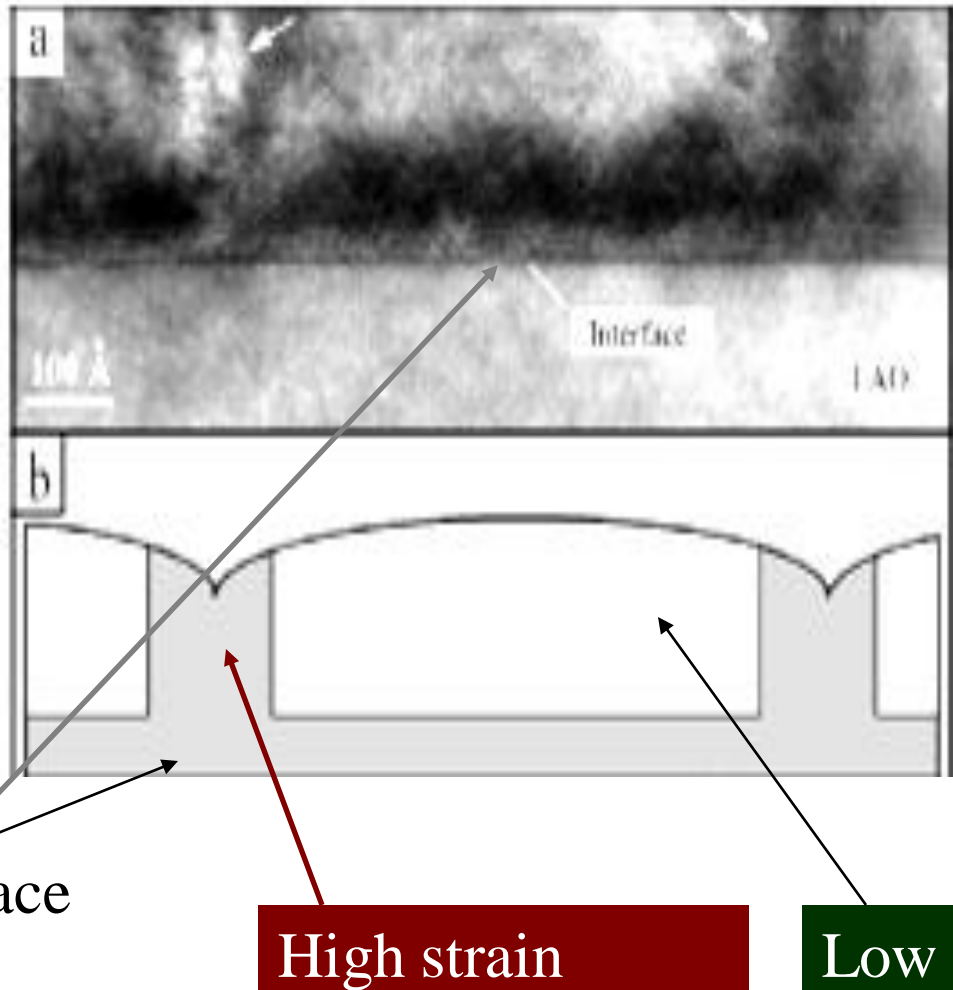


Reactive co-sputtering process

• Substrate ⇒	Si (100) , LaAlO₃(100)
• Target ⇒	YBCO, LSMO
• RF power ⇒	80 Watt
• Base pressure ⇒	3 × 10⁻⁷ torr
• Mixed gas ⇒	Ar:O₂=98:2
• Sputtering pressure	70 mtorr
• Base temperature ⇒	Room temperature
• pre-sputtering ⇒	3 minutes
• Working distance ⇒	10 cm
• Annealing tempert.	800 – 920 °C (700 °C)
• Annealing time ⇒	1 hrs



Non-uniform strain in $\text{La}_{0.67}\text{Ca}_{0.33}\text{MnO}_3$ film



Lattice parameter a

$\text{LCMO}=3.86\text{\AA}$

$\text{NGO}(110)=3.86 \text{ \AA} \text{ (no strain)}$

$\text{LAO}(100)=3.79 \text{ \AA} \text{ (Compressive)}$

$\text{STO}(100)=3.91 \text{ \AA} \text{ (Tensile)}$

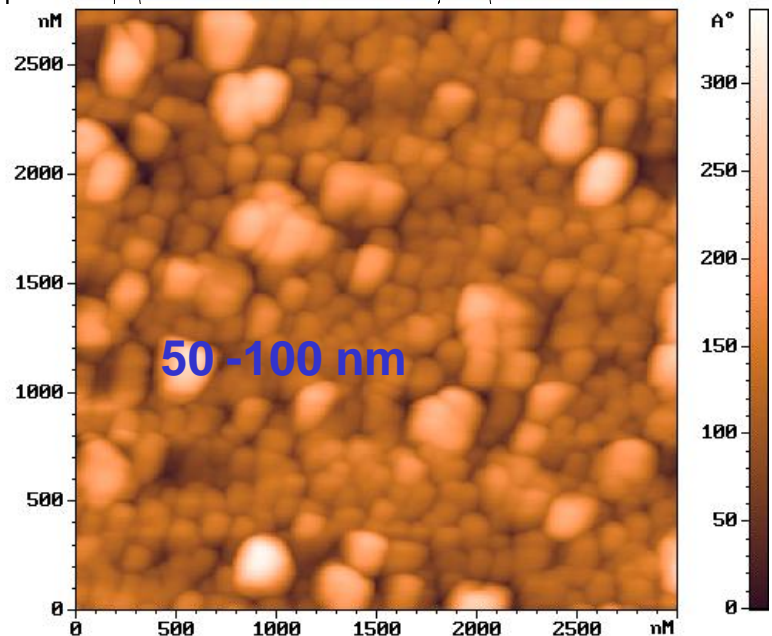
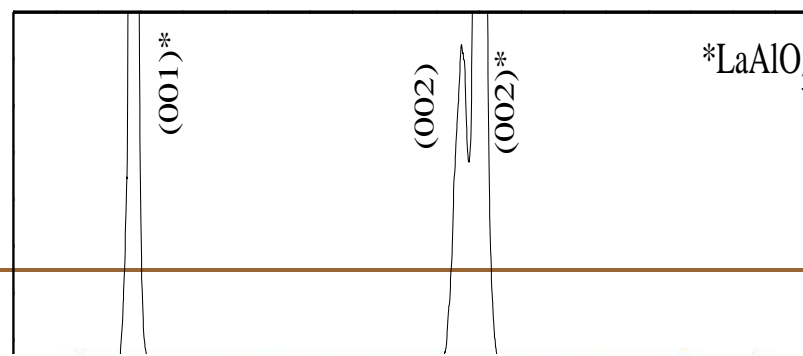
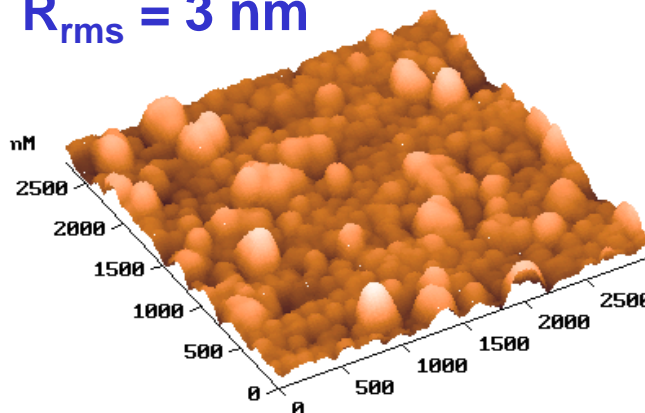
Structures of LSMO layer

XRD – monoclinic
c-oriented



AFM - granular

$R_{rms} = 3 \text{ nm}$

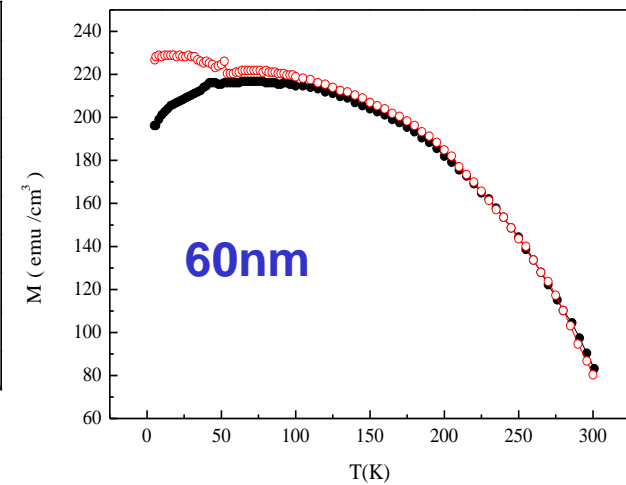
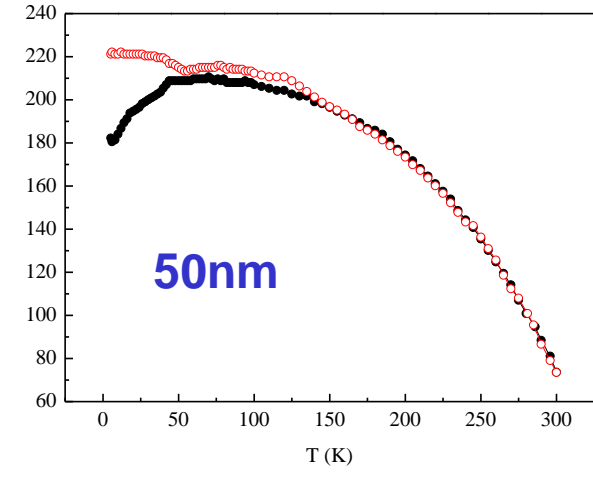
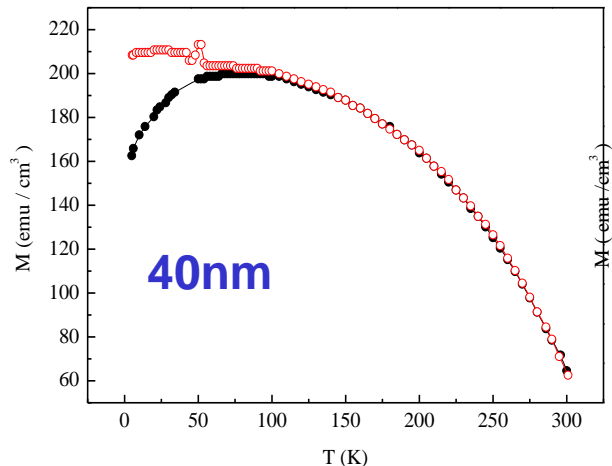
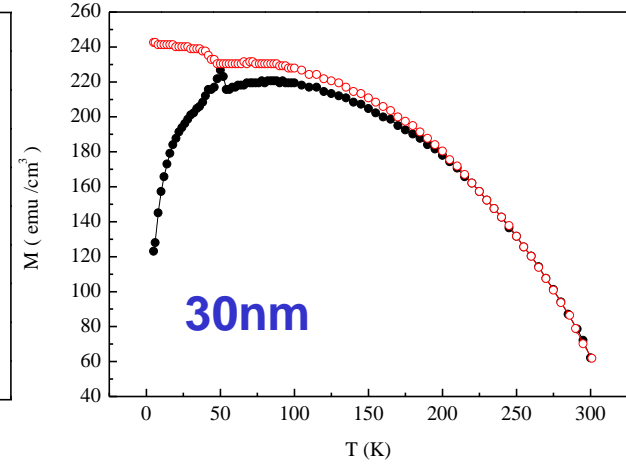
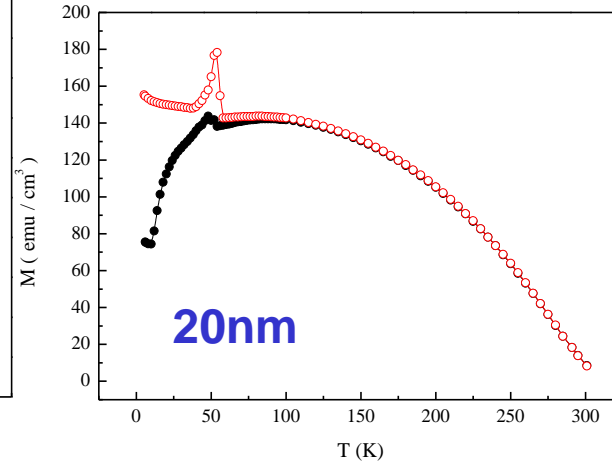
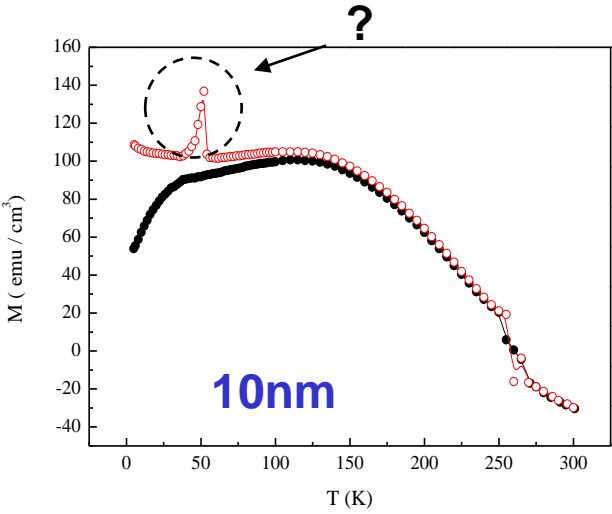


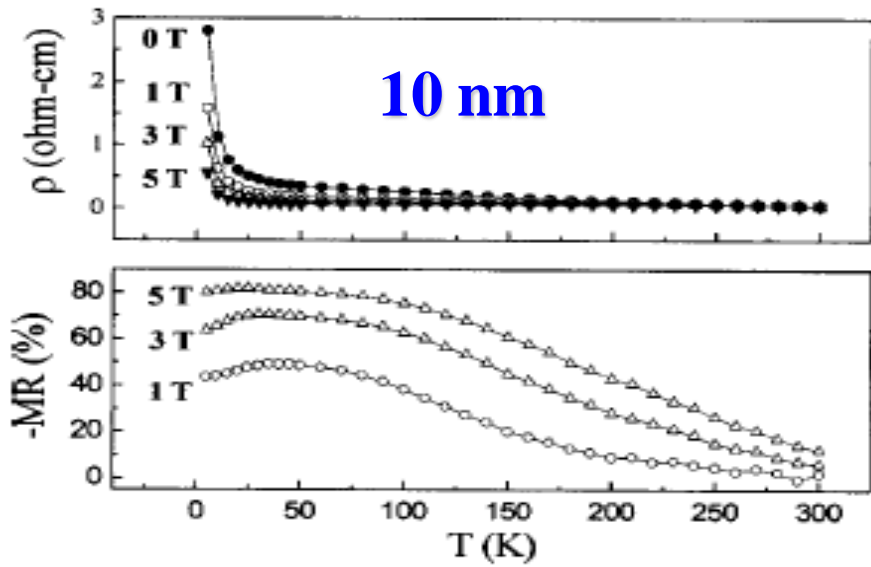
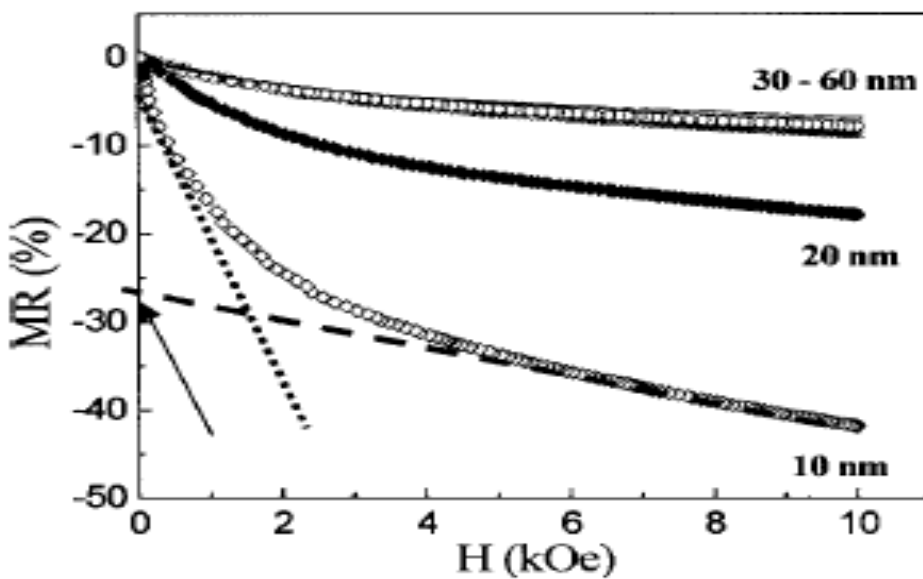
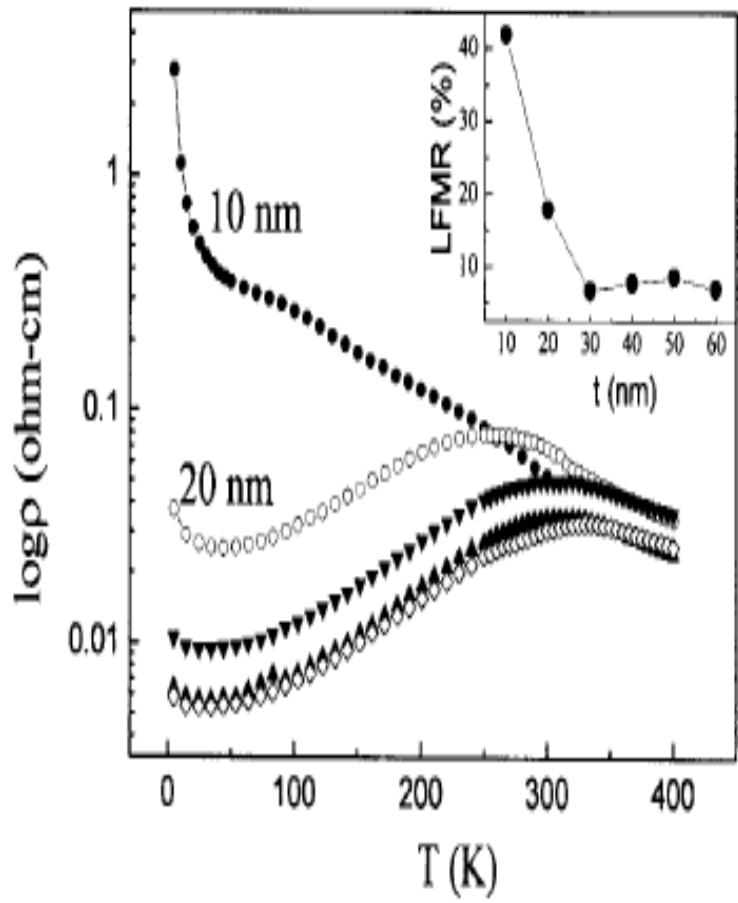


Magnetization for LSMO

H=500 Gauss

ZFC(black line); FC (red line)





Low-field magnetoresistance in nanocrystalline $\text{La}_{0.7}\text{Sr}_{0.3}\text{MnO}_3$ films

S. L. Cheng and J. G. Lin^{a)}

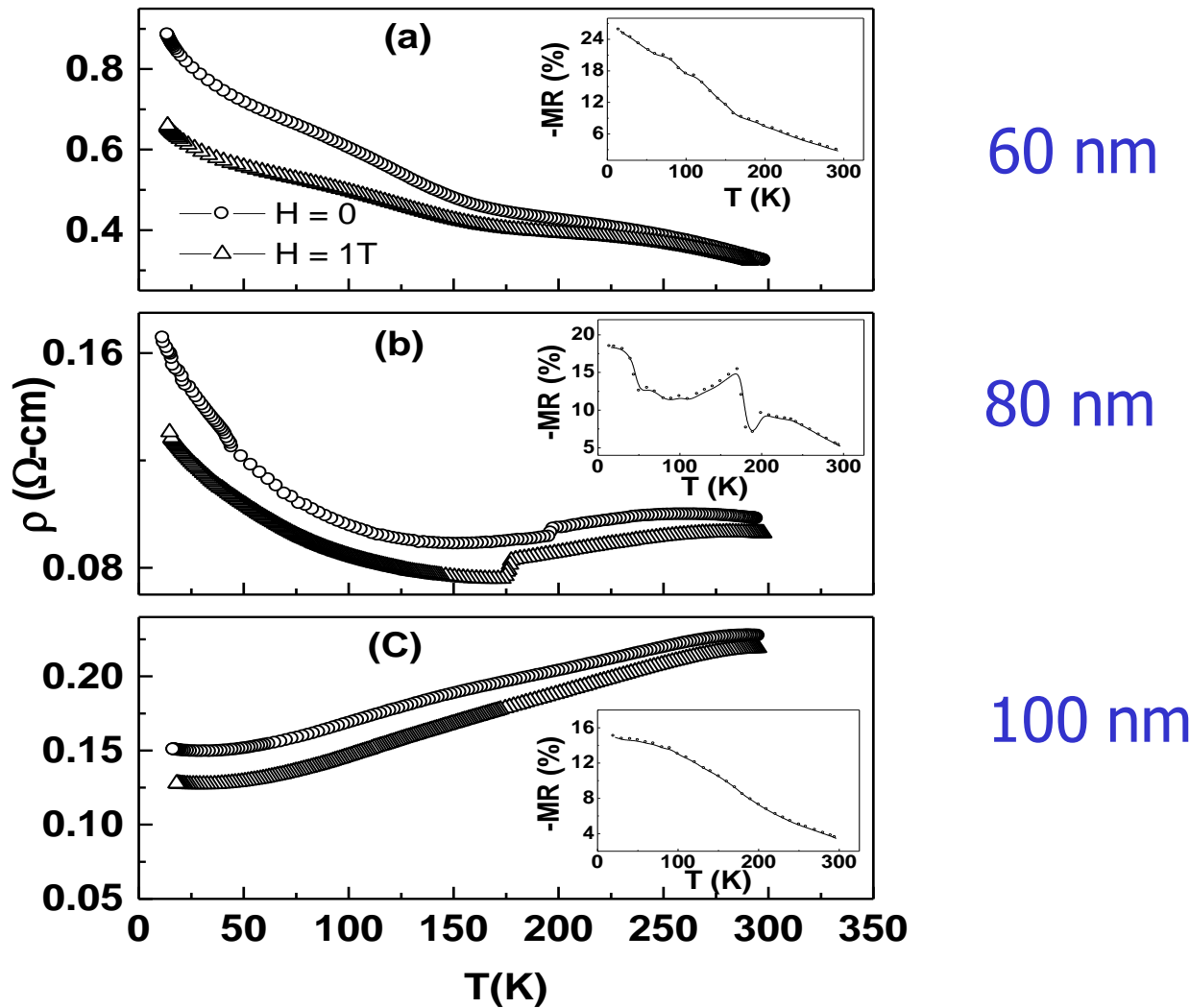
Center for Condensed Matter Sciences/Center for Nanostorage Research, National Taiwan University, Taipei 106, Taiwan

(Received 28 March 2005; accepted 1 November 2005; published online 14 December 2005)

Nanocrystalline $\text{La}_{0.7}\text{Sr}_{0.3}\text{MnO}_3$ films with thickness $t=10\text{-}60\text{ nm}$ were grown on $\text{LaAlO}_3(100)$ substrates by radio-frequency magnetron sputtering. Their electrical resistivity and low-field magnetoresistance (MR) were measured. Metal-insulator transitions occur above 275 K for films with $t=20\text{-}60\text{ nm}$, but the electron localization prevails in the 10 nm thick film. Furthermore, only the 10 nm thick film has an MR that depends on the inverse of temperature, consistent with the model of spin-polarized tunneling. This relationship may reflect a critical aspect of the structure of grain/grain-boundaries. Accordingly, the tunneling MR in this film is 27% at 75 K. © 2005 American Institute of Physics. [DOI: [10.1063/1.2140081](https://doi.org/10.1063/1.2140081)]

Current-induced giant electroresistance in La_{0.7}Sr_{0.3}MnO₃ thin films

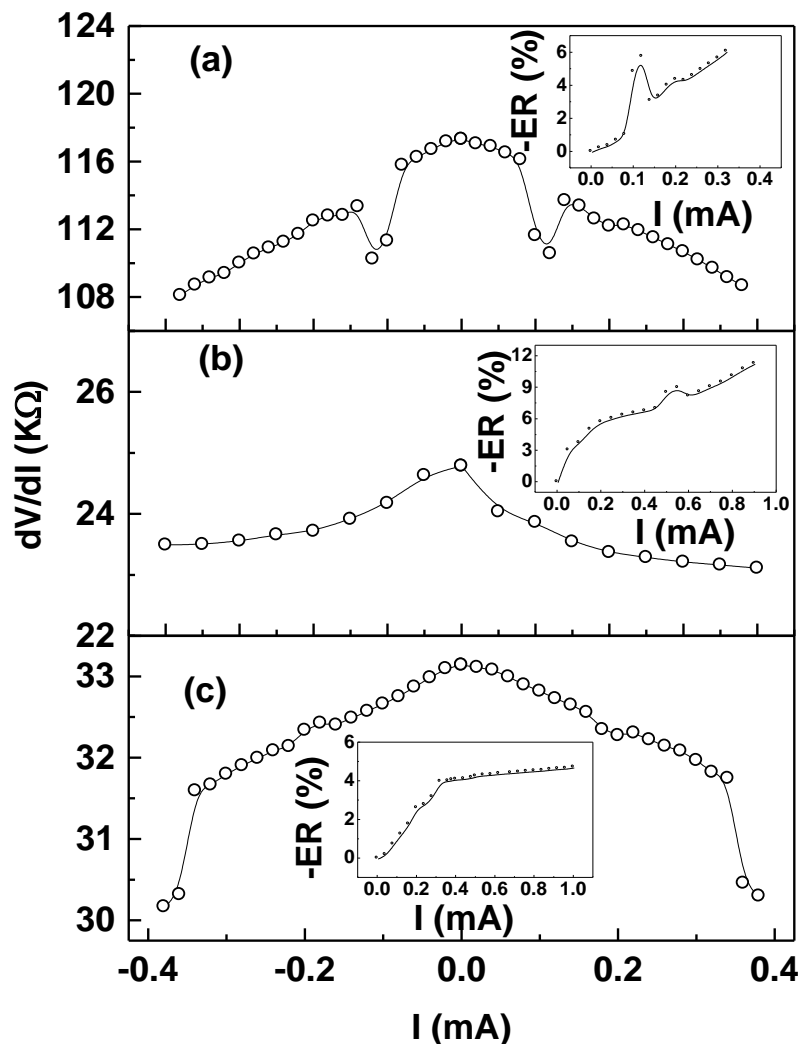
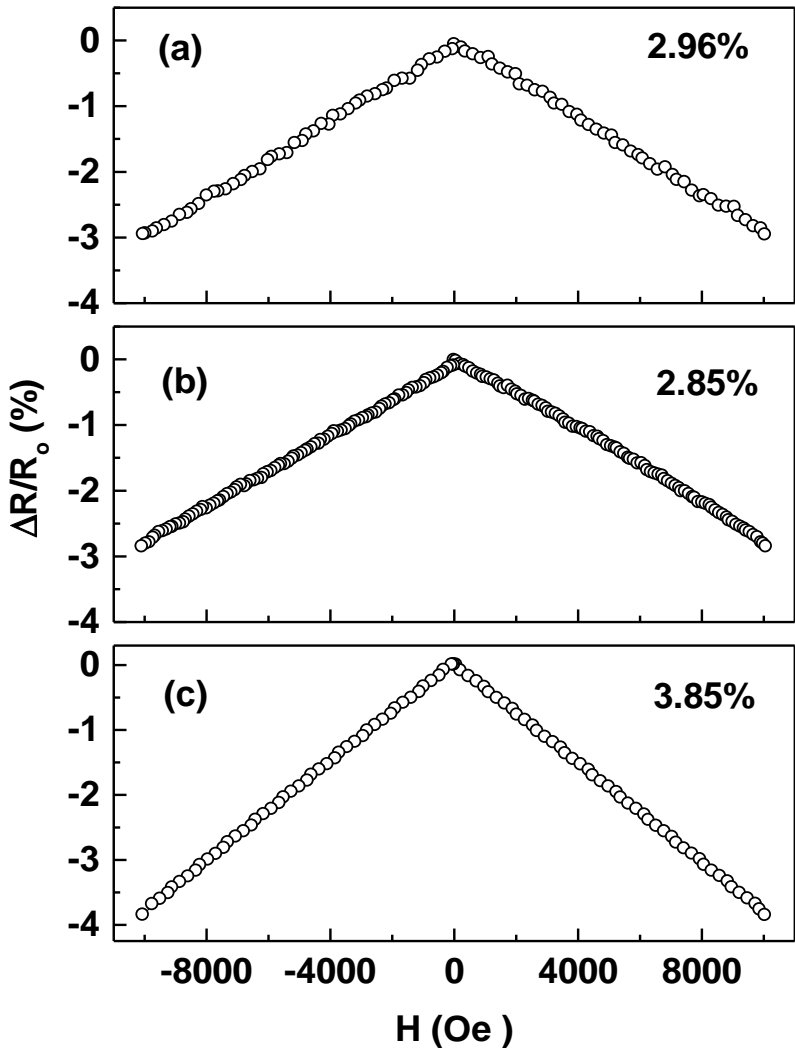
A. K. Debnath* and J. G. Lin†

Center for Condensed Matter Sciences, National Taiwan University, Taipei 10617, Taiwan

Current-induced giant electroresistance in La_{0.7}Sr_{0.3}MnO₃ thin films

A. K. Debnath* and J. G. Lin†

Center for Condensed Matter Sciences, National Taiwan University, Taipei 10617, Taiwan



Current-induced giant electroresistance in La_{0.7}Sr_{0.3}MnO₃ thin films

A. K. Debnath* and J. G. Lin†

Center for Condensed Matter Sciences, National Taiwan University, Taipei 10617, Taiwan

Current in nanowire of LSMO induced magnetic field, and the thermal energy delocalized the electrons.

thickness (nm)	MR_H (%)	MR_I (%)	ratio
60	2.96	5.6 (I = 0.3)	1.9
80	2.85	6.4 (I = 0.3)	2.3
		11.3 (I = 0.9)	4.0
100	3.85	3.5 (I = 0.3)	0.9
		4.6 (I = 0.9)	1.2

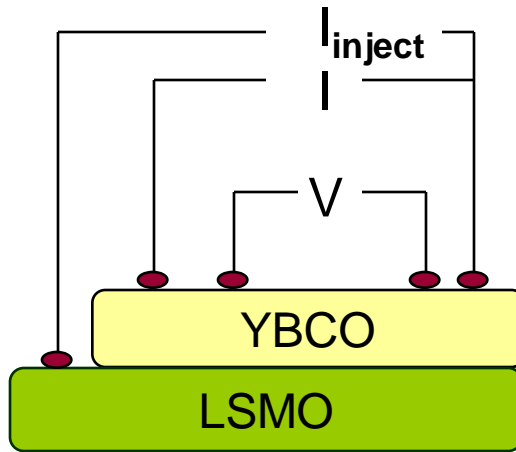


Subject (2): Nanocrystalline YBCO/LSMO
bilayers

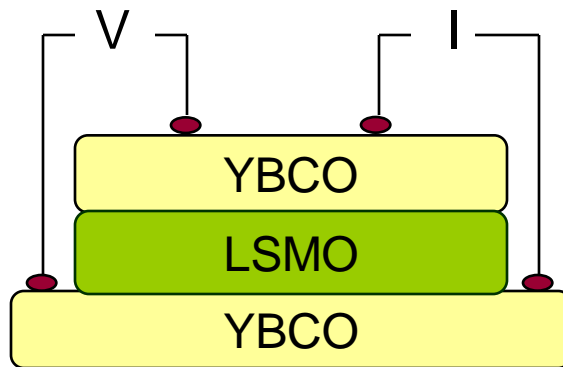
--- Proximity effect, spin injection
& vortex pinning



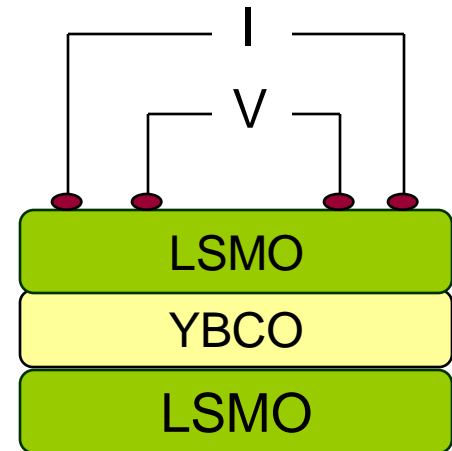
Multilayer spintronic devices



Spin-injection
 I_c - depression



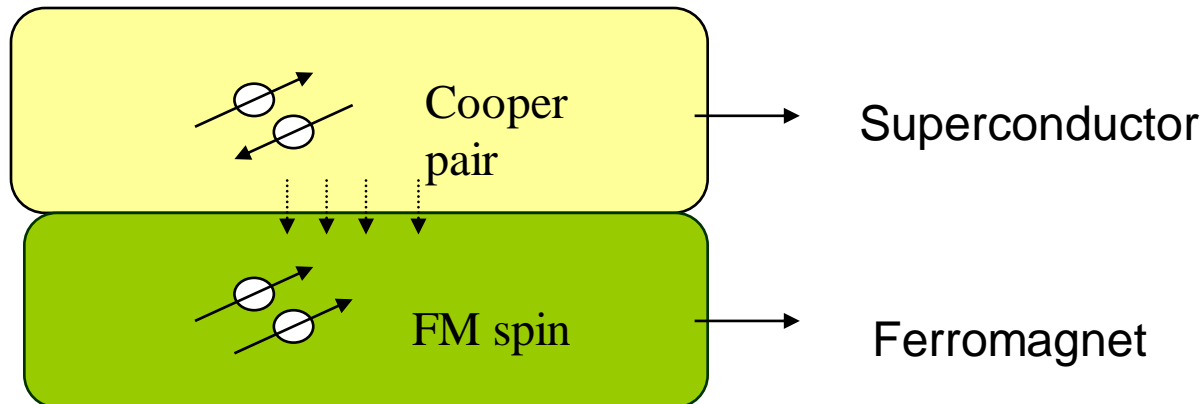
proximity effect
 T_c - depression



FM/N/FM structure
MR enhancement



Interesting topics on YBCO/LSMO



- 1) Proximity effects**
- 2) Andreev reflection**
- 3) Spin injection**
- 4) Spin-accumulation**
- 5) π –phase shift**



Proximity effect

1) Influence of magnetism on supercond.

Intermixing \Rightarrow effective exchange field

$$H_{\text{effect}} = H_{\text{ex}} [d_F/(d_s+d_F)], T_c \text{ oscillation}$$

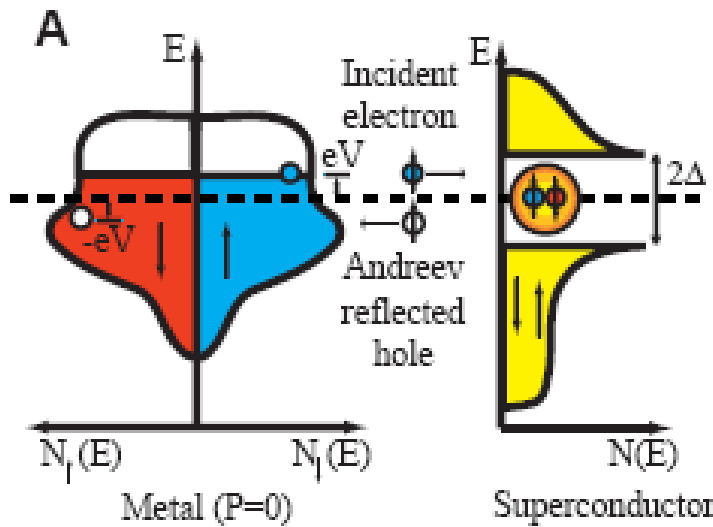
2) Influence of supercond. on magnetism

Intermixing \Rightarrow reconstruction of magnetic order

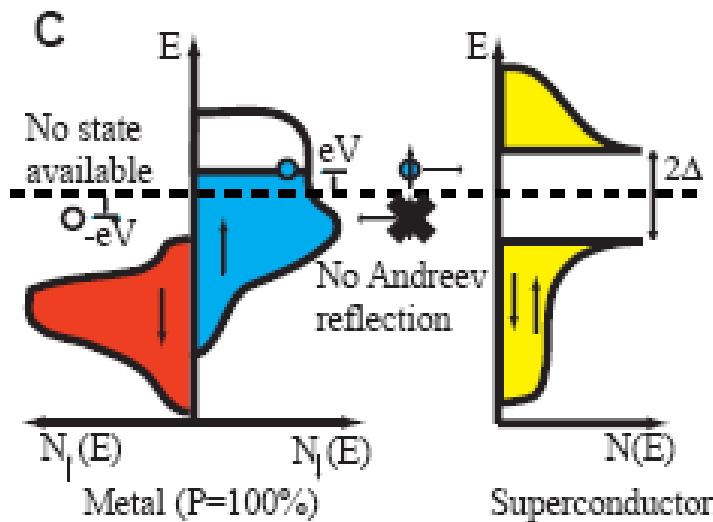
T_{curie} oscillation



Spin-injection

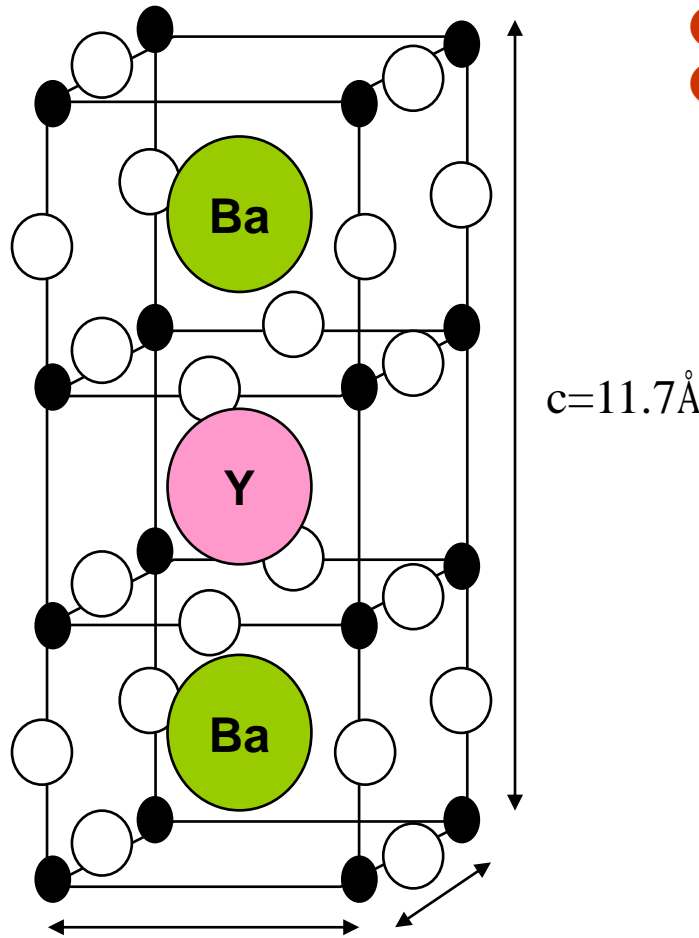


- Normal electron injected to superconductor will be reflected as a hole;
- Polarized electron injected into superconductor will kill a Cooper pair.

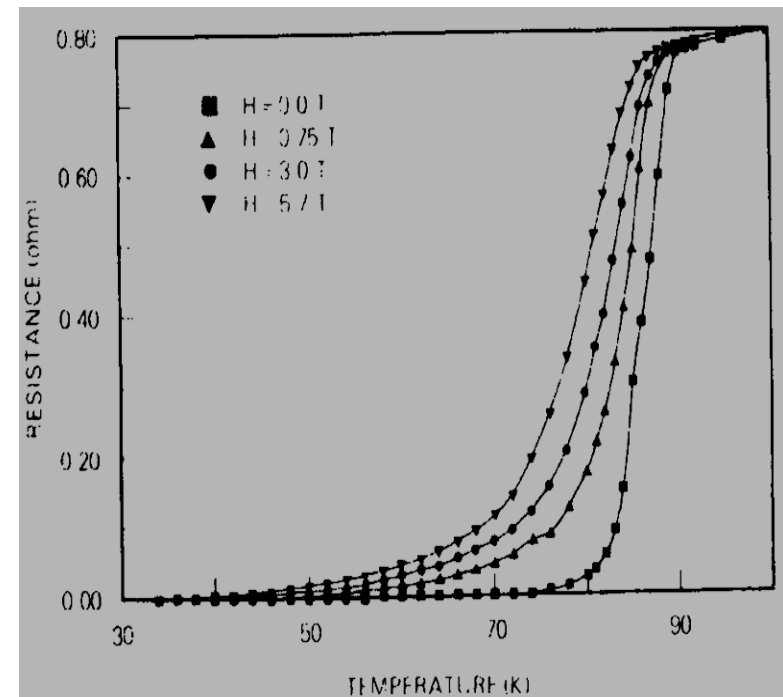




Superconductor: $\text{RBa}_2\text{Cu}_3\text{O}_7$, R = Y or rare earth element



- $\text{YBa}_2\text{Cu}_3\text{O}_7$ $\xi_S \sim 3\text{-}10 \text{ nm}$
- Critical parameter $T_c = 90 \text{ K}$, $H_{c2} \sim 165 \text{ T}$
- SQUID, Bolometer, Filter, Resonator...

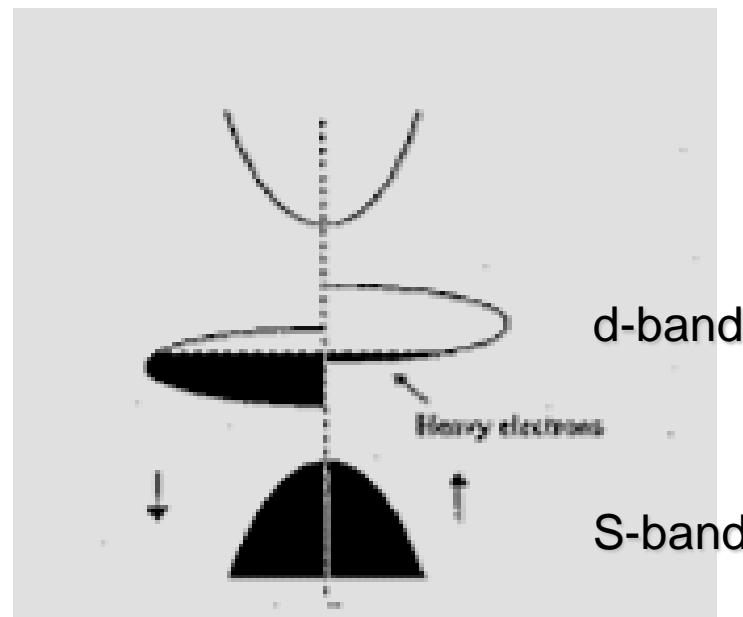
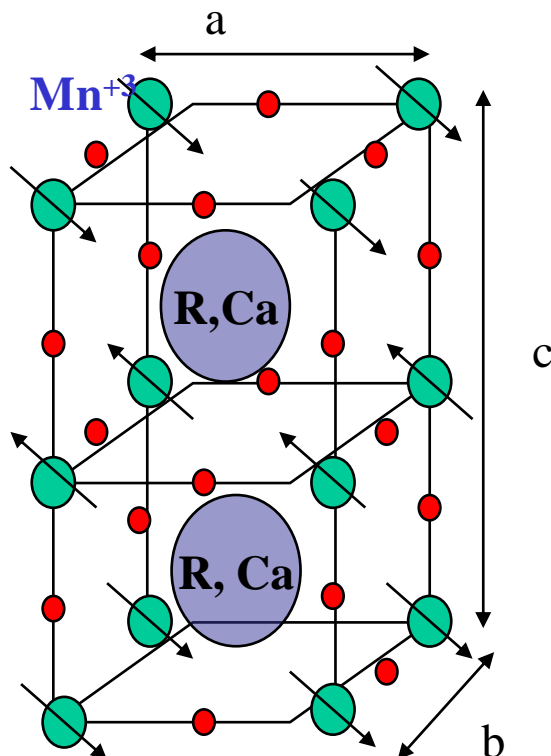


Wu, Chu et al., PRL (1987)



Half metal: $(R,Ca)MnO_3$, R = La, Nd, Pr....

- Ferromagnetic with 90 % polarization for LCMO. $\xi_M \sim 10 - 15$ nm
- Colossal magnetoresistance (CMR)
- Sensor, pick-up head, MRAM





Superconductivity depression in ultrathin $\text{YBa}_2\text{Cu}_3\text{O}_{7-\delta}$ layers in $\text{La}_{0.7}\text{Ca}_{0.3}\text{MnO}_3/\text{YBa}_2\text{Cu}_3\text{O}_{7-\delta}$ superlattices

Z. Sefrioui, M. Varela, V. Peña, D. Arias,^{a)} C. León, and J. Santamaría^{b)}

GFMC, Departamento de Física Aplicada III, U Complutense, 28040 Madrid, Spain

J. E. Villegas

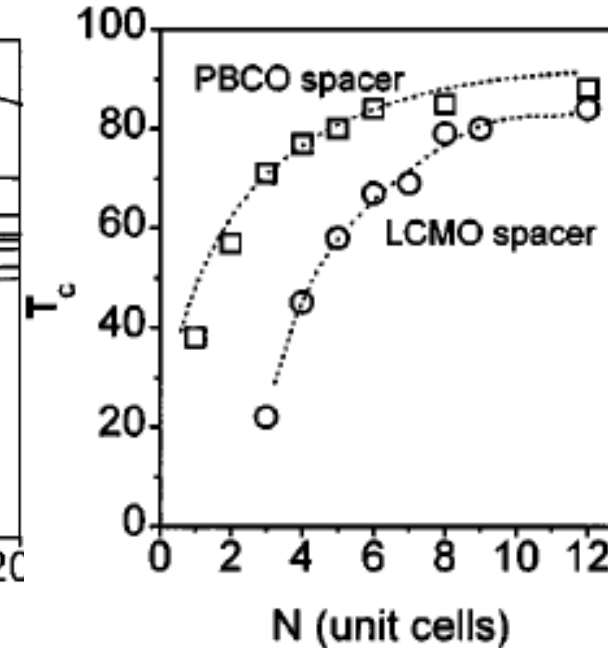
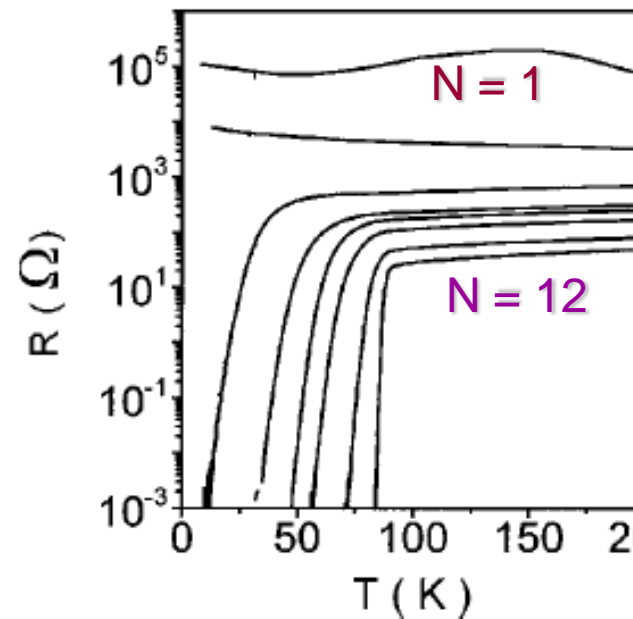
Departamento de Física de los Materiales, U. Complutense, 28040 Madrid, Spain

J. L. Martínez

Instituto de Ciencia de Materiales de Madrid (ICMM-CSIC), Cantoblanco 28049 Madrid, Spain

W. Saldarriaga and P. Prieto

Departamento de Física, Universidad del Valle A. A. 25360 Cali, Colombia



$\text{LCMO} = 15 \text{ unit cell} \sim 10 \text{ nm}$

$\text{N} = \text{unit cell of YBCO}$

$\text{N} = 3 \text{ to } 12$

$\sim 3.5 \text{ to } 14 \text{ nm}$

$\Delta T_c \sim 62 \text{ to } 2 \text{ K}$

$E_{\text{eff-ex}} \sim 0.74 \text{ to } 0.42 \text{ of } E_{\text{ex}}$

Superconducting and transport properties of $\text{YBa}_2\text{Cu}_3\text{O}_7/\text{La}_{0.7}\text{Sr}_{0.3}\text{MnO}_3$ bilayers

J. G. Lin^{a)} and S. L. Cheng

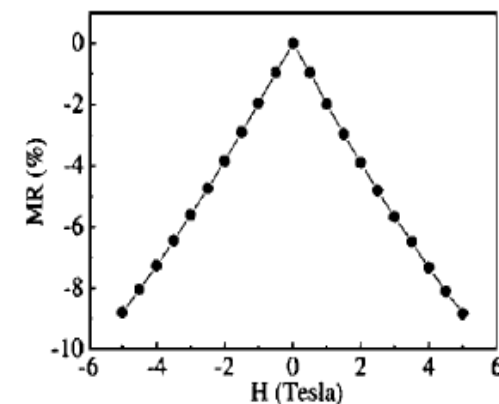
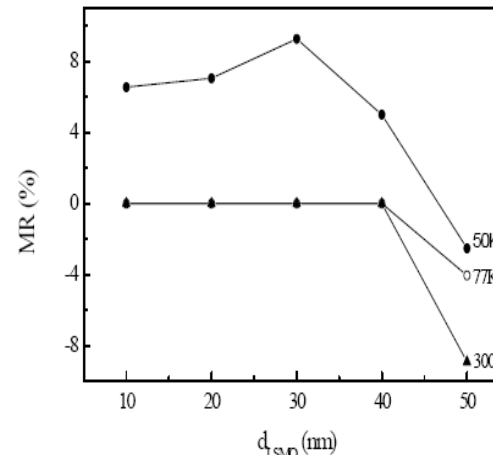
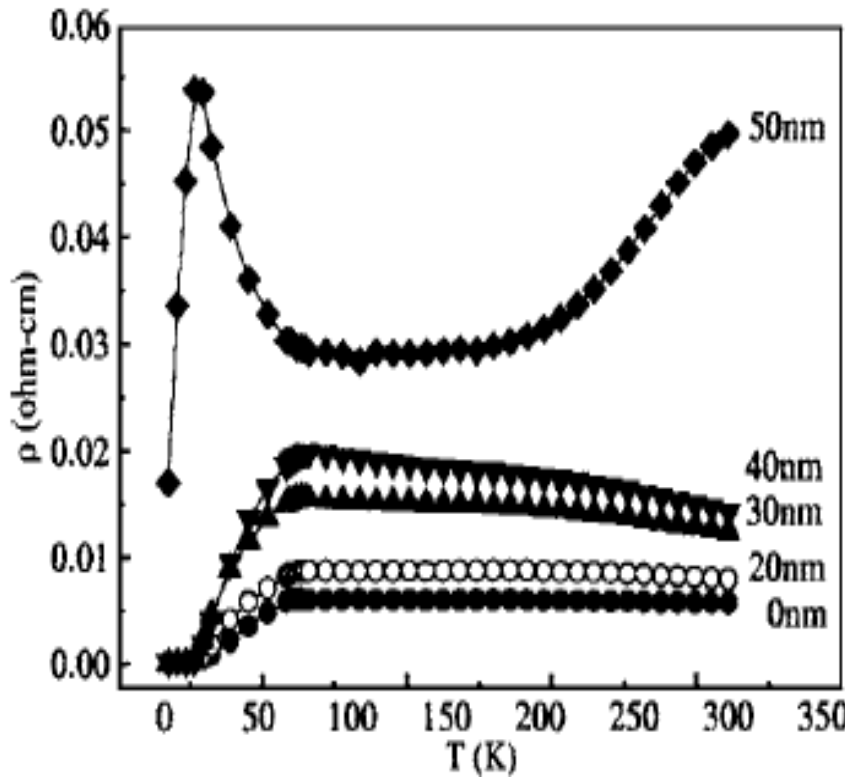
Center for Condensed Matter Science and Center for Nanostorage Research, National Taiwan University, Taipei 106, Taiwan

C. R. Chang

Department of Physics and Center for Nanostorage Research, National Taiwan University, Taipei 106, Taiwan

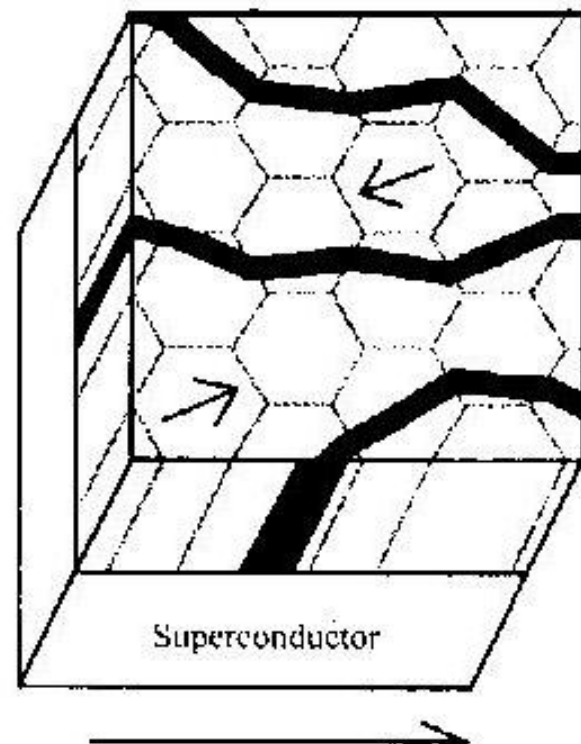
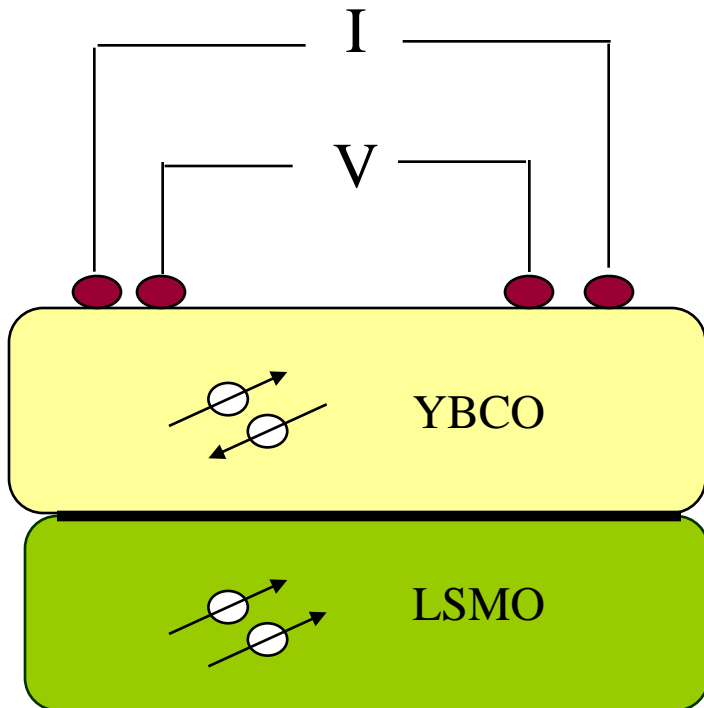
D. Y. Xing

National Laboratory of Solid State Microstructures and Department of Physics, Nanjing University, Nanjing 210093, China





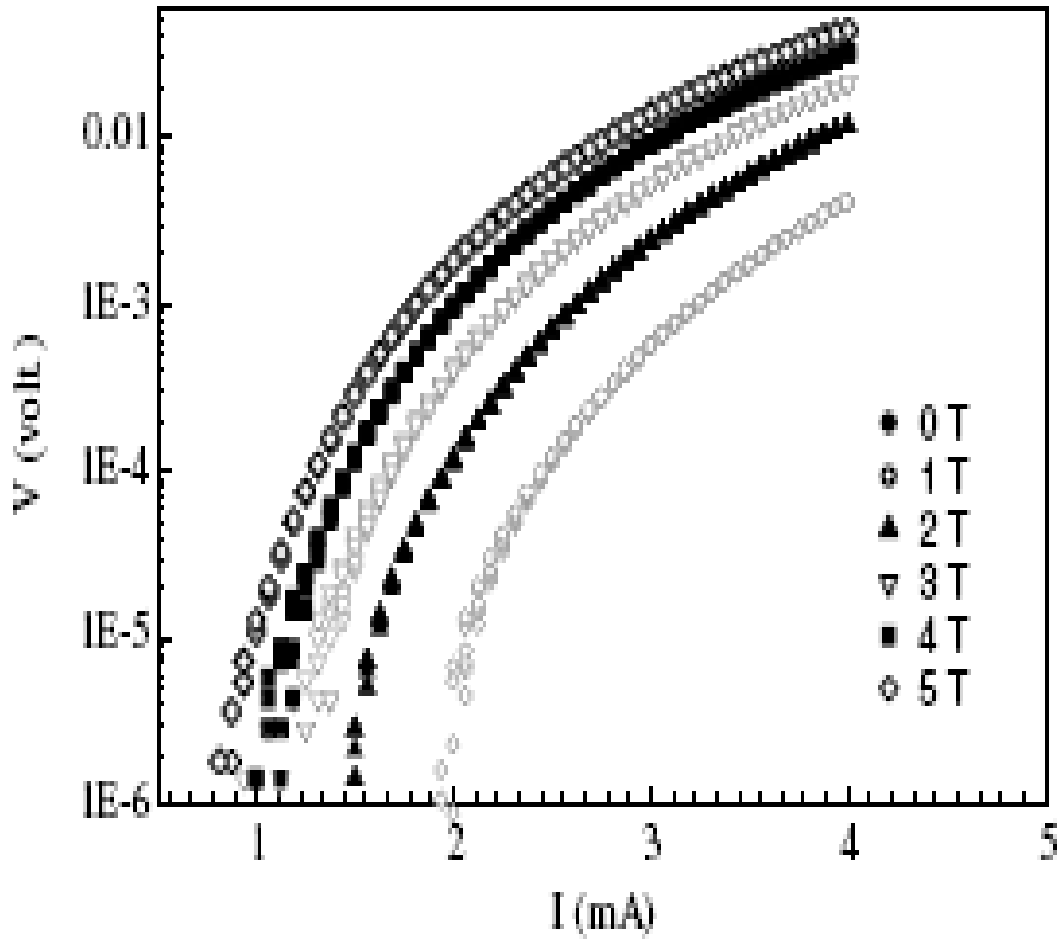
Vortex pinning device



Current flow



I-V characteristic



Critical current I_C
Normal state resistance R_n
Energy gap Δ

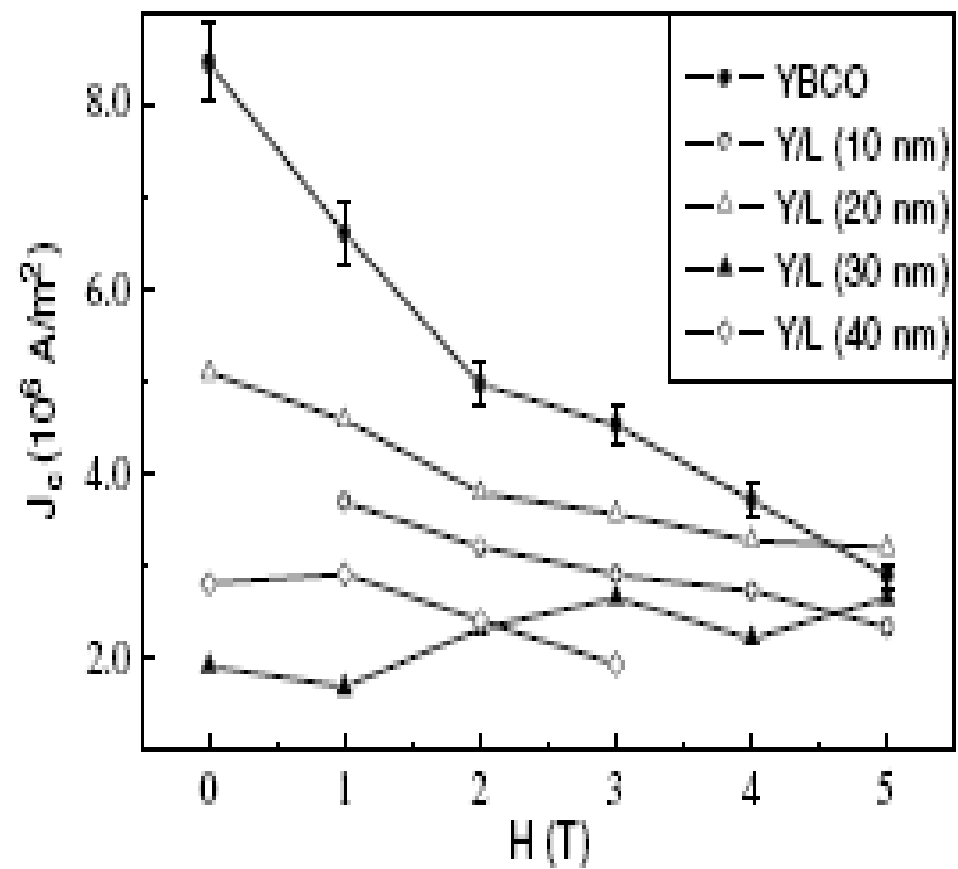
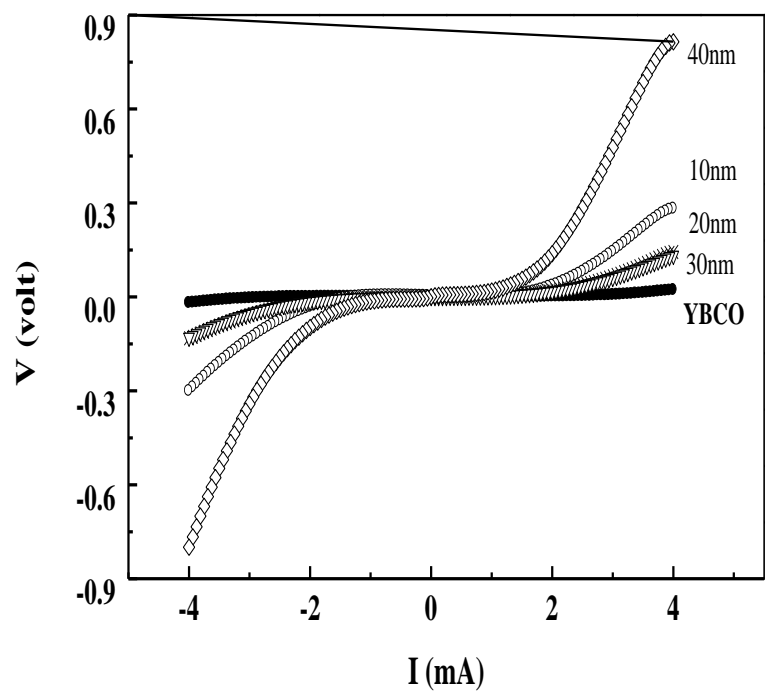
$$I_C = I(V=1 \mu\text{V})$$

$$I_C R_n = \pi \Delta / 2$$

$$= 3.52 \pi K_B T_C / 4$$



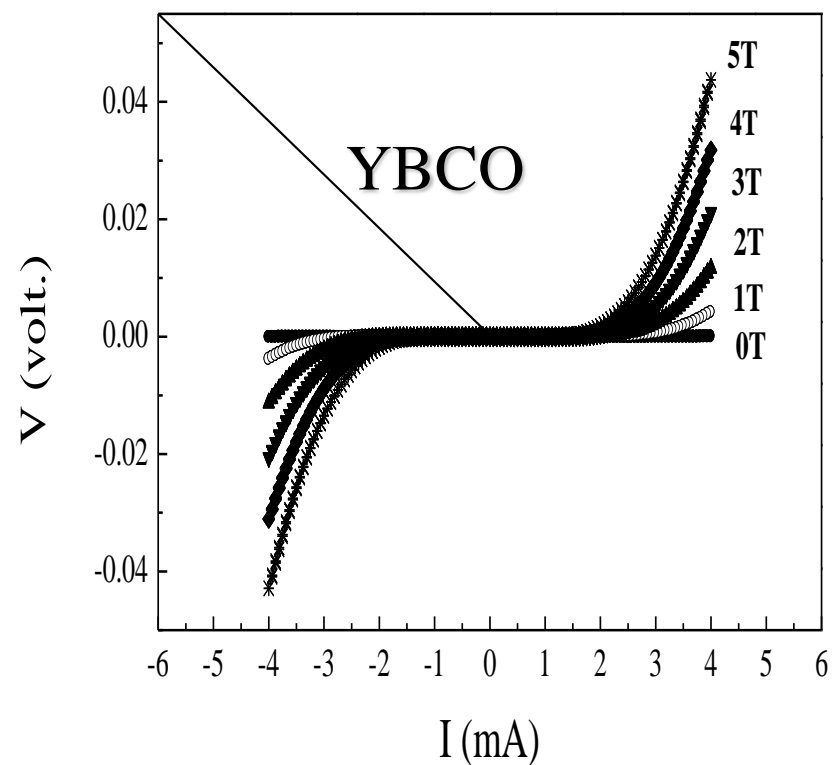
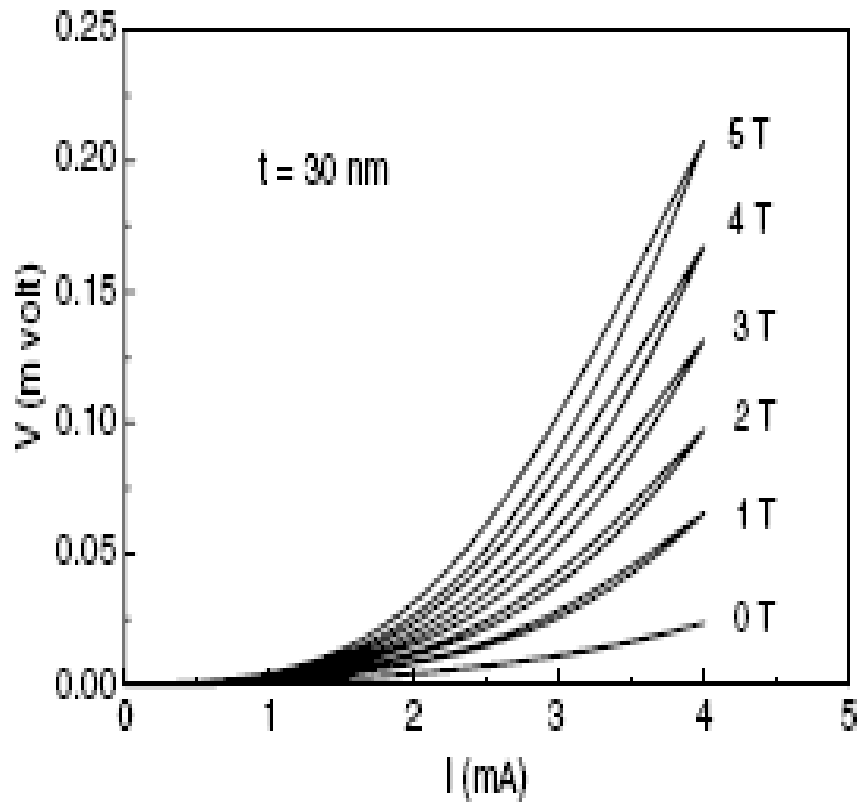
I-V Characteristic (1.9 K)



I_c decreases with increasing thickness of LSMO



Hysteresis in YBCO/LSMO(30nm)





Available online at www.sciencedirect.com



Physica C 437–438 (2006) 187–189

PHYSICA C

www.elsevier.com/locate/physc

High field pinning-effects in $\text{YBa}_2\text{Cu}_3\text{O}_7/\text{La}_{0.7}\text{Sr}_{0.3}\text{MnO}_3$ nanocrystalline bilayers

J.G. Lin ^{a,b,*}, S.L. Cheng ^b

^a *Center for Condensed Matter Sciences, National Taiwan University, Taipei 106, Taiwan*

^b *Center for Nanostorage Research, National Taiwan University, Taipei 106, Taiwan*

Available online 26 January 2006

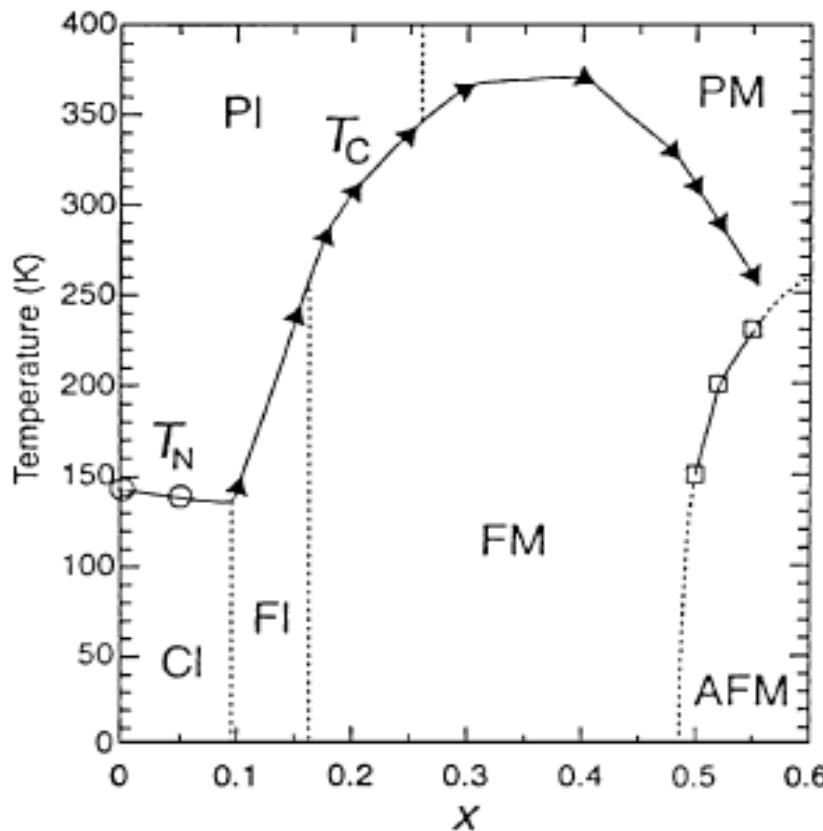


Subject (3): Epitaxial YBCO/NCMO bilayers

--- **How the superconductivity is affected
by weak ferromagnetic insulator ?**

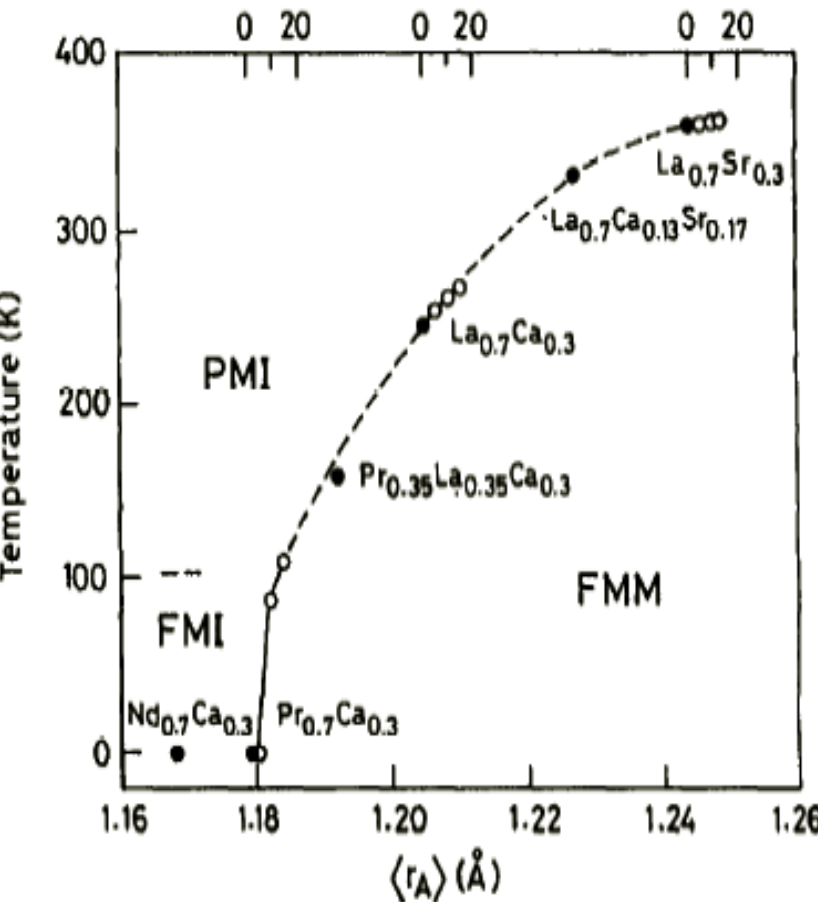


$\text{La}_{1-x}\text{Sr}_x\text{MnO}_3$



E. Dagotto *et. al.*, Physics Reports 344, 1-153 (2001)

$\text{R}_{0.7}(\text{Ca},\text{Sr})_{0.3}\text{MnO}_3$



C. N. R. Rao *et al.* J. Phys. Chem. Solids 59, 487 (1998)

Low-current-induced electrical hysteresis in $\text{Nd}_{0.7}\text{Ca}_{0.3}\text{MnO}_3$

Daniel Hsu

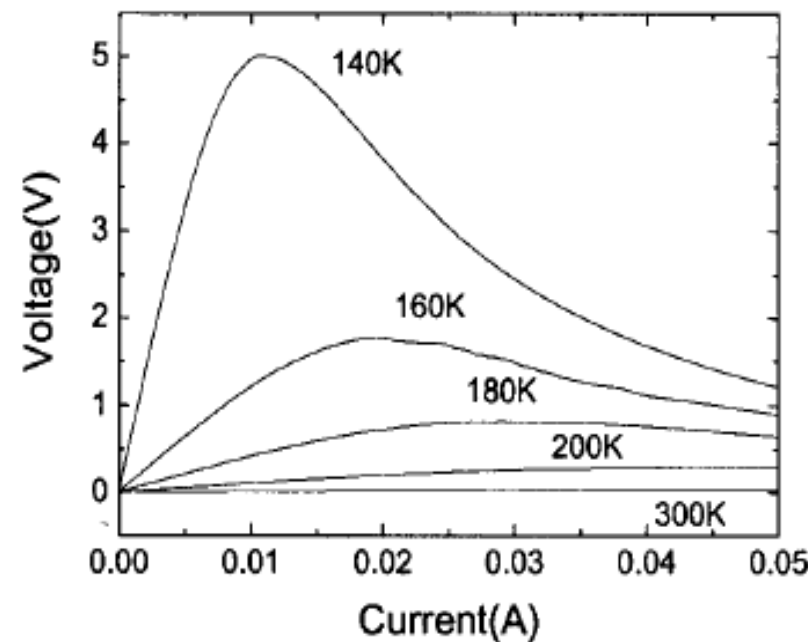
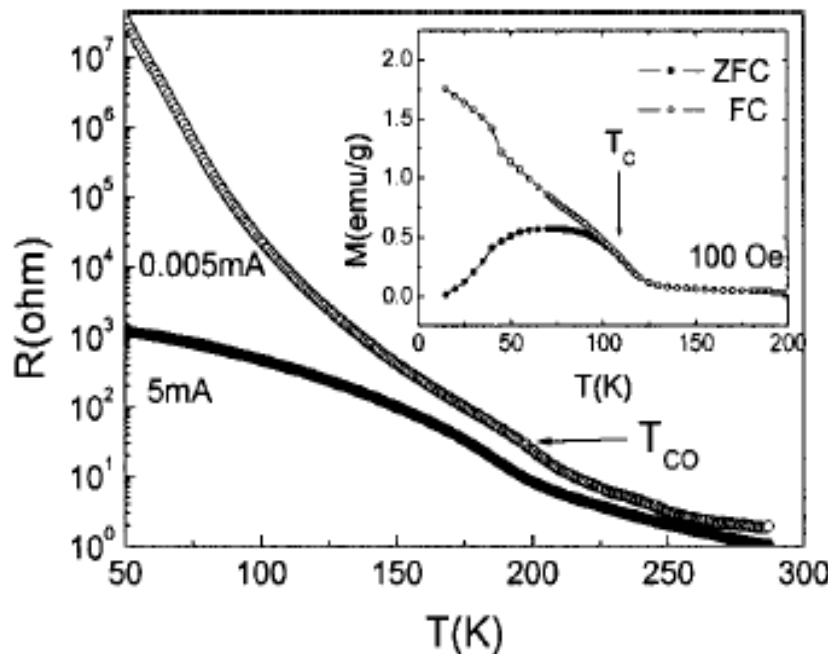
Center for Condensed Matter Science, National Taiwan University, Taipei 106, Taiwan; Center for Nanostorage Research, National Taiwan University, Taipei 106, Taiwan; and Institute of Mechanical Engineering, National Taiwan University, Taipei 106, Taiwan

J. G. Lin^{a)}

Center for Condensed Matter Science, National Taiwan University, Taipei 106, Taiwan and Center for Nanostorage Research, National Taiwan University, Taipei 106, Taiwan

W. F. Wu

Institute of Mechanical Engineering, National Taiwan University, Taipei 106, Taiwan





Substrate criteria

1. Atomically flat
2. Chemically comparable
3. Well lattice mismatch

For YBCO, LaAlO_3 (100) is $\sim 0.4\%$;

SrTiO_3 (100) is 0.2% for a -parameter, 0.3%
for b -parameter;

NdGaO_3 (110) is 0.7 % for a - and b -parameters



$\text{Nd}_{0.7}\text{Ca}_{0.3}\text{MnO}_3$ (001), orthorhombic

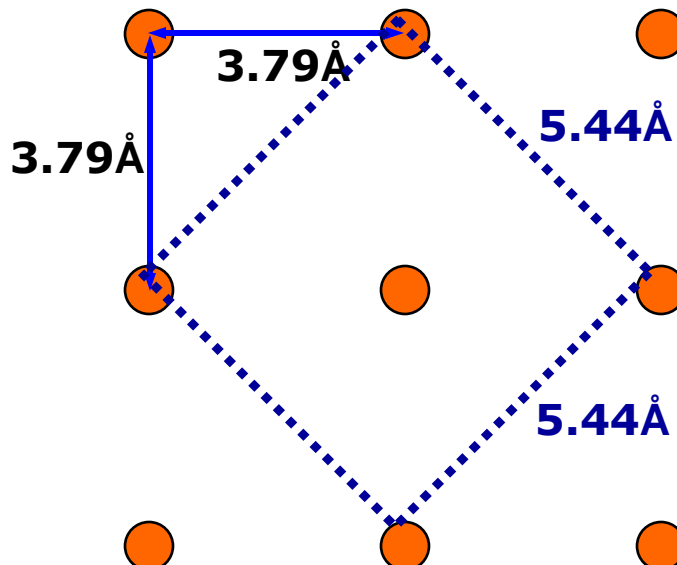
$\text{YBa}_2\text{Cu}_3\text{O}_7$ (001), orthorhombic

LaAlO_3 (100), rhombohedra

$\underline{\text{LaAlO}_3}$

$a=b=c=3.79 \text{ \AA}$

$\alpha=\beta=\gamma=90.12^\circ$



$\underline{\text{o-YBa}_2\text{Cu}_3\text{O}_7}$

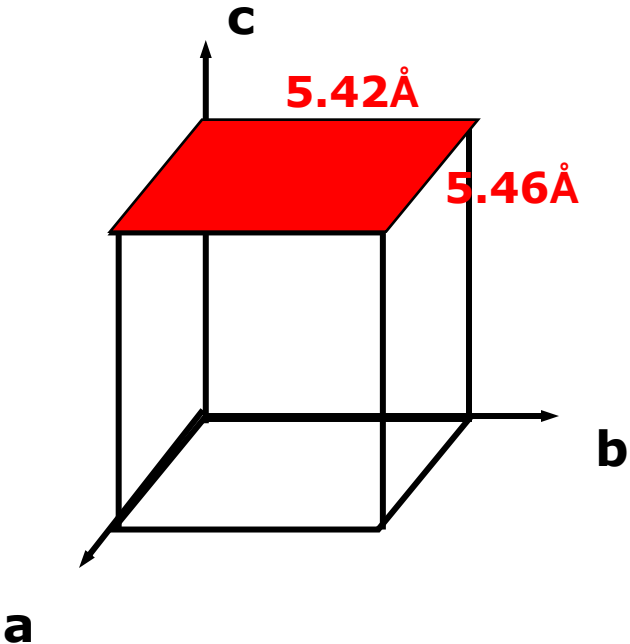
$a=3.82 \text{ \AA}, b=3.85 \text{ \AA},$

$c=11.63 \text{ \AA}; \alpha=\beta=\gamma=90^\circ$

$\underline{\text{o-Nd}_{0.7}\text{Ca}_{0.3}\text{MnO}_3}$

$a=5.42 \text{ \AA}, b=5.46 \text{ \AA},$

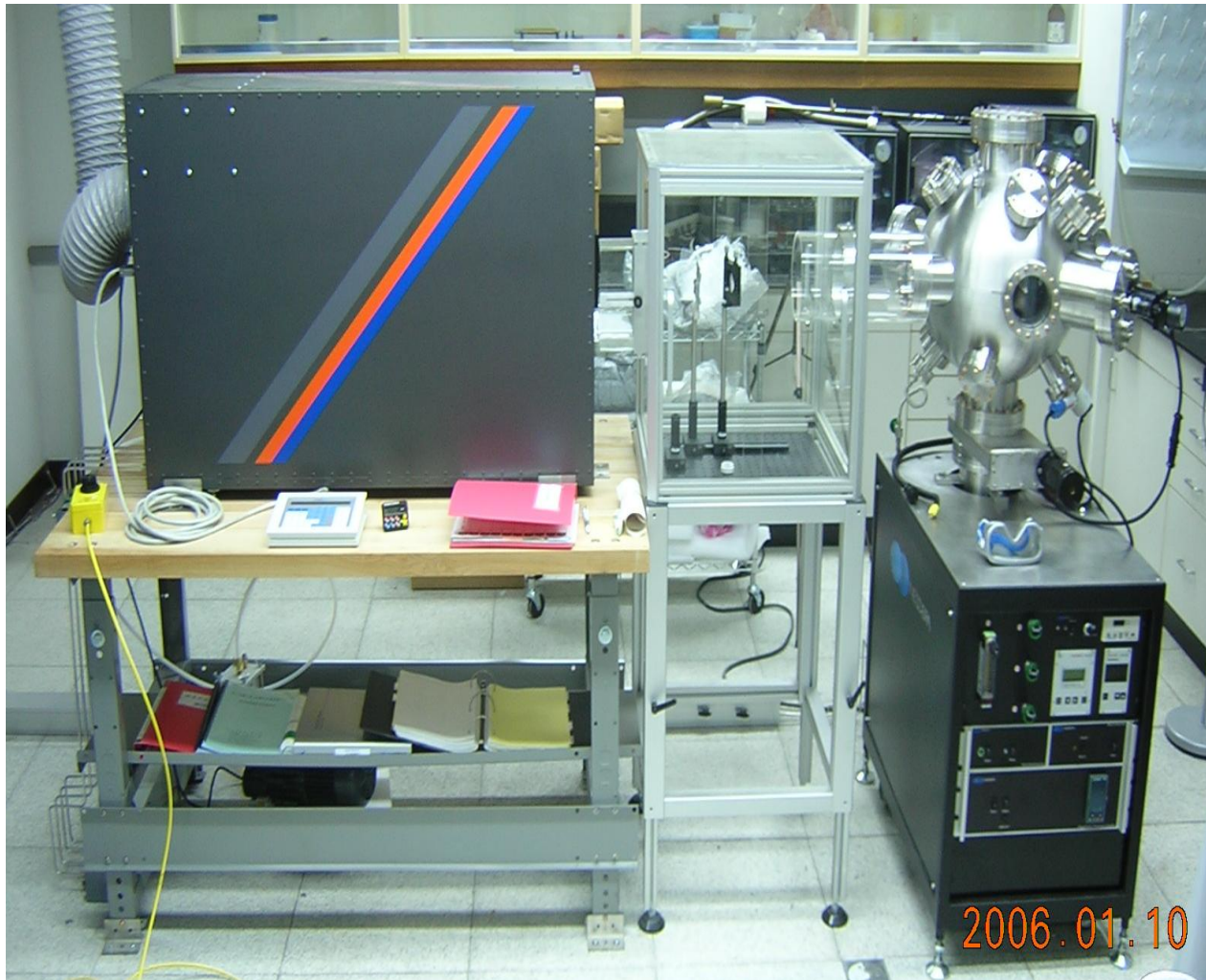
$c=7.72 \text{ \AA}; \alpha=\beta=\gamma=90^\circ$



Pulse-Laser-Deposition system –Neocera 180

KrF Laser (248 nm)

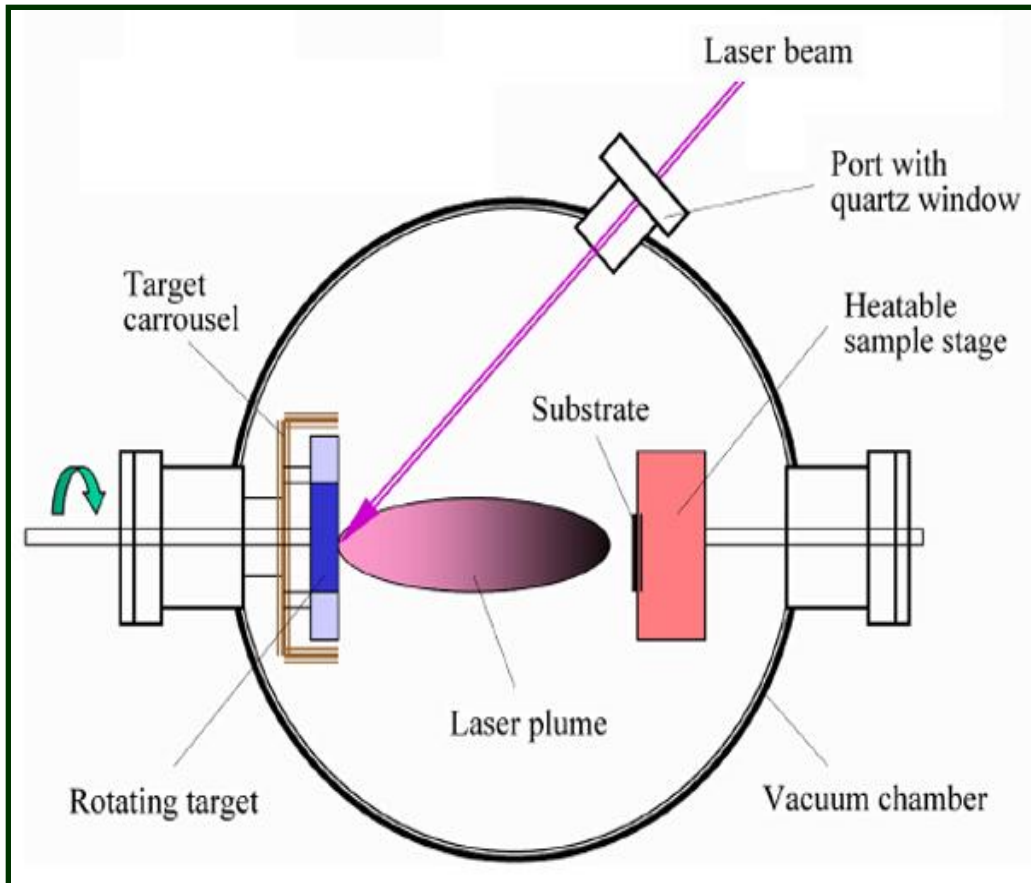
Focus Len



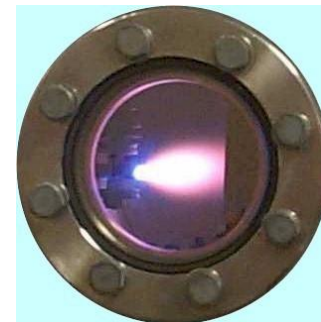
Chamber
 10^{-8} torr

Pump
Flow meter
Vacuum gauge

Pulse-Laser Deposition system (II) - Chamber



YBCO

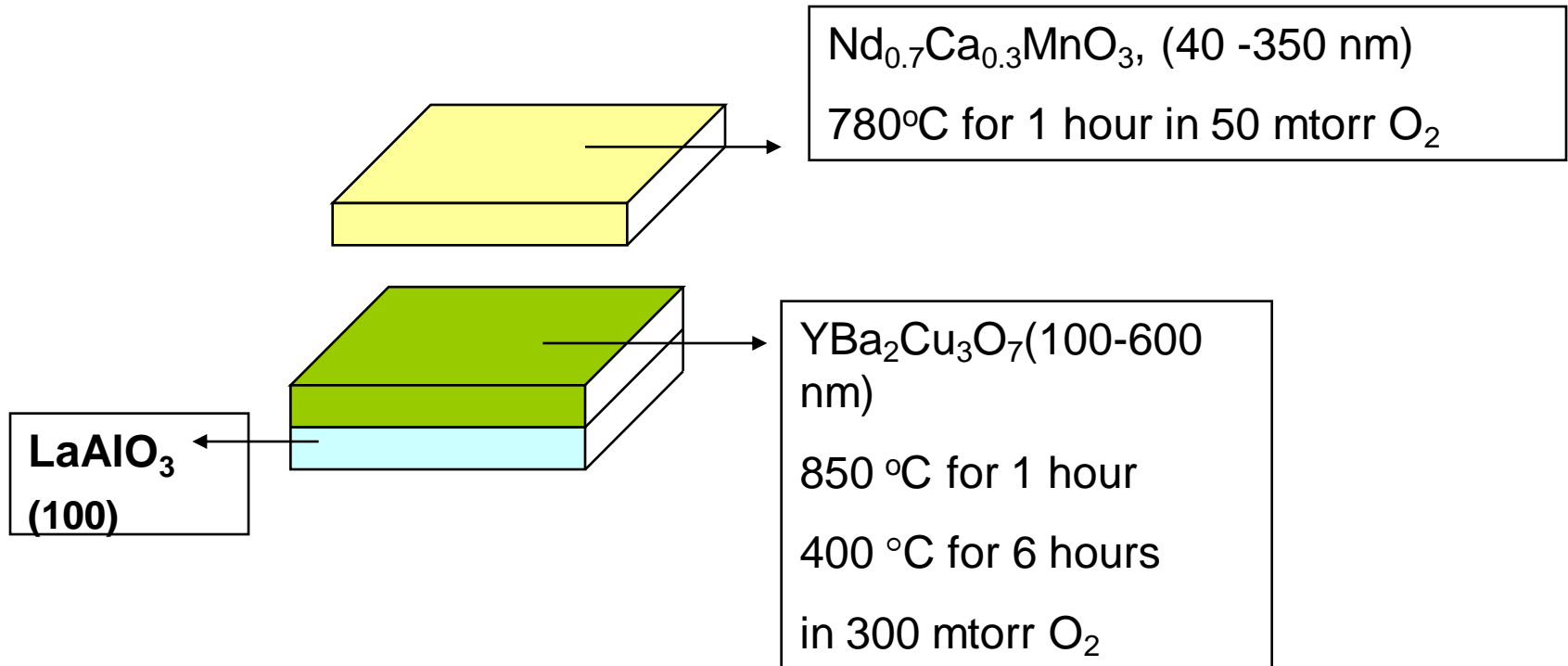


NCMO





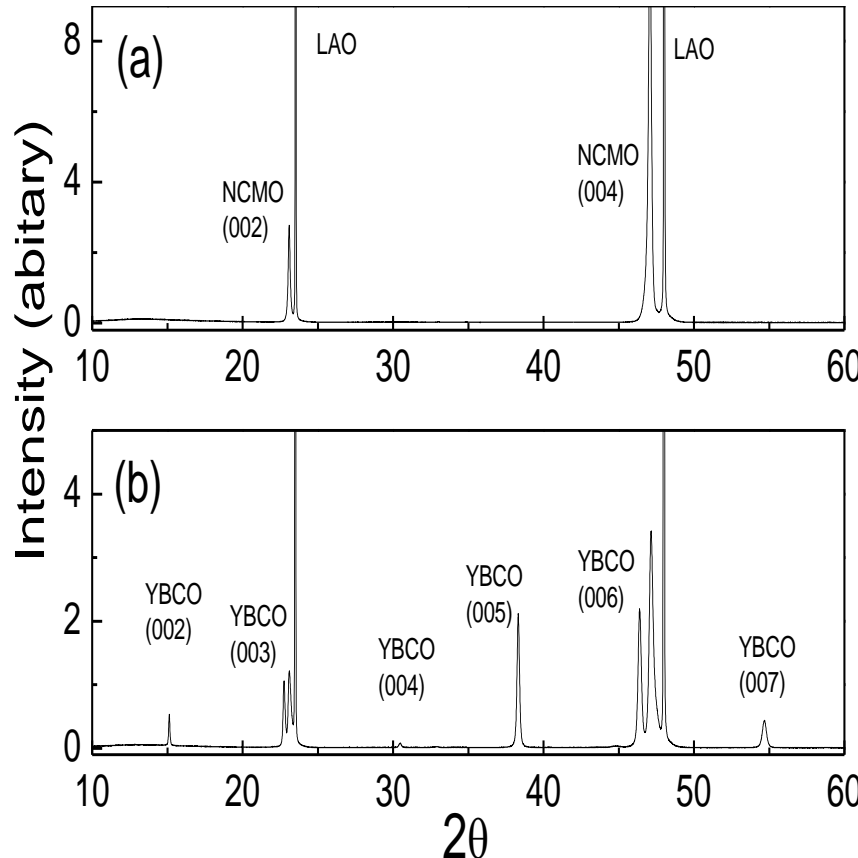
NCMO/YBCO heterostructure



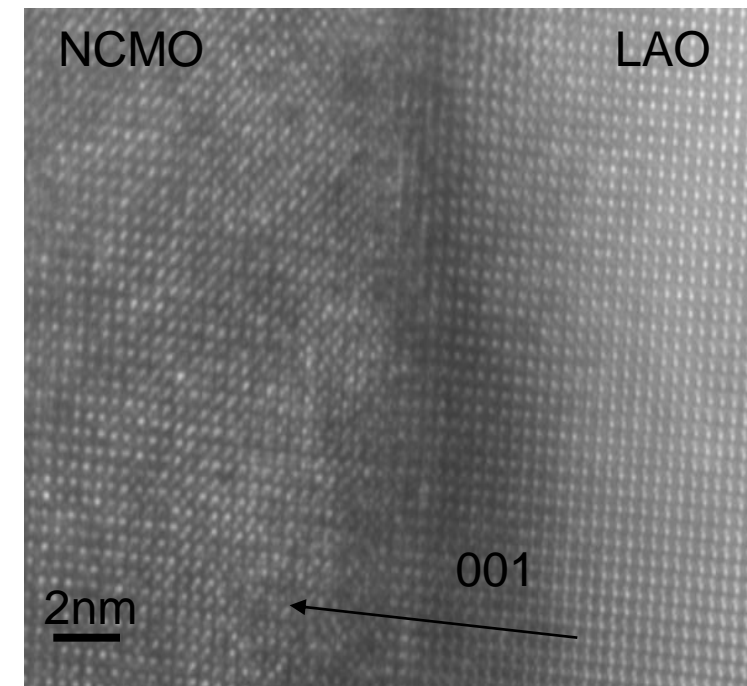


X-ray Diffraction Patterns & TEM image

- Both NCMO & YBCO are with c-axis perpendicular to the film surface



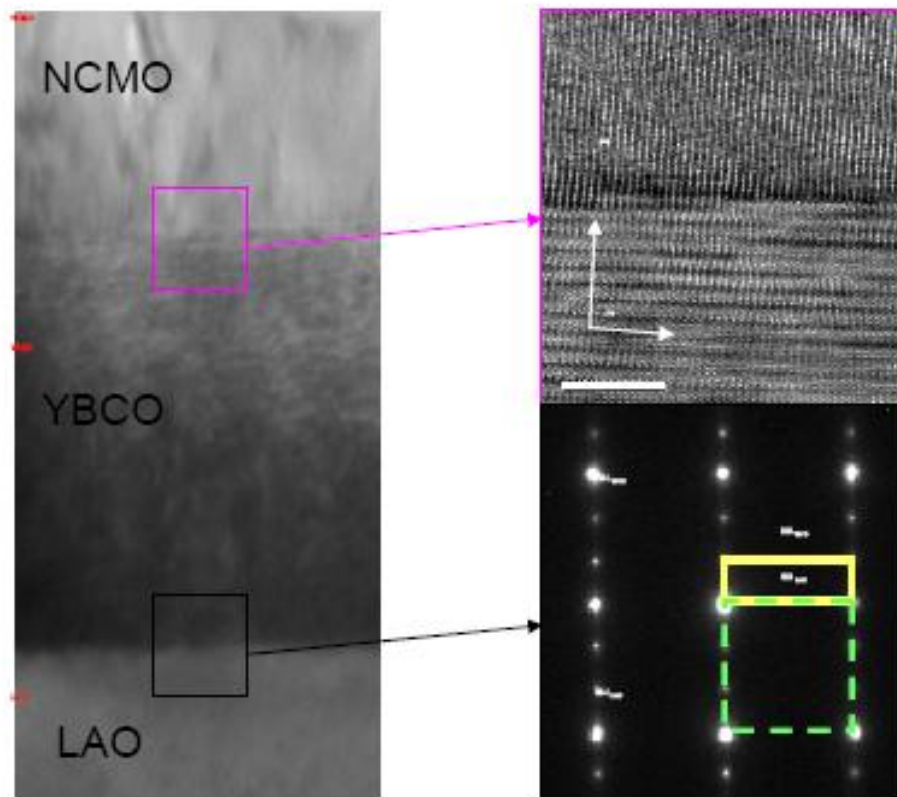
- Epitaxial growth along [001]



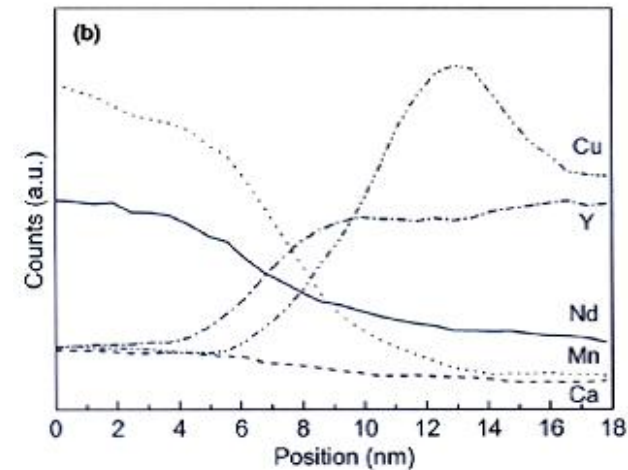
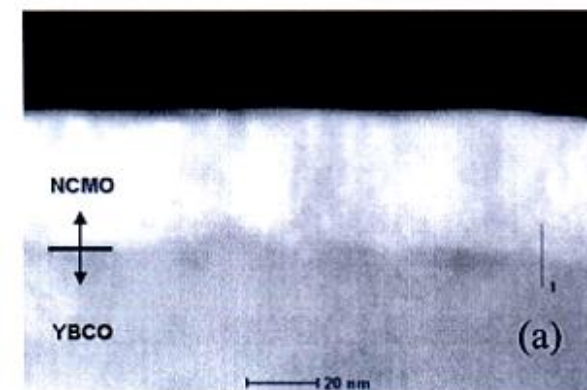


Basic characterization

(High resolution TEM & electron diffractions)



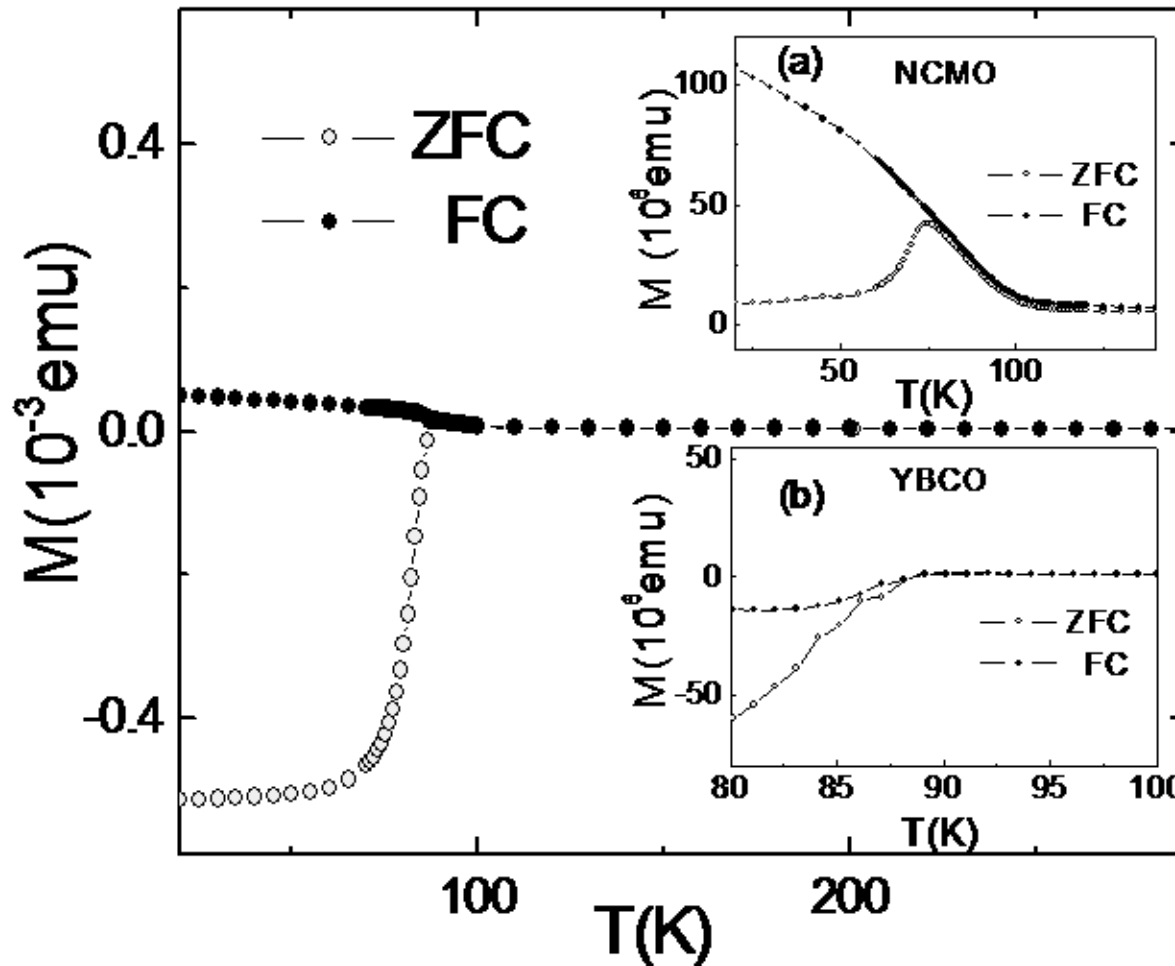
(Scanning EDX)





Magnetization(M) vs. Temperature (T) – by SQUID

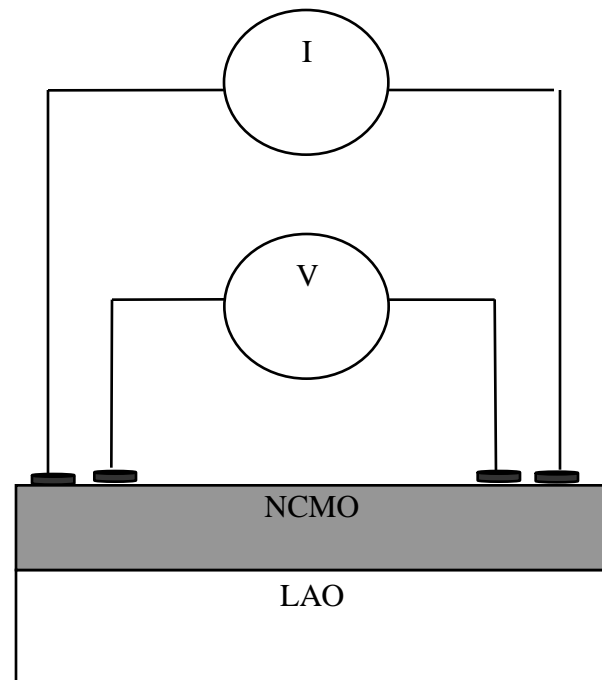
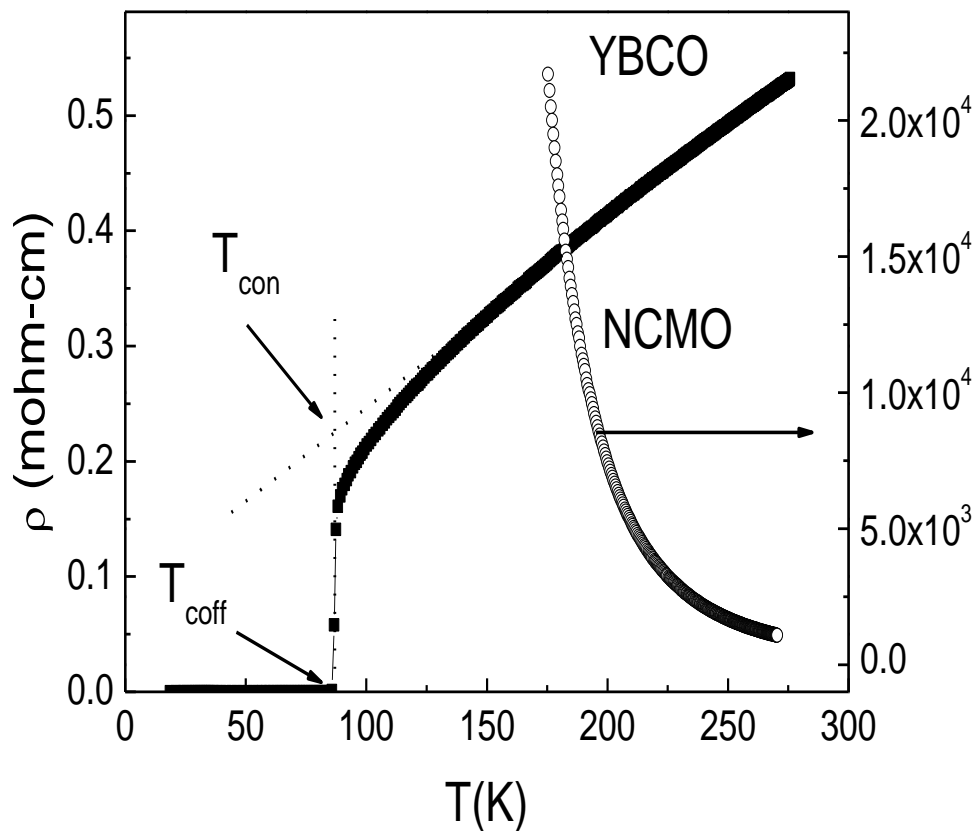
- T_c is 88 K for YBCO; T_N is ~ 75 K for NCMO;
Both transition temperature do not change in
NCMO(40nm)/YBCO(160nm).





4-Probe method

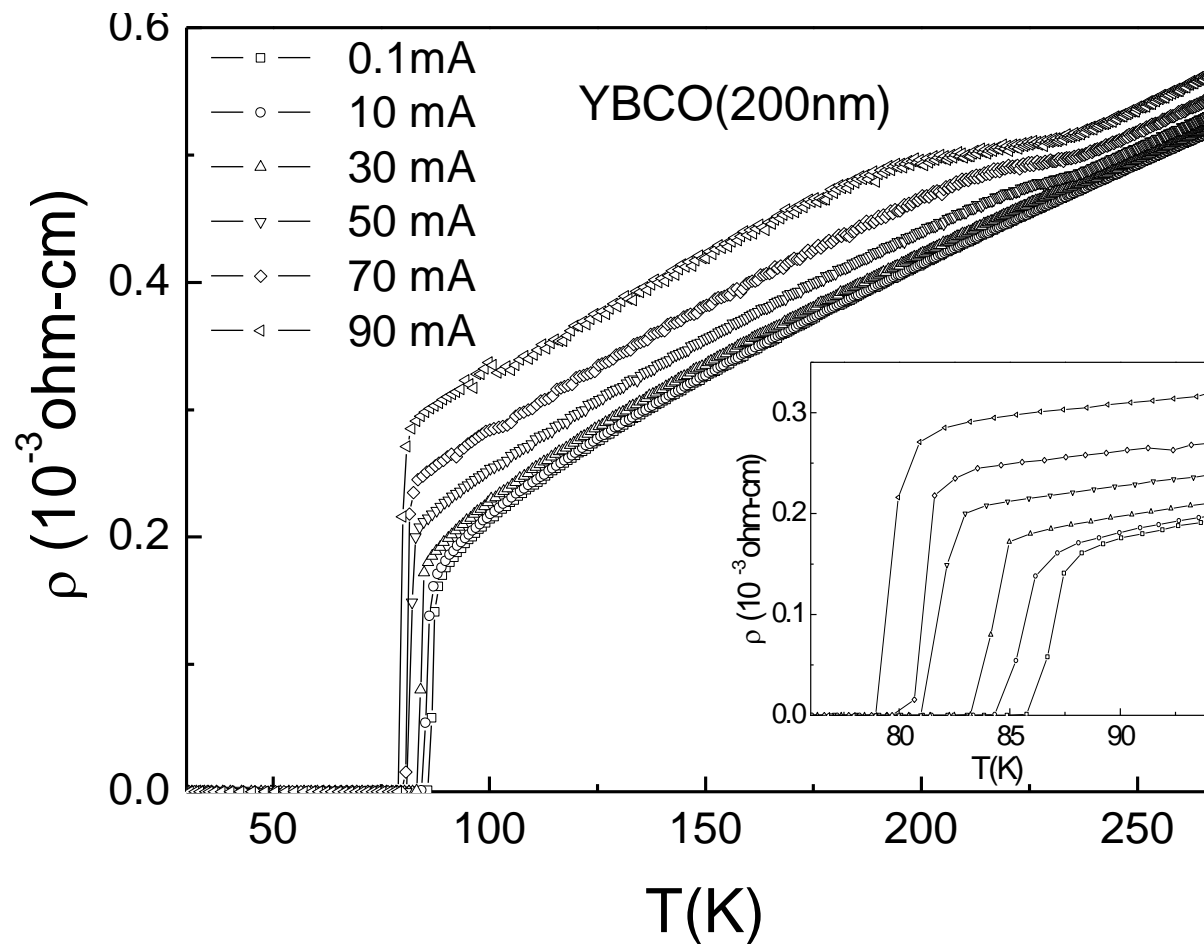
- YBCO : $T_c \sim 88$ K & $\Delta T < 2$ K; NCMO: Insulating





Resistivity (ρ) vs. Temperature (T)

- For $I_a = 1 - 90$ mA, normal state increases & T_c drops with a rate 0.1K/mA.
- open a gap at 230 K ?

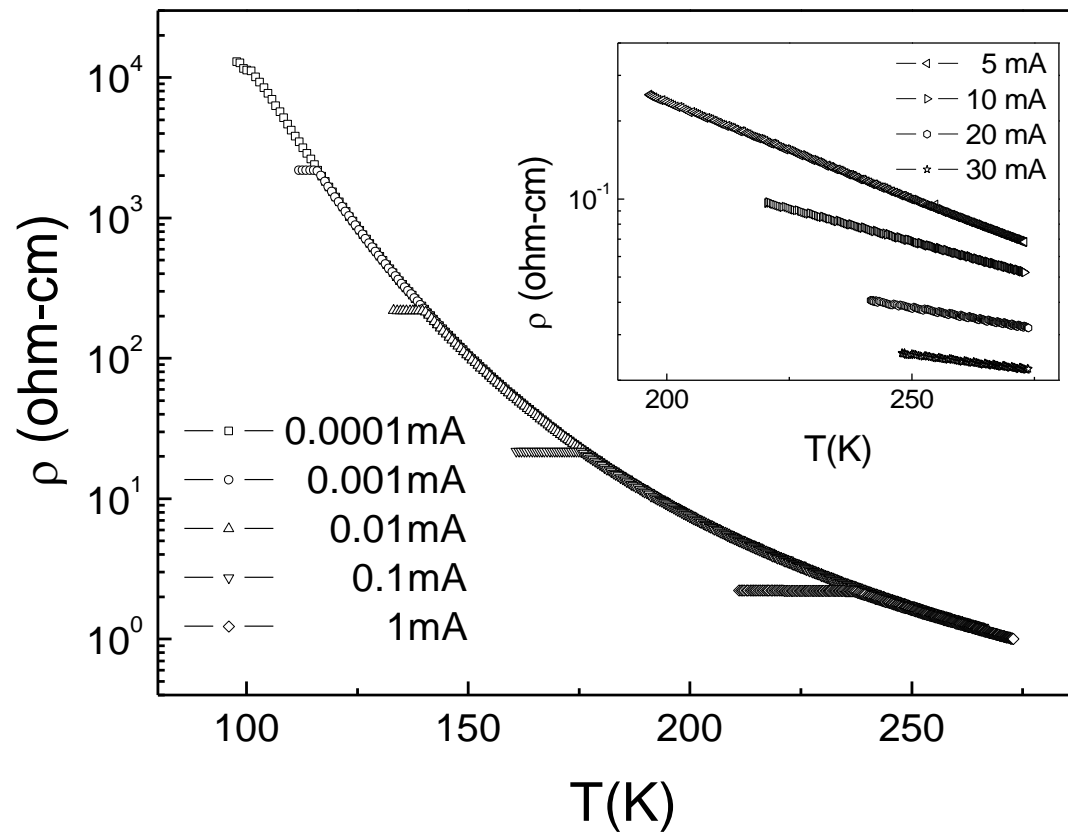




Resistivity (ρ) vs. Temperature (T)

- For $I_a = 5 - 30$ mA, resistivity decreases.

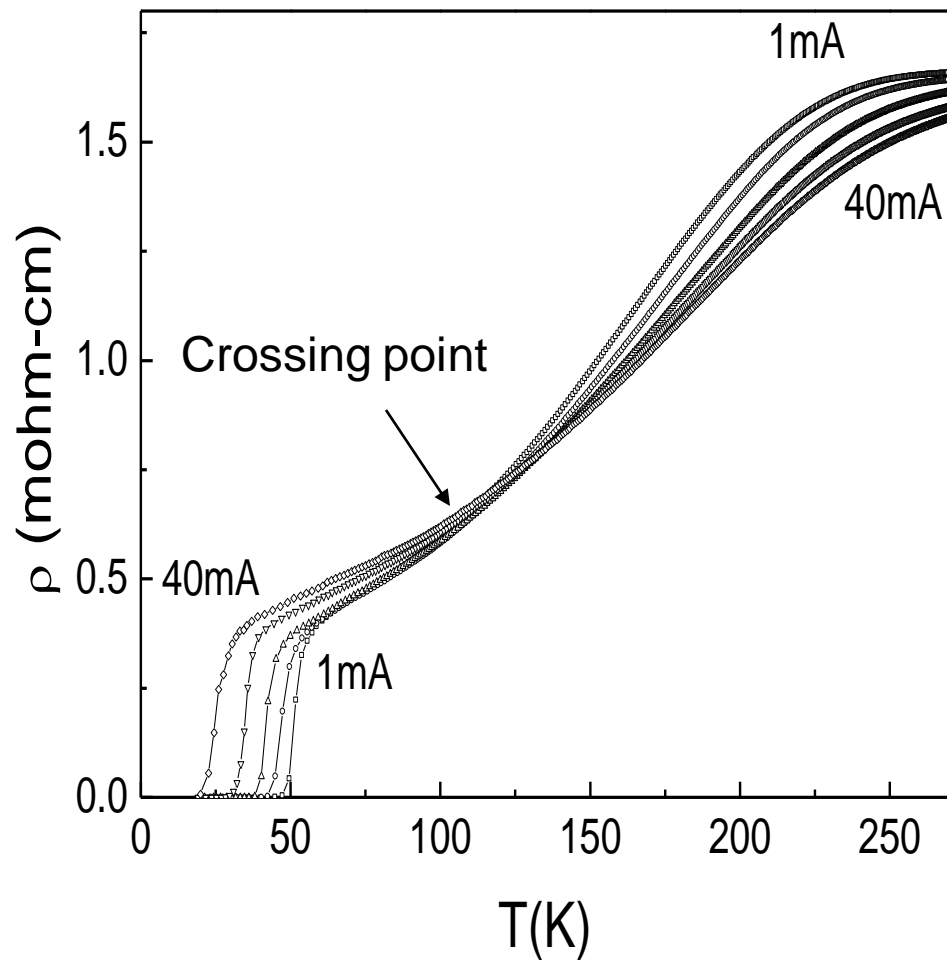
NCMO(200nm)



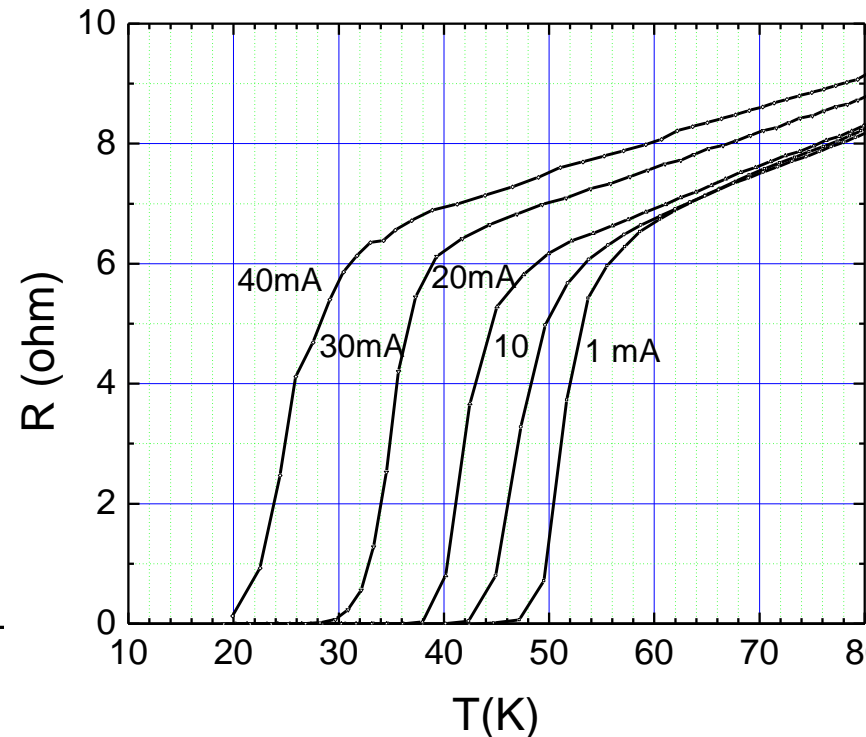


Resistivity (ρ) vs. Temperature (T)

NCMO(200nm)/YBCO(200nm)



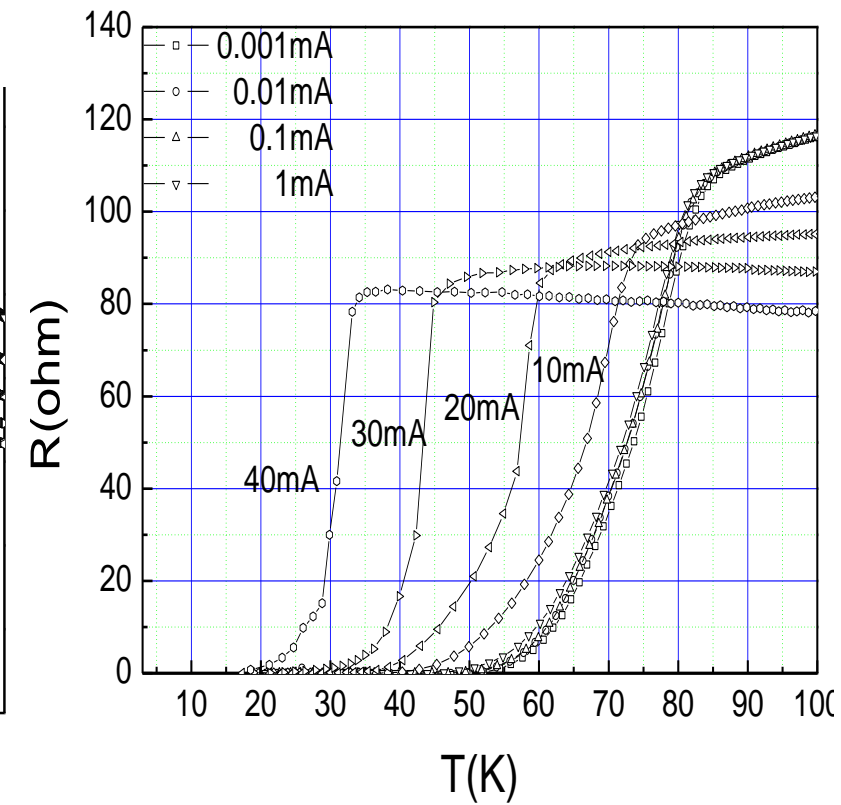
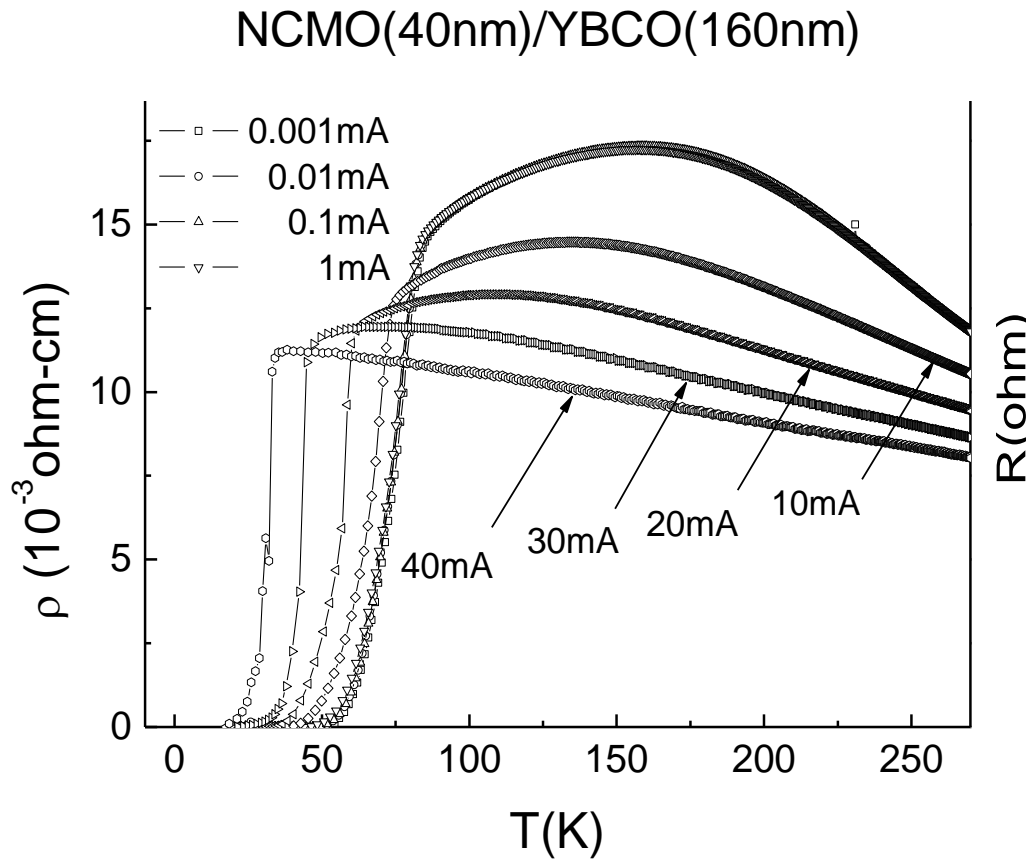
- For $I_a = 1 - 40$ mA, normal state increases & T_c drops with a rate of 1.0 K/mA.





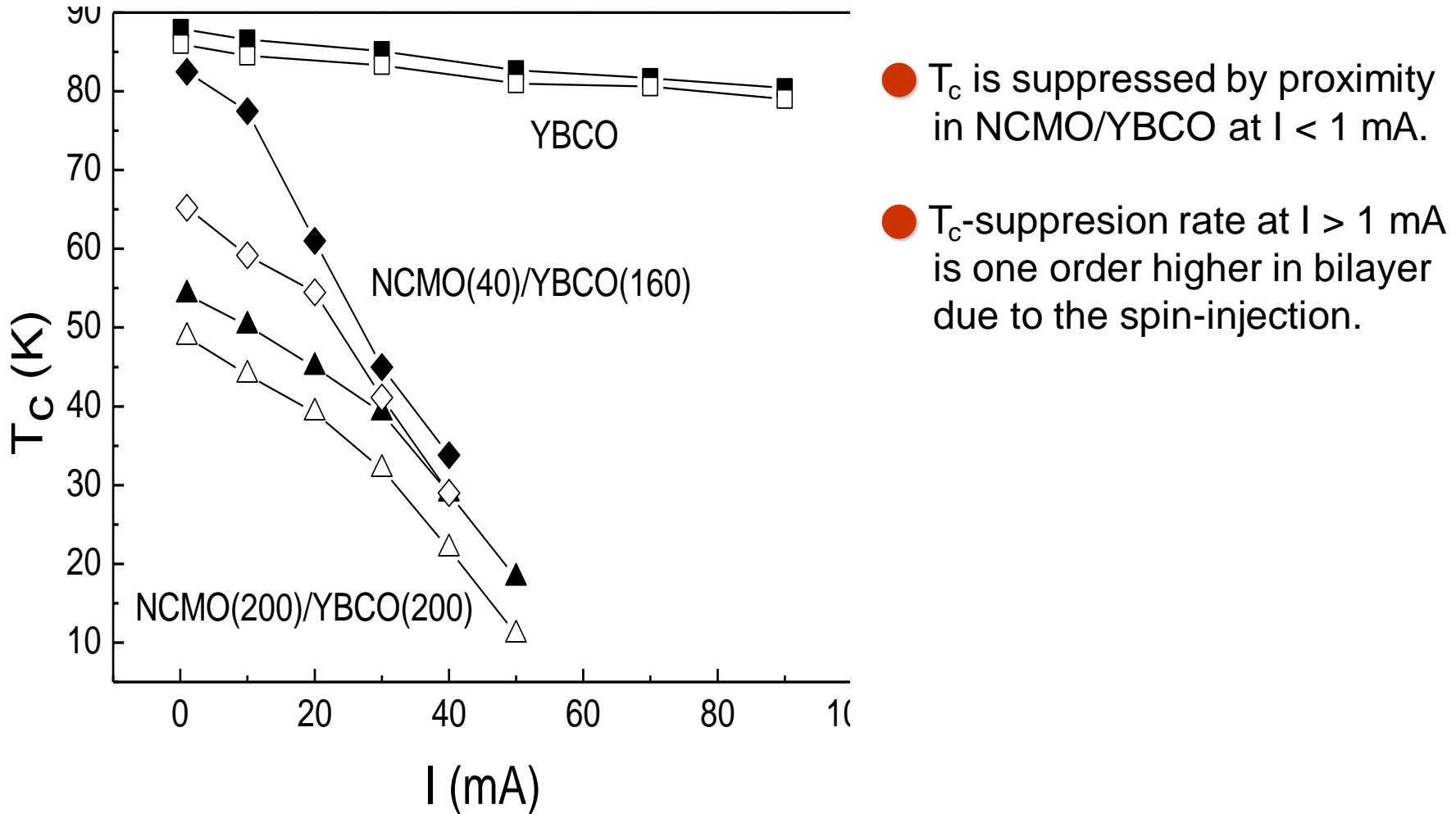
Resistivity (ρ) vs. Temperature (T)

- For $I_a = 1 - 40$ mA, normal state decreases 30% & T_c drops with a rate of 1.4 K/mA.





Superconducting temperature vs. applying current





● Proximity effect

$$H_{\text{eff-ex}} = H_{\text{ex}} \{d_F/(d_S + d_F)\}$$

0.5H_{ex} for NCMO(200nm)/YBCO(200nm)
0.2H_{ex} for NCMO(40nm)/YBCO(160nm)

$\Delta T_c \sim 34K / 16K$

● Current induces spin-injection effect

Observe a threshold of effective current $I > 1$ mA

Large T_c-suppresion in a rate of 1.4 K/mA.

Proximity effect of superconductivity and magnetism in the $\text{Nd}_{0.7}\text{Ca}_{0.3}\text{MnO}_3/\text{YBa}_2\text{Cu}_3\text{O}_7$ bilayer

J. G. Lin^{a)}

*Center for Condensed Matter Sciences, National Taiwan University, Taipei, 106 Taiwan, Republic of China
and Center for Nanostorage Research, National Taiwan University, Taipei, 106 Taiwan,
Republic of China*

Daniel Hsu

*Center for Condensed Matter Sciences, National Taiwan University, Taipei, 106 Taiwan, Republic of China;
Center for Nanostorage Research, and Department of Mechanical Engineering, National Taiwan
University, Taipei, 106 Taiwan, Republic of China*

W. F. Wu

Department of Mechanical Engineering, National Taiwan University, Taipei, 106 Taiwan, Republic of China

C. H. Chiang and W. C. Chan

Department of Physics, Tamkang University, Tamsui, Taipei, 251 Taiwan, Republic of China

(Presented on 10 January 2007; received 31 October 2006; accepted 2 December 2006;
published online 10 April 2007)

Current enhanced magnetic proximity in $\text{Nd}_{0.7}\text{Ca}_{0.3}\text{MnO}_3/\text{YBa}_2\text{Cu}_3\text{O}_7$ bilayer

Daniel Hsu

Center for Condensed Matter Sciences, Center for Nanostorage Research, and Department of Mechanical Engineering, National Taiwan University, Taipei, Taiwan 106, Republic of China

J. G. Lin^{a)}

Center for Condensed Matter Sciences and Center for Nanostorage Research, National Taiwan University, Taipei, Taiwan 106, Republic of China

C. P. Chang and C. H. Chen

Center for Condensed Matter Sciences, National Taiwan University, Taipei, Taiwan 106, Republic of China

W. F. Wu

Department of Mechanical Engineering, National Taiwan University, Taipei, Taiwan 106, Republic of China

C. H. Chiang and W. C. Chan

Department of Physics, Tamkang University, Taipei, Taiwan 251, Republic of China

Thickness dependent spin-injection effects in $\text{Nd}_{0.7}\text{Ca}_{0.3}\text{MnO}_3/\text{YBa}_2\text{Cu}_3\text{O}_7$ bilayers

Daniel Hsu,^{1,2} J. G. Lin,^{1,2,a)} C. P. Chang,¹ C. H. Chen,¹ C. H. Chiang,³ W. C. Chan,³ and W. F. Wu⁴

¹*Center for Condensed Matter Sciences, National Taiwan University, Taipei 106, Taiwan, Republic of China*

²*Center for Nanostorage Research, National Taiwan University, Taipei 106, Taiwan, Republic of China*

³*Department of Physics, Tamkang University, Tamsui, Taipei 251, Taiwan, Republic of China*

⁴*Department of Mechanical Engineering, National Taiwan University, Taipei 106, Taiwan, Republic of China*

(Presented on 9 November 2007; received 10 September 2007; accepted 26 October 2007; published online 8 February 2008)

Two $\text{Nd}_{0.7}\text{Ca}_{0.3}\text{MnO}_3/\text{YBa}_2\text{Cu}_3\text{O}_7$ (NCMO/YBCO) bilayers with different thickness ratios are fabricated and the spin-injection effects are investigated. The NCMO/YBCO samples have thicknesses of 100 nm/200 nm and 200 nm/200 nm, which are denoted as N/Y(1) and N/Y(2), respectively. It is shown that the current-induced suppression rate of superconducting transition temperature (dT_c/dI) in YBCO is enhanced by four to six times of magnitude in N/Y(1) and N/Y(2) compared with that in pure YBCO. Furthermore, dT_c/dI in N/Y(2) is larger than that in N/Y(1), which suggests that the thickness of NCMO has influence on the pair breaking in YBCO.

© 2008 American Institute of Physics. [DOI: [10.1063/1.2833819](https://doi.org/10.1063/1.2833819)]

Conclusion Remark



Half metal is the future material for various kinds of spintronic devices